International Journal of Peptides

Natural Peptides with Potential Applications in Drug Development, Diagnosis, and/or Biotechnology

Guest Editors: Mirian A. F. Hayashi, Frédéric Ducancel, and Katsuhiro Konno

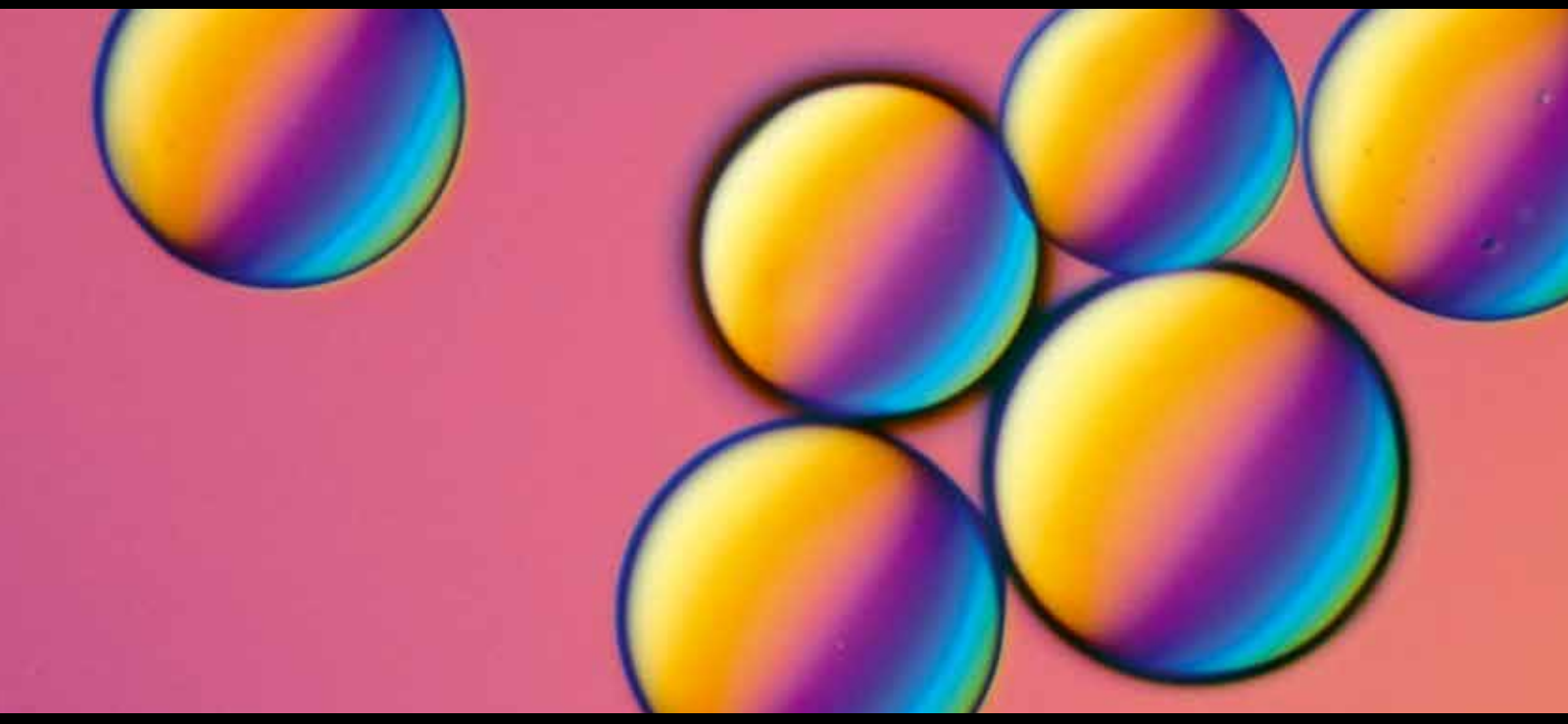

Natural Peptides with Potential Applications in Drug Development, Diagnosis, and/or Biotechnology

International Journal of Peptides

Natural Peptides with Potential Applications in Drug Development, Diagnosis, and/or Biotechnology

Guest Editors: Mirian A. F. Hayashi, Frédéric Ducancel, and Katsuhiro Konno

Editorial Board

Contents

Hindawi Publishing Corporation
International Journal of Peptides
Volume 2012, Article ID 757838, 2 pages
doi:10.1155/2012/757838

Editorial

Natural Peptides with Potential Applications in Drug Development, Diagnosis, and/or Biotechnology

Mirian A. F. Hayashi,[1] Frédéric Ducancel,[2] and Katsuhiro Konno[3]

[1] *Laboratory of Molecular Pharmacology, Departamento de Farmacología, Universidade Federal de São Paulo (Medical School of São Paulo), São Paulo, SP, Brazil*
[2] *Responsable du Laboratoire d'Ingénierie des Anticorps pour la Santé Head of the Laboratory of Antibody Engineering for Health (CEA/iBiTecS/SPI/LIAS), CEA de Saclay, Bt 152, 91191 Gif-sur-Yvette Cedex, France*
[3] *Institute of Natural Medicine, University of Toyama, 2630 Sugitani, Toyama-shi, Toyama 930-0194, Japan*

Correspondence should be addressed to Mirian A. F. Hayashi, mhayashi@unifesp.br

Received 19 July 2012; Accepted 19 July 2012

Natural peptides are central and crucial in many physiological processes playing either direct or indirect roles. Peptides are short linear chains of up to fifty amino acid residues, stabilized or not by disulphide bonds. They occur naturally in all living beings and exert highly specific biological activities, whose specificity is mainly based on and dependent on their primary sequence and, ultimately, to their conformational structure. The primary function of most peptides is the cell signalling role aiming to translate and deliver the biochemical "message" that triggers structural, molecular, cellular, and eventually biological effects. Thus, peptides can play roles as agonists, antagonists, modulators, mediators, hormones, effectors, cofactors, activators, stimulators, and so on.

Also, many peptides can act directly as enzyme inhibitors or as antimicrobial compounds with possible activity on biological membranes, although with no necessary membrane lipid bilayer permeabilisation ability, acting by interfering with metabolism and targeting cytoplasmic components. They are also potentially antigenic compounds and several other peptides are used as pathological biomarkers, since they can be easily and specifically detected and quantified in various biological fluids.

Based on the huge variety of mode of actions and physiological/pathological roles played by the peptides, in general, their structural and functional relationship has been widely studied by scientific researchers. Their functional roles, their reduced size, their low immunogenicity, their stability, in addition to the recent development of powerful strategies for chemical synthesis and/or recombinant expression, have given to the peptides the status of the most promising family of compounds with potential application for human diagnosis and therapy. Furthermore, their scaffold can been engineered to design compounds with modified biochemical, functional, or biophysical properties, allowing their labelling for *in vivo* imaging and vectorization applications, or also to functionalize nanoparticles.

This special issue aims to gather a recent set of six original articles that mainly further emphasizes the molecular diversity and the variety of mode of action of natural peptides.

Thus, C. Kairane and colleagues, from Estonia (Faculty of Medicine of University of Tartu), have examined the influence of the replacement of γ-Glu moiety to α-Glu in two gluthatione- (GSH-) related tetrapeptides UPF1 (Tyr (Me)-γ-Glu-Cys-Gly) and UPF17 (Tyr (Me)-α-Glu-Cys-Gly) in the antioxidative defense system in a human erythroleukemia K562 cell line. By monitoring the effects in these K562 cells via measurements of the cytosolic superoxide dismutase CuZnSOD activity and variations of intracellular GSH levels, followed by addressing the question of the stability of these two peptides against the action of the γ-glutamyltranspeptidase (GGT), allowed to the authors to open promising perspectives for the usage of GSH analogues as regulators of the oxidative status of cells. In fact, UPF1 was shown to be resistant to the degradation by GGT. Nonetheless, attention was brought to the fact that UPF1/GSH and UPF17/α-GSH have paradoxal effects, suggesting that the

effective antioxidative character of peptides is not depend solely on the reactivity of the thiol group, but it might also be dependent of other functional groups and on the spatial structure of peptides.

The short communication by L. B. Bondarenko and V. M. Kovalenko aimed at investigating the potential effect of pyrazinamide on the type II collagen amino acid composition. Indeed, pyrazinamide is a drug classically used for tuberculosis treatment, and the establishment of its effect on a so important cell structural protein is clearly of worth. A dose-dependent quantitative and qualitative effect of pyrazinamide on the male rat extracellular matrix cartilage type II collagen amino acid composition was demonstrated, but additional studies are now necessary to precise and complete this preliminary study.

D. J. Sánchez-González and colleagues, from Mexico, provided to the readers of this special issue a review article on platelet-rich plasma peptides, revealing the central and important roles of these nonnuclear cellular fragments in mammals. Indeed, platelets are characterized by an important role on proteins and peptides synthesis, whose pattern and release in the plasma seems to be modulated in response to different cellular activations. Numerous peptidic growth factors present in the platelet-rich plasma are listed and their activities are also described. Also, the content in bioactive molecules, among which several peptides, present in the alpha granules of platelets are described, and their classification accordingly to their general known activity is shown. Finally, the therapeutic potential of several plasma-derived plasma peptides and their actual clinical status are presented, shedding some light on their potential use in both tissue repair and regenerative medicine.

The K. Wong group's article, from United Kingdom, consisted in a meta-analysis of the existing literature about the therapeutic effects of glucagon-like peptide-1 (GLP-1) agonist in the treatment of heart failure due to ischaemia. The leading cause of systolic heart failure is myocardial ischemia, resulting in the lack of chemical energy transfer from the metabolism of carbon fuels to the contractile work. Thus, metabolic modulators are able to improve the cardiac energetics by altering the substrate from free fatty acids to glucose. This shift results in an optimization of the metabolic efficiency of the heart. The GLP-1 agonist is among these metabolic modulator agents. This comprehensive review of medical literature (including information on preclinical or clinical trials) gives an overall estimate of the therapeutic effectiveness of using GLP-1 agonist in heart failure.

And, in a different topic, the review article presented by M. S. Akhtar and colleagues, from Pakistan, illustrates the particular interest that represents antimicrobial peptides as infection imaging agents. Indeed, differentiation between infection and inflammation by nuclear techniques using radiolabeled compounds is usually difficult. In this review, the authors describe and discuss the merits and demerits that can be attributed to specific radiotracers such as antimicrobial peptides compared to radiolabeled antibiotics for infection localization. Thus, antimicrobial peptides seems to be more specific agents for localizing infections, as they bind specifically to bacterial cell membranes. In fact, gram positive and negative bacteria, *Candida albicans* and also *Aspergillus fumigatus* infections are detected by such tracers. Furthermore, the use of these radiolabeled peptides for monitoring the efficacy and duration of antibiotic treatments is also proposed.

Venom fluids from venomous animals are complex mixtures of several hundreds of components, among which including a number of peptides reticulated or not by disulfide bridges, or sometimes posttranslationaly modified by for instance amidation or phosphorylation. Classically, they bind with high affinity and specificity to different target proteins such as enzymes, ion channels, and receptors. Consequently, they constitute useful and powerful tools for physiological, biochemical and pharmacological studies, supporting further progress in the understanding of the sophisticated relationships between the main biological molecular actors. Interestingly, several of these natural peptides are either the therapeutic molecules by themselves or they have inspired the design of synthetic chemical small molecule drugs. Thus the importance of performing an inventory of the existing natural molecular biodiversity is unquestionable. Classically, mass spectrometry analysis and/or precursors cloning followed by sequencing are the most frequently employed techniques. Also, several groups have successfully applied the next generation sequencing (NGS) strategies, initially used in genome elucidation, to perform exhaustive transcriptomic studies. Actually, T. Kubo's group, from Japan, described the identification of a large variety of venom bioactive peptides by sequencing of cDNA library clones isolated from the Chilean common tarantula *Grammostola rosea* venom gland. The cDNA sequences analysis of about 1,500 clones out of 4,000 clones allowed the identification of 48 novel toxin-like peptides (GTx1 to GTx7, and GTx-TCTP and GTx-CRISP), and among them 24 toxins are ICK motif peptides, 11 peptides are MIT1-like peptides, and 7 are ESTX-like peptides. Peptides similar to JZTX-64, aptotoxin, CRISP or TCTP were also described. Moreover, GTx-CRISP is the first CRISP-like protein identified from the arthropod venom, demonstrating once more the power of applying ESTs techniques to cDNA library to the discovery of novel peptide sequences with potential application in biomedicine.

Together, these articles composing this special issue papers provide to the readers a new and recent set of information on bioactive peptide studies, either in form of original papers or as concise review articles. The common motivation of these different publications is to illustrate the high therapeutic or diagnostic potential associated to the use of natural peptides, or to the design of new drugs inspired in the natural biodiversity of sequences and their wide biological roles.

Mirian A. F. Hayashi
Frédéric Ducancel
Katsuhiro Konno

Hindawi Publishing Corporation
International Journal of Peptides
Volume 2012, Article ID 249827, 7 pages
doi:10.1155/2012/249827

Review Article

A Meta-Analysis of the Therapeutic Effects of Glucagon-Like Peptide-1 Agonist in Heart Failure

Mohammed Munaf, Pierpaolo Pellicori, Victoria Allgar, and Kenneth Wong

Department of Cardiovascular and Respiratory Studies, Hull and East Yorkshire Medical Research and Teaching Centre, Daisy Building, Castle Hill Hospital, Castle Road, Kingston upon Hull HU16 5JQ, UK

Correspondence should be addressed to Kenneth Wong, kenneth.wong@hey.nhs.uk

Received 15 September 2011; Revised 8 March 2012; Accepted 9 March 2012

Academic Editor: Frédéric Ducancel

We conducted a meta-analysis of the existing literature of the therapeutic effects of using GLP-1 agonists to improve the metabolism of the failing heart. Animal studies showed significant improvement in markers of cardiac function, such as left ventricular ejection fraction (LVEF), with regular GLP-1 agonist infusions. In clinical trials, the potential effects of GLP-1 agonists in improving cardiac function were modest: LVEF improved by 4.4% compared to placebo (95% C.I 1.36–7.44, $P = 0.005$). However, BNP levels were not significantly altered by GLP-1 agonists in heart failure. In two trials, a modest increase in heart rate by up to 7 beats per minute was noted, but meta-analysis demonstrated this was not significant statistically. The small number of studies plus variation in the concentration and length of the regime between the trials would limit our conclusions, even though statistically, heterogeneity chi-squared tests did not reveal any significant heterogeneity in the endpoints tested. Moreover, studies in non-diabetics with heart failure yielded conflicting results. In conclusion, the use of GLP-1 agonists has at best a modest effect on ejection fraction improvement in heart failure, but there was no significant improvement in BNP levels in the meta-analysis.

1. Introduction

Heart failure (HF) is defined as "*a complex clinical syndrome that can result from any structural or functional cardiac disorder that impairs the ability of the ventricle to fill with or eject blood*" [1]. HF is a major public health issue, with a prevalence of over 5.8 million in the USA, and over 23 million (and rising) worldwide. The lifetime risk of developing HF is one in five [2]. Despite advances in treatment, the number of deaths from heart failure has increased steadily and only one quarter to one-third of people with heart failure survive 5 years after admission [3]. The cause of heart failure has shifted in the last two decades: in the late 1970s, rheumatic valvular disease was the primary cause, nowadays the leading cause is ischemic heart disease [4]. A deficit in the "pump" function as cause of signs or symptoms attributed to HF, or systolic dysfunction, is frequently well diagnosed due to widespread availability of echocardiography but, an increased left ventricular (LV) "stiffness," or diastolic dysfunction, is often missed. To further complicate matters, the two components—systolic and diastolic dysfunction—often coexist. Some studies [5, 6] reported that isolated diastolic dysfunction could be responsible for up to 50% of heart failure admissions (often labelled as "heart failure with normal ejection fraction," HFnEF), with a major impact on patient outcome. Moreover, in patients with impaired glucose tolerance, the extent of diastolic dysfunction seems to be more severe [7] and HFnEF seems to be more common in patients with a history of hypertension and/or diabetes [8, 9].

The standard treatment of systolic heart failure is currently angiotensin-converting enzyme (ACE) inhibitors, angiotensin II receptor blockers (ARBs), beta blockers, and aldosterone antagonists. These all improve prognosis of heart failure. However, there is no specific treatment for HFnEF: diuretics are often used for symptom control; digoxin is particularly beneficial for ventricular rate control when atrial fibrillation (AF) is the predominant rhythm.

In recent years, progress in basic research has led to the identification of multiple new possible therapeutic targets for the treatment of systolic heart failure, and many promising drugs have subsequently been developed. These include novel vasodilators, such as natriuretic peptides, metabolic substrates, urocortins, guanylyl cyclase activators, and adrenomedullin. They also include drugs such as direct renin inhibitors, and aldosterone synthase inhibitors [10]. There have been numerous large randomised controlled trials (RCT) of these new drugs. They have not yet been licensed as results regarding the efficacy of these new drugs have not been entirely positive. Further evidence is needed as many of the positive results that have been observed in preclinical studies and Phase II trials have not always been confirmed in Phase III studies [10].

As mentioned above, the leading cause of systolic HF is myocardial ischaemia, whereby the myocardium is oxygen starved and thus has a decreased ability to generate ATP by oxidative metabolism. As a result, it is unable to effectively transfer the chemical energy from the metabolism of carbon fuels to contractile work. This leads the myocardium to utilise other compounds, such as free fatty acids (FFAs), for energy production. However, if the heart uses FFAs as a substrate for energy generation, there is much greater oxygen consumption per unit ATP produced than there is with glucose. This increased demand for oxygen can lead to worsening heart failure. Thus, improvement of cardiac energetics is an important therapeutic target in patients with heart failure [10].

Metabolic modulators do exactly this by altering the substrate that is oxidized by the myocardium to derive energy. They shift this substrate from FFA to glucose and thus optimize metabolic efficiency of the heart. These compounds exert their effects through several mechanisms: inhibiting carnitine *O*-palmitoyltransferase 1, long-chain 3-ketoacyl-CoA thiolase or malonyl-CoA decarboxylase, reducing plasma levels of FFA and myocardial uptake of FFA, and/or activating the 5′-AMP-activated protein kinase (AMPK). Thus it follows that, using metabolic manipulating agents to either promote glucose utilisation or reduce fatty acid utilisation, will improve the metabolic efficiency of the heart by decreasing oxygen demand and thus be used therapeutically in heart failure. Amongst these metabolic agents are glucagon like peptide-1 (GLP-1) agonists [10].

GLP-1 is an incretin that is released from intestinal L cells in response to glucose ingestion and is known to be a potent glucose-dependent insulinotropic hormone. It has important actions on gastric motility, on the suppression of plasma glucagon levels, and possibly on the promotion of satiety and stimulation of glucose disposal in peripheral tissues independent of the actions of insulin. It does this by increasing insulin secretion from the pancreas and myocardial glucose uptake via the translocation of glucose-transporting vesicles (glucose transporter type 1 (GLUT1) and GLUT4) to the sarcolemma. GLP-1 exerts its direct cardioprotective effects through the stimulation of G-protein-coupled receptors (i.e., GLP1Rs) that are coupled to adenylyl cyclase, and via its rapid metabolism to the GLP1 (9–36) amide [11].

Therefore, GLP-1 agonists can be used to bring about the same effects. These agents have been investigated widely as an adjunct to therapy in diabetes as they offer an obvious alternative to insulin, but their metabolic effect could also be extended to the heart as they can enable the heart to switch to the more energy-efficient glucose-dependent pathway [10]. Moreover, there are GLP-1 specific receptors in cardiac tissue so the potential for using these peptide agonists holds promise for treating heart failure [12].

However, whilst GLP-1-related compounds have proven efficacy in the treatment of hyperglycaemia associated with type 2 diabetes [13, 14], little was known about the effectiveness of GLP-1 agonist or other peptides substrates in improving cardiac function in heart failure. Because the half-life of GLP-1 in only a few minutes, several Phase III-Phase IV trials are analysing the effects of its analogues, such as exenatide, which are not degraded so quickly [15].

2. Aims and Objectives

We aimed to carry out a comprehensive review of medical literature on the therapeutic advantage of using peptide agonists to improve cardiac metabolism in heart failure. We included all papers regardless of size, whether they were pre-clinical or clinical trials, either randomized, blinded, or not. The results of these papers have been combined to give an overall estimate of the effectiveness of using GLP-1 agonists in heart failure. Furthermore, we conducted a meta-analysis of each primary outcome if contained in more than two papers.

3. Methods

3.1. Search Strategy of the Meta-Analysis. Highly sensitive search strategies were developed using appropriate subject headings and text word terms. Full details of the search strategies used are appended. The following electronic databases were searched: the Cochrane Library (Issue 7, 2011); MEDLINE (via OVID, from 1948 to August week 1 2011); Pubmed (via NCBI); EMBASE (via OVID, from 1996 to week 30, 2011); BMJ's Clinical Evidence; DARE (Issue 7, 2011). British and American medical journals were also hand-searched, such as The Lancet, NEJM, and BMJ. In addition, conference proceedings and reference lists of all included studies were scanned to identify additionally potentially relevant studies. There were no start year or language restrictions.

3.2. Data Extraction. One reviewer screened the titles (and abstracts if available) of all reports identified by the search strategy. Full copies of potentially relevant reports were obtained, studied, and assessed for inclusion. Data was discussed with the senior author, and disagreements were resolved by consensus.

3.3. Selection Criteria. Papers that had details of trials conducted of peptide agonists versus placebo or usual treatment alone for heart failure were included. All papers, whether

they included human or animal trials were included. For humans, randomized controlled trials, regardless of whether they were blinded, were included along with pilot and observational studies.

3.4. Meta-Analysis Methodology

3.4.1. Data Synthesis. The eligible trials were entered into RevMan 5 software package, and the statistical methods were those programmed into RevMan 5.1 analysis software.

For continuous data, the mean difference and 95% confidence intervals were calculated. Where applicable, for dichotomous data, the relative risk and 95% confidence intervals would be calculated. The results from the trials were pooled using the fixed effects models. We tested for heterogeneity with the chi squared statistic, which was considered to be significant at $P < 0.10$. If significant, a random effect model would be used to allow generalisation of the results and sources of heterogeneity would be investigated. Z tests were used to test for the overall effect.

4. Results

A total of 16 papers were found in Medline and 32 in Embase. Handsearching in Pubmed yielded a further 22 papers. There were no Cochrane or DARE reviews of the use of GLP-1 agonist due to the scarcity of clinical trials on these agents and there were no additional papers found in American or British journals. The full references of the papers which contained studies are listed below in the references section.

The general finding from Medline, Embase, and Pubmed was that the papers that were found to mention GLP-1 agonists in HF, generally only detailed their pharmacology and suggested their potential for therapeutic benefit with very few containing any experimental evidence for the application of these agents [10–23]. When these papers containing studies were examined, they pertained to the use of GLP-1 agonists in diabetics with HF due to their insulinotropic effects instead of looking at their use as metabolic substrates for the ischaemic heart as has been suggested by some other papers. In the present paper, we only focused on papers that had experimental evidence for the use of GLP-1 agonists as therapeutic agents. These are discussed below.

4.1. Preclinical Experiments. Work on rats [24, 25], rabbits [26], mice [27], and dogs [28, 29] showed favourable functional effects of GLP-1 in failing hearts with significant improvements in LV systolic and diastolic function.

Nikolaidis et al. [28] found that short-term infusion of recombinant GLP-1 over 48 hours increased myocardial insulin sensitivity and glucose uptake in a canine model of rapid pacing-induced dilated cardiomyopathy. Interestingly, GLP-1 (9–36) was found to exert similar beneficial effects to native GLP-1 in this model, supporting the growing suggestion that the metabolically inactive form of GLP-1 [GLP-1 (9–36)] may play an active role in the cardiovascular system.

Furthermore, spontaneously hypertensive heart-failure-prone rats (characterized by obesity, insulin resistance, hypertension, and dilated cardiomyopathy), treated chronically with GLP-1 from 9 months of age (when they begin to progress to advanced heart failure and death) exhibited preserved cardiac contractile function, increased myocardial glucose uptake, improved survival, and a significant reduction in cardiac myocyte apoptosis [22]. Although this study also reported GLP-1 to stimulate myocardial glucose uptake in the failing myocardium, it was unclear whether its beneficial effects on contractile function occurred due to a direct cardiac action or was secondary to its established insulinotropic effects. These promising findings led the way for clinical trials and these are discussed below.

4.2. Clinical Trials. The beneficial effects on contractile function seen in animals treated with GLP-1 were supported by preliminary clinical studies in humans, indicating that GLP-1 may also improve LV contractile function in patients with chronic heart failure.

Thrainsdottir et al. [30], in an early nonrandomised pilot investigation conducted on 6 hospitalised type 2 diabetic hospitalised with ischaemic but stable heart failure New York Heart Association (NYHA) class II-III, with LVEF < 40%, found that short-term GLP-1 infusion for 3 days tended to improve both systolic and diastolic function, although these changes did not reach statistical significance.

However, we also found another three-day study that was conducted on 10 patients with acute myocardial infarction (AMI) or left ventricular ejection fraction (LVEF) of <40% compared with 11 controls [20]. Baseline demographics and background therapy were similar, and both groups had severe LV dysfunction at baseline (LVEF = 29 ± 2%). The study demonstrated that GLP-1 significantly improved LVEF (from 29 ± 2% to 39 ± 2%, $P \leq 0.01$), global wall motion score indexes (1.94 ± 0.11 → 1.63 ± 0.09, $P \leq 0.01$), and regional wall motion score indexes (2.53 ± 0.08 → 2.02 ± 0.11, $P \leq 0.01$) compared with control subjects. The benefits of GLP-1 were independent of AMI location or history of diabetes. Moreover, GLP-1 was well tolerated, with only transient gastrointestinal effects.

Moreover, longer-term treatment with GLP-1 has shown positive results in both diabetics and nondiabetics. Sokos and colleagues [31] compared a 5-week infusion of GLP-1 added to standard therapy in 12 patients with NYHA class III/IV heart failure and the results were compared with those of 9 patients with heart failure on standard therapy. They found that patients treated with GLP-1 infusion had significantly better LV systolic function (LVEF changed from 21 ± 3% to 27 ± 3% $P < 0.01$), exercise tolerance (VO_2 max changed from 10.8 ± .9 mL/O_2/min/kg to 13.9 ± .6 mL/O_2/min/kg; $P < 0.001$, as well as the 6-minute walk distance, from 232 ± 15 m to 286 ± 12 m; $P < 0.001$), and quality of life (Minnesota Living with Heart Failure quality of life score (MNQOL) score: from 64 ± 4 to 44 ± 5; $P < 0.01$). However, no significant changes in any of the parameters were observed in the control group on standard therapy. GLP-1

was well tolerated with minimal episodes of hypoglycaemia and gastrointestinal side effects. Like the aforementioned study [20], this study suggests a role for GLP-1 agonists beyond glycaemic control as significant improvements were seen in both diabetic and nondiabetic patients.

However, we found no further evidence for the extension of GLP-1 to nondiabetics. In a randomized, double-blind crossover trial of 20 normoglycaemic patients without diabetes and with HF with ischemic heart disease, severe left ventricular impairment, NYHA II, and III, Halbirk et al. [32] found that GLP-1 infusion over 48 h increased circulating insulin levels and reduced plasma glucose concentration but had no major cardiovascular effects in patients with chronic heart failure when compared with a placebo. The only significant cardiovascular impacts of the infusion were increases in heart rate (67 ± 2 beats/min versus 65 ± 2 beats/min; $P = 0.016$) and diastolic blood pressure (71 ± 2 mmHg versus 68 ± 2 mmHg; $P = 0.008$). GLP-1 had no effect on systolic blood pressure (113 ± 5 mmHg versus 113 ± 4 mmHg; $P = 0.95$) or on LVEF (GLP-1 treatment from 28 ± 2% to 30 ± 2% versus placebo 30 ± 2% to 30 ± 2%; $P = 0.93$). Importantly, also, GLP-1 infusion did not affect exercise capacity, VO_2 max, cardiac index, stroke volume, and systemic vascular resistance during exercise. Unlike other studies, hypoglycemia was frequent with eight patients experiencing nine episodes of hypoglycaemia (capillary glucose < 3.5 mmol/L) versus none with placebo. This calls for caution in patients without diabetes but with HF and also reiterates the need for further studies with regard to the use of GLP-1 agonists in nondiabetics. Intriguingly, both GLP-1 and placebo significantly dropped BNP, although the effects of the two infusions did not differ (−112 ± 54 pg/mL versus −65 ± 54 pg/mL, $P = 0.17$). Future trials looking at changes in BNP in heart failure should bear in mind that small changes need to be interpreted with caution, as it was intriguing that placebo might have produced a significant reduction in BNP. The authors of that paper attributed this drop in natriuretic peptide to be due to patients' reduced exercise during their hospital stay, more than a direct effect of the infusion. However, a recent study conducted in healthy subjects found exenatide had significant haemodynamic effects, including natriuretic properties [33].

4.3. Meta-Analysis. Individually, some of the studies that we have discussed would suggest that GLP-1 agonist might be potentially effective for heart failure. We performed a meta-analysis on all the primary endpoints that were contained in at least two papers. The results were summarised in Table 1, and Figures 1, 2, and 3.

There was at best a modest improvement in ejection fraction (4.4%; 95% CI 1.36–7.44%). There was no significant change in BNP or heart rate in our meta-analysis. Thus, although some of the preliminary clinical studies provided some encouragement for the potential use of GLP-1 in the treatment of heart failure, it is clear that significant further research is required to confirm these initial observations, investigate the underlying mechanisms, and explore possible interactions with current heart failure therapies.

Table 1: Summary of all trials studying GLP-1 effects in human heart failure.

Study	Endpoints
Thrainsdottir et al., 2004 [30]	HR, BP (rest + exercise), rate pressure product, global systolic and diastolic function, LVEF, LV end-diastolic diameter
Nikolaidis et al., 2004 [20]	LVEF, ED +ESV, SV, global WMSI
Sokos et al., 2006 [31]	HR, BNP, LVEF, VO_2, 6-min walk
Halbirk et al., 2010 [32]	BNP, BP, HR, SV, CI, LVEF, SVR, 6 min hall walk test

4.4. Limitations of Meta-Analysis. As with any meta-analysis, the quality is dependent on the quality of the studies and any limitations the included studies have. Firstly, the most obvious limitation is the lack of a large number of studies available to meta-analyse. Secondly, the total sample size of patients in all four studies combined is small. A further limitation in our meta-analysis is that all four studies investigated different concentrations of GLP-1 agonist infusion: 1.0 pmol/kg/min (Halbirk); 1.5 pmol/kg/min (Nikolaidis); 2.5 pmol/kg/min (Sokos) and 4 pmol/kg/min (Thrainsdottir). Moreover, the studies measured improvements at different intervals of time, with Halbirk looking at effects after 48 hours, Thrainsdottir and Nikkolaidis at 3 days and Sokos investigating a 5-week infusion. This has definite implications for interpretation of the results. Another limitation was that not all the studies included were double blinded and randomised, for example, Thrainsdottir was an open observation study, whereas Halbirk was a double-blinded crossover placebo study. This leads to methodological heterogeneity.

4.5. Clinical Implications and Future Research. The Carvedilol Hibernating Reversible Ischaemia Trial: Marker of Success (CHRISTMAS trial) [34] found patients with more hibernation/ischaemia had greater improvement in left ventricular systolic function with beta-blocker treatment. Our Academic Cardiology Department in Hull also conducted the Heart Failure Revascularisation Trial which showed how myocardial ischaemia and hibernation could not effectively be resuscitated by revascularization in patients with chronic HF [35]. Recently, the large STITCH trial [36] did not demonstrate any survival benefit of coronary artery bypass surgery in patients with heart failure with severe coronary artery disease. Thus, to optimally treat ischaemic heart failure, we need to explore other avenues to improve myocardial metabolism, to try and optimize cardiac function.

GLP-1 is an endogenous peptide which is released from the gut following food intake. It is one of a number of factors that can augment insulin release, so as expected, its role in improving glycaemic control in diabetics is now fairly well established.

Our meta-analysis of clinical trials involving patients with heart failure demonstrated some promising evidence to suggest possible beneficial effects of the GLP-1 peptide agonist in improving cardiac function, in both diabetics and

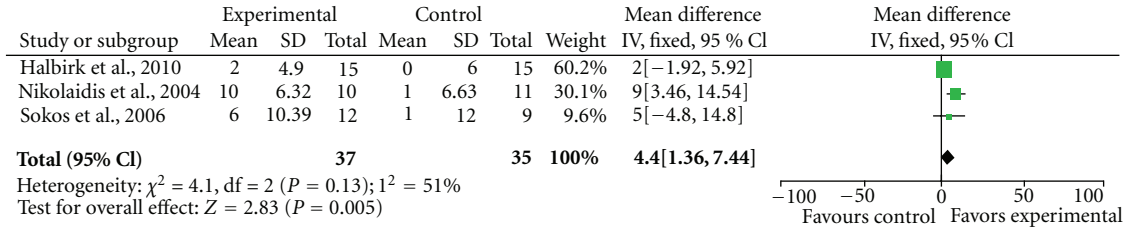

Figure 1: Forrest plot demonstrating GLP-1 improves ejection fraction.

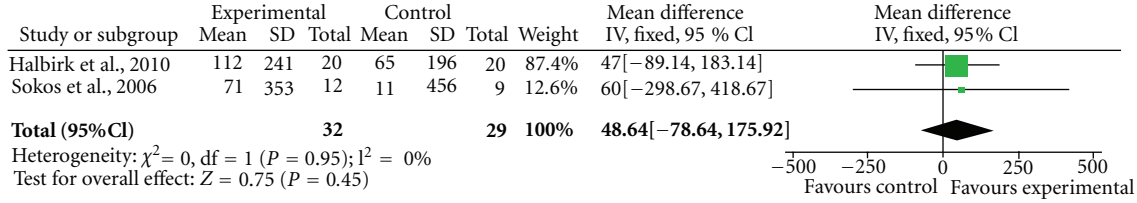

Figure 2: Forrest plot demonstrating the negligible effect of GLP-1 on BNP levels.

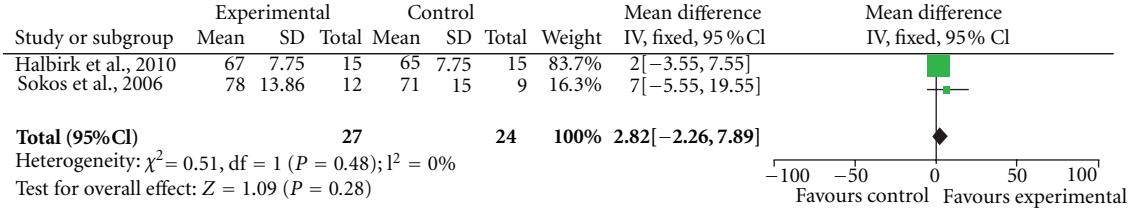

Figure 3: Forrest plot demonstrating the effect of GLP-1 agonist on heart rate.

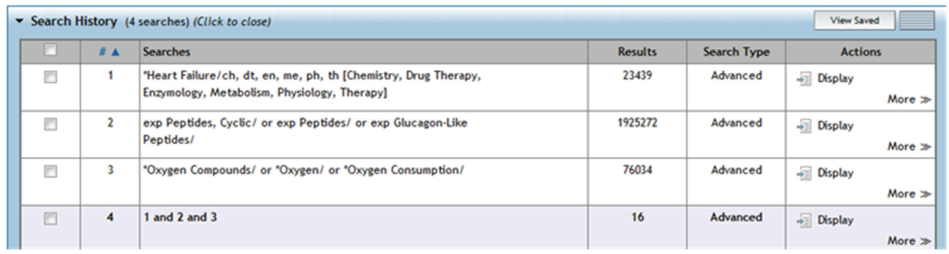

Figure 4: Full Medline search with MeSH terms.

nondiabetics. This was seen with the statistically significant increase in left ventricular ejection fraction, although the absolute change was very modest (4.4%). An absence of lowering effect on systolic blood pressure may be particularly appealing to clinicians who find their patients with heart failure often have relatively low blood pressure on a combination of ACE-inhibitors, beta blockers, spironolactone or eplerenone, and loop diuretics. It should be noted that the drug might drop patients' diastolic blood pressure.

Minor increase in heart rate may also turn out to be a concern as recent evidence have confirmed the hypothesis that patients with heart failure have better prognosis if their heart rate is less than 70 beats per minute [37]. However, whilst in the two individual trials (Halbirk and Sokos), there was a modest increase in heart rate by up to 7 beats per minute, our meta-analysis demonstrated this was not significant statistically. In nondiabetics with heart failure, caution must be exercised to ensure they do not develop hypoglycaemia, which again is potentially hazardous.

Before the peptide agonist can be recommended for routine clinical use, large multicentre, double-blinded randomised controlled trials are needed, investigating the effects of GLP-1 or its analogue in patients with acute or chronic HF including hard endpoints, such as mortality, cardiovascular death, or hospitalization for heart failure. Further, as suggested previously, heart failure with normal ejection fraction (HFnEF) is often difficult to treat specifically. Future trials should study the effect of GLP-1 agonists in this challenging group of patients. Recent work suggested that advanced echocardiography techniques using speckle tracking to assess

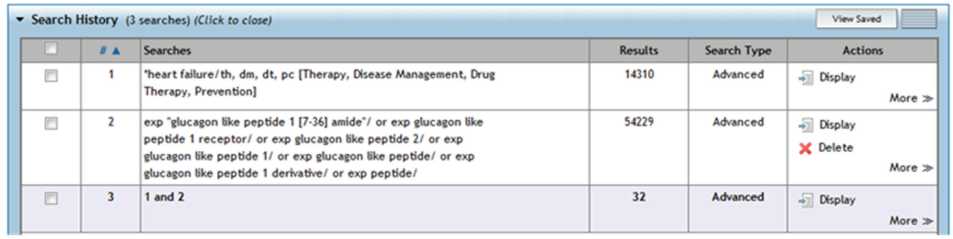

Figure 5: Full Embase search with MeSH terms.

the so-called global longitudinal strain (GLS) might identify patients with subtle systolic dysfunction [38] and might even be better than ejection fraction at predicting poor cardiovascular outcome in patients with chronic heart failure [39].

5. Conclusions

This meta-analysis of the potential therapeutic benefits of GLP-1 agonists in heart failure involved a thorough literature search using Embase and Medline plus hand-search strategies. The animal studies gave evidence in favour of these peptide agonists. There were only a few small clinical trials involving patients with heart failure. The use of GLP-1 agonists has at best a modest effect on ejection fraction improvement in patients with heart failure, but there was no significant improvement in BNP levels in the meta-analysis.

Appendix

Medline Search Strategy. The search focused on heart failure, mapped to subject headings, and included the following MESH terms: chemistry, drug therapy, enzymology, metabolism, physiology, and therapy.

The second search term was for peptide and this term was again mapped to include medical subject headings. From this the following mesh terms were exploded: Glucagon-like peptides; peptides and peptides, cyclic.

The third search term was oxygen, including oxygen compounds, oxygen, and oxygen consumption as these were central to our review.

The fourth search item combined the above three and produced 16 papers.

The full search is shown in Figure 4.

Embase Search Strategy. For Embase, again heart failure was the first search term, including disease management, drug therapy, prevention, and therapy.

The second search term was for peptide and all the similar MeSH including "glucagon like peptides" were selected. All these were exploded so similar terms could be included.

The third search combined the previous two searches with "AND," thus returning 32 results: see Figure 5.

Hand-Searching. Pubmed yielded a further 22 papers. Of these, only three papers contained results of studies done on humans. These, along with the papers found with Medline and Embase, were cited fully in the references section. There were no additional papers found in the medical journals that were hand-searched (BMJ, Lancet, NEJM).

References

[1] S. A. Hunt, D. W. Baker, M. H. Chin et al., "ACC/AHA guidelines for the evaluation and management of chronic heart failure in the adult: executive summary. A report of the American college of cardiology/American heart association task force on practice guidelines (committee to revise the 1995 guidelines for the evaluation and management of heart failure): developed in collaboration with the international society for heart and lung transplantation; endorsed by the heart failure society of America," *Circulation*, vol. 104, no. 24, pp. 2996–3007, 2001.

[2] A. L. Bui, T. B. Horwich, and G. C. Fonarow, "Epidemiology and risk profile of heart failure," *Nature Reviews Cardiology*, vol. 8, no. 1, pp. 30–41, 2011.

[3] J. J. V. McMurray and S. Stewart, "The burden of heart failure," *European Heart Journal*, vol. 4, supplement D, pp. D50–D58, 2002.

[4] J. G. Cleland, A. Torabi, and N. K. Khan, "Epidemiology and management of heart failure and left ventricular systolic dysfunction in the aftermath of a myocardial infarction," *Heart*, vol. 91, supplement 2, pp. ii7–ii13, ii31–ii43, 2005.

[5] K. Hogg, K. Swedberg, and J. McMurray, "Heart failure with preserved left ventricular systolic function: epidemiology, clinical characteristics, and prognosis," *Journal of the American College of Cardiology*, vol. 43, no. 3, pp. 317–327, 2004.

[6] J. G. F. Cleland, T. McDonagh, A. S. Rigby, A. Yassin, T. Whittaker, and H. J. Dargie, "The national heart failure audit for England and Wales 2008-2009," *Heart*, vol. 97, no. 11, pp. 876–886, 2011.

[7] A. M. Salmasi, P. Frost, and M. Dancy, "Left ventricular diastolic function in normotensive subjects 2 months after acute myocardial infarction is related to glucose intolerance," *American Heart Journal*, vol. 150, no. 1, pp. 168–174, 2005.

[8] T. Tsujino, D. Kawasaki, and T. Masuyama, "Left ventricular diastolic dysfunction in diabetic patients: pathophysiology and therapeutic implications," *American Journal of Cardiovascular Drugs*, vol. 6, no. 4, pp. 219–230, 2006.

[9] M. Fujita, H. Asanuma, J. Kim et al., "Impaired glucose tolerance: a possible contributor to left ventricular hypertrophy and diastolic dysfunction," *International Journal of Cardiology*, vol. 118, no. 1, pp. 76–80, 2007.

[10] J. Tamargo and J. Löpez-Sendón, "Novel therapeutic targets for the treatment of heart failure," *Nature Reviews Drug Discovery*, vol. 10, no. 7, pp. 536–555, 2011.

[11] T. J. Kieffer and J. F. Habener, "The glucagon-like peptides," *Endocrine Reviews*, vol. 20, no. 6, pp. 876–913, 1999.

[12] C. Saraceni and T. L. Broderick, "Effects of glucagon-like peptide-1 and long-acting analogues on cardiovascular and metabolic function," *Drugs in R and D*, vol. 8, no. 3, pp. 145–153, 2007.

[13] M. B. Toft-Nielsen, S. Madsbad, and J. J. Holst, "Determinants of the effectiveness of glucagon-like peptide-1 in type 2 diabetes," *Journal of Clinical Endocrinology and Metabolism*, vol. 86, no. 8, pp. 3853–3860, 2001.

[14] J. J. Meier, D. Weyhe, M. Michaely et al., "Intravenous glucagon-like peptide 1 normalizes blood glucose after major surgery in patients with type 2 diabetes," *Critical Care Medicine*, vol. 32, no. 3, pp. 848–851, 2004.

[15] M. Monami, F. Cremasco, C. Lamanna et al., "Glucagon-like peptide-1 receptor agonists and cardiovascular events: a meta-analysis of randomized clinical trials," *Experimental Diabetes Research*, vol. 2011, Article ID 215764, 2011.

[16] W. C. Stanley, F. A. Recchia, and G. D. Lopaschuk, "Myocardial substrate metabolism in the normal and failing heart," *Physiological Reviews*, vol. 85, no. 3, pp. 1093–1129, 2005.

[17] M. F. Essop and L. H. Opie, "Metabolic therapy for heart failure," *European Heart Journal*, vol. 25, no. 20, pp. 1765–1768, 2004.

[18] H. Taegtmeyer, "Cardiac metabolism as a target for the treatment of heart failure," *Circulation*, vol. 110, no. 8, pp. 894–896, 2004.

[19] D. J. Grieve, R. S. Cassidy, and B. D. Green, "Emerging cardiovascular actions of the incretin hormone glucagon-like peptide-1: potential therapeutic benefits beyond glycaemic control?" *British Journal of Pharmacology*, vol. 157, no. 8, pp. 1340–1351, 2009.

[20] L. A. Nikolaidis, S. Mankad, G. G. Sokos et al., "Effects of glucagon-like peptide-1 in patients with acute myocardial infarction and left ventricular dysfunction after successful reperfusion," *Circulation*, vol. 109, no. 8, pp. 962–965, 2004.

[21] K. Ban, M. H. Noyan-Ashraf, J. Hoefer, S. S. Bolz, D. J. Drucker, and M. Husain, "Cardioprotective and vasodilatory actions of glucagon-like peptide 1 receptor are mediated through both glucagon-like peptide 1 receptor-dependent and -independent pathways," *Circulation*, vol. 117, no. 18, pp. 2340–2350, 2008.

[22] E. Mannucci and C. M. Rotella, "Future perspectives on glucagon-like peptide-1, diabetes and cardiovascular risk," *Nutrition, Metabolism and Cardiovascular Diseases*, vol. 18, no. 9, pp. 639–645, 2008.

[23] A. K. Bose, M. M. Mocanu, R. D. Carr, C. L. Brand, and D. M. Yellon, "Glucagon-like peptide 1 can directly protect the heart against ischemia/reperfusion injury," *Diabetes*, vol. 54, no. 1, pp. 146–151, 2005.

[24] I. Poornima, S. B. Brown, S. Bhashyam, P. Parikh, H. Bolukoglu, and R. P. Shannon, "Chronic glucagon-like peptide-1 infusion sustains left ventricular systolic function and prolongs survival in the spontaneously hypertensive, heart failure-prone rat," *Circulation*, vol. 1, no. 3, pp. 153–160, 2008.

[25] T. Zhao, P. Parikh, S. Bhashyam et al., "Direct effects of glucagon-like peptide-1 on myocardial contractility and glucose uptake in normal and postischemic isolated rat hearts," *Journal of Pharmacology and Experimental Therapeutics*, vol. 317, no. 3, pp. 1106–1113, 2006.

[26] M. Matsubara, S. Kanemoto, B. G. Leshnower et al., "Single dose GLP-1-tf ameliorates myocardial ischemia/reperfusion injury," *Journal of Surgical Research*, vol. 165, no. 1, pp. 38–45, 2011.

[27] M. H. Noyan-Ashraf, M. Abdul Momen, K. Ban et al., "GLP-1R agonist liraglutide activates cytoprotective pathways and improves outcomes after experimental myocardial infarction in mice," *Diabetes*, vol. 58, no. 4, pp. 975–983, 2009.

[28] L. A. Nikolaidis, D. Elahi, T. Hentosz et al., "Recombinant glucagon-like peptide-1 increases myocardial glucose uptake and improves left ventricular performance in conscious dogs with pacing-induced dilated cardiomyopathy," *Circulation*, vol. 110, no. 8, pp. 955–961, 2004.

[29] L. A. Nikolaidis, D. Elahi, Y. T. Shen, and R. P. Shannon, "Active metabolite of GLP-1 mediates myocardial glucose uptake and improves left ventricular performance in conscious dogs with dilated cardiomyopathy," *American Journal of Physiology-Heart and Circulatory Physiology*, vol. 289, no. 6, pp. H2401–H2408, 2005.

[30] I. Thrainsdottir, K. Malmberg, A. Olsson, M. Gutniak, and L. Rydén, "Initial experience with GLP-1 treatment on metabolic control and myocardial function in patients with type 2 diabetes mellitus and heart failure," *Diabetes & Vascular Disease Research*, vol. 1, no. 1, pp. 40–43, 2004.

[31] G. G. Sokos, L. A. Nikolaidis, S. Mankad, D. Elahi, and R. P. Shannon, "Glucagon-Like Peptide-1 Infusion Improves Left Ventricular Ejection Fraction and Functional Status in Patients With Chronic Heart Failure," *Journal of Cardiac Failure*, vol. 12, no. 9, pp. 694–699, 2006.

[32] M. Halbirk, H. Nørrelund, N. Møller et al., "Cardiovascular and metabolic effects of 48-h glucagon-like peptide-1 infusion in compensated chronic patients with heart failure," *American Journal of Physiology-Heart and Circulatory Physiology*, vol. 298, no. 3, pp. H1096–H1102, 2010.

[33] B. Mendis, E. Simpson, I. Macdonald, and P. Mansell, "Investigation of the haemodynamic effects of exenatide in healthy male subjects," *British Journal of Clinical Pharmacology*. In press.

[34] J. G. Cleland, D. J. Pennell, S. G. Ray et al., "Carvedilol hibernating reversible ischaemia trial: marker of success investigators. Myocardial viability as a determinant of the ejection fraction response to carvedilol in patients with heart failure (CHRISTMAS trial): randomised controlled trial," *The Lancet*, vol. 362, no. 9377, pp. 14–21, 2003.

[35] A. P. Coletta, J. G. F. Cleland, D. Cullington, and A. L. Clark, "Clinical trials update from heart rhythm 2008 and heart failure 2008: ATHENA, URGENT, INH study, HEART and CK-1827452," *European Journal of Heart Failure*, vol. 10, no. 9, pp. 917–920, 2008.

[36] E. J. Velazquez, K. L. Lee, M. A. Deja et al., "Coronary-artery bypass surgery in patients with left ventricular dysfunction," *The New England Journal of Medicine*, vol. 364, no. 17, pp. 1607–1616, 2011.

[37] K. Fox, I. Ford, P.G. Steg, M. Tendera, M. Robertson, and R. Ferrari, "On behalf of the BEAUTIFUL investigators/Heart rate as a prognostic risk factor in patients with coronary artery disease and left-ventricular systolic dysfunction (BEAUTIFUL): a subgroup analysis of a randomised controlled trial," *The Lancet*, vol. 372, no. 9641, pp. 817–821, 2008.

[38] M. Galderisi, V. S. Lomoriello, A. Santoro et al., "Differences of myocardial systolic deformation and correlates of diastolic function in competitive rowers and young hypertensives: a speckle-tracking echocardiography study," *Journal of the American Society of Echocardiography*, vol. 23, no. 11, pp. 1190–1198, 2010.

[39] J. Nahum, A. Bensaid, C. Dussault et al., "Impact of longitudinal myocardial deformation on the prognosis of chronic heart failure patients," *Circulation Cardiovascular Imaging*, vol. 3, no. 3, pp. 249–256, 2010.

Hindawi Publishing Corporation
International Journal of Peptides
Volume 2012, Article ID 965238, 19 pages
doi:10.1155/2012/965238

Review Article

Antimicrobial Peptides as Infection Imaging Agents: Better Than Radiolabeled Antibiotics

Muammad Saeed Akhtar, Muhammad Babar Imran, Muhammad Afzal Nadeem, and Abubaker Shahid

Nuclear Medicine Division, Punjab Institute of Nuclear Medicine (PINUM), Faisalabad 38000, Pakistan

Correspondence should be addressed to Muammad Saeed Akhtar, saeed_pinum@yahoo.com

Received 8 December 2011; Revised 9 February 2012; Accepted 11 March 2012

Academic Editor: Mirian A. F. Hayashi

Nuclear medicine imaging techniques offer whole body imaging for localization of number and site of infective foci inspite of limitation of spatial resolution. The innate human immune system contains a large member of important elements including antimicrobial peptides to combat any form of infection. However, development of antibiotics against bacteria progressed rapidly and gained popularity over antimicrobial peptides but even powerful antimicrobials failed to reduce morbidity and mortality due to emergence of mutant strains of bacteria resulting in antimicrobial resistance. Differentiation between infection and inflammation using radiolabeled compounds with nuclear medicine techniques has always been a dilemma which is still to be resolved. Starting from nonspecific tracers to specific radiolabeled tracers, the question is still unanswered. Specific radiolabeled tracers included antibiotics and antimicrobial peptides which bind directly to the bacteria for efficient localization with advanced nuclear medicine equipments. However, there are merits and demerits attributed to each. In the current paper, radiolabeled antibiotics and radiolabeled peptides for infection localization have been discussed starting with the background of primitive nonspecific tracers. Radiolabeled antimicrobial peptides have certain merits compared with labeled antibiotics which make them superior agents for localization of infective focus.

1. General Introduction

Blood-derived antimicrobial proteins and peptides being part of innate immunity target the microbial membranes leading to growth arrest and, in some instants, neutralization of proinflammatory surface components like lipopolysaccharides. Different inflammatory response blood cells like neutrophils, eosinophils, macrophages, and platelets contain antimicrobial proteins and peptides which have affinity for surface lipids of microbial as opposed to eukaryotic cells. Neutrophils contain primary and secondary granules in their cytoplasm which contain antimicrobial proteins and peptides. Lactoferrin is localized in the secondary granules, which has direct microbicidal effect, presumably via membrane disruption. Activated neutrophils release bactericidal/permeability increasing protein (BPI) into inflammatory fluids where it is potentially bactericidal. Serprocidins are proteases with cytotoxic activity localized in neutrophil primary granules. Cathelicidins are also antimicrobial peptides within secondary granules of neutrophils. The defensins are a family of 4-Kd peptides with broad cytotoxic activity against bacteria, fungi, parasites, viruses, and host cells. Humans express α-defensins in neutrophils and β-defensins in intestinal Paneth cell, as well as pulmonary and reproductive epithelia. The defensins peptides, calprotectin protein, and ubiquicidin cationic peptides are found in macrophages [1]. Platelet α-grounds contain certain cationic antimicrobial peptides having broad spectrum antimicrobial activity [2]. Multiple proteins and peptides have been radiolabelled by multiple investigators for specific localization of infection foci but each had certain demerits. More attention diverted to development of new antibiotics followed by radiolabeling but these face the growing problem of microbial resistance.

Differentiation between infection and inflammation is usually difficult. Clinicians use a variety of clues, for example, clinical, laboratory, and radiological tests, to aid in diagnosis

and influence decision making. Commonly employed and useful modalities for demonstration of any focal lesion include conventional radiological techniques such as X-ray, ultrasound, computerized tomography (CT), magnetic resonance imaging (MRI), which demonstrate structural abnormalities which take some time to become visible, may not always be present, and their resolution lag behind cure. In addition they are neither inflammation nor infection specific. Nuclear medicine has enhanced infection imaging because it depends on the demonstration of pathophysiological and pathological changes, which occur earlier in infection process and also resolve quicker after cure of the infection compared with gross changes in structure [3]. Scintigraphic imaging of inflammation can be achieved in two ways. The first is to utilize the locally enhanced vascular permeability by injecting radiolabelled molecules that show increased extravasation at the site of infection/inflammation. The alternative is to exploit the diapedesis and chemotaxis of leucocytes, either by radiolabelling white blood cells of the patients *ex vivo* or by directly targeting leukocyte antigens or receptors *in vivo* via administration of radiolabelled antigranulocyte monoclonal antibodies on receptor-binding ligands [4]. However, nuclear medicine utilizes radiation and must be used as a diagnostic modality in cases where other nonisotopic and noninvasive techniques fail to achieve the target.

Scintigraphy has the advantage of early elucidation of pathophysiological changes in the infective process; however, it is limited by poor resolution. Recent advances in nuclear medicine technology resulted in commercially available instrumentation such as single-photon emission computed tomography (SPECT) and positron emission tomography (PET) that have markedly improved anatomical details. Autologous *in vitro* ^{111}In-oxinate- or ^{99m}Tc-HMPAO-labeled leukocytes are still the gold standard for imaging infections [5–7]. Planar images with gamma cameras are handicapped with limited resolution that is not sufficient for assessing the extent of disease. SPECT increases the sensitivity of the nuclear medicine procedures [8, 9], but precise anatomical localization of organs is still not possible. Hybrid SPECT/CT improves the diagnostic accuracy when subjected to ^{99m}Tc-HMPAO-labeled leukocytes in patients with suspected osteomyelitis [10]. Marked improvement in sensitivity and definition of the extent of infection has been documented with SPECT/CT using ^{67}Ga- and ^{111}In-labeled leukocytes [11]. PET/CT with ^{18}F-FDG-labeled autologous leukocytes has further improved the diagnosis and localization of infection lesions [12]; however, the technique is time consuming, demands a sterile environment, and carries the risk of transmission of blood-borne diseases. Antimicrobial compounds that bind to the bacteria would be specific for infection localization if labeled with a suitable isotope because of their selective adhesion to the causative agents [3]. An early antibiotic radiopharmaceutical was ^{99m}Tc-ciprofloxacin, which is an analog of a broad-spectrum quinolone antibiotic having the property of binding to DNA gyrase of bacteria and inhibiting DNA synthesis [13]. This ^{99m}Tc agent showed encouraging results in various infections [14–16]; however, specificity was lower than expected, and its accumulation in noninfectious/inflammatory sites has also been reported [17]. Due to nonspecific accumulation in inflammatory sites, this agent has been proposed for identifying the presence and distribution of inflammation within joints [18]. Bacterial resistance to ciprofloxacin is another disadvantage, which results in false-negative results [19].

Antimicrobial peptides, produced by phagocytes, epithelial cells, endothelial cells, and many other cell types, are an important component of innate immunity against infection by a variety of pathogens [20]. These peptides show antibacterial, antiviral, and antifungal activities *in vitro.* Bacterial infections with *Staphylococcus aureus* and *Klebsiella pneumoniae* have been visualized in mice by ^{99m}Tc-labeled human neutrophil peptide-1 [21]. The basis of the antimicrobial activity of these peptides is the interaction of the cationic domains with the negatively charged surface of the microorganisms. The antimicrobial peptide ubiquicidin UBI (29–41) (TGRAKRRMQYNRR; 1,693 Da) was originally isolated from mouse macrophage cells. This peptide is identical or highly homologous to S30, a protein that was purified from the small ribosomal subunit fraction of rat liver and shown to be present in various human and murine tissues [22]. Later, an identical UBI was isolated from human airway epithelial cells. This peptide was labeled with ^{99m}Tc, which targeted bacterial cells but not sterile inflammatory processes in experimental animals [23]. In later experiments, it also showed accumulation with high accuracy in fungal infections. This tracer was also used for detection of *Staphylococcus aureus* infections in mice and *Klebsiella pneumoniae* in rabbits. As controls, inflammation was produced by lipopolysaccharides (LPSs) and heat-killed microorganisms [24]. Interactions of cationic peptides with bacterial envelopes involve insertion of the peptide into microbial membranes [25] and possibly a sequence-dependent interaction of the antimicrobial peptides with microorganisms [26]. Multiple animal studies using ^{99m}Tc-labeled ubiquicidin (29–41) showed encouraging results for differentiation between infection and inflammation model. ^{99m}Tc-UBI (29–41) scintigraphy showed more accumulation of tracer in *Staphylococcus-aureus*-induced infection compared with that of *Escherichia coli* infection model. Optimum time for imaging was 60 min after tracer injection [27]. In another study with this radiolabelled peptide, it was concluded that its accumulation is directly related to viable number of bacteria as tracer accumulation in infective foci declined after administration of ciprofloxacin which reduced the number of bacteria sensitive to this antibiotic. However, serial imaging with ^{99m}Tc-UBI can be utilized for monitoring efficacy and direction of antibiotic treatment [28]. Use of radiolabeled antimicrobial peptides is only recommended in cases where physician or surgeon is in dilemma to differentiate infection from inflammation. This would avoid blind use of prophylactic antibiotics or as broad spectrum coverage of infection, which results in heavy expenditure and side effects of unnecessary medicines.

Phase-I clinical trial with this novel radiolabelled peptide showed overall sensitivity, specificity, and accuracy of 100%, 80%, and 94.4%, respectively, in patients with soft tissue infections and osteomyelitis. However, optimum time for imaging was 30 min after intravenous administration of radiotracer [29].

2. Detection of Infection by Nonspecific Tracers

2.1. Gallium-67-Citrate. The oldest radiopharmaceutical proposed for imaging inflammation is Gallium-67 citrate which has been used for infection and inflammation ever since its discovery in 1971 [30]. ^{67}Ga is a cyclotron-produced radionuclide, with a half-life of 78 hours, emits a broad spectrum of gamma rays between 93 keV and 880 keV. The energy peaks that are most suitable for gamma camera imaging are 93 keV, 184 keV, 296 keV, and 388 keV [31]. After intravenous injection, ^{67}Ga binds to transferrin. This complex extravasates at the site of inflammation due to the locally enhanced vascular permeability, and in the inflammatory lesion it may transchelate to lactoferrin as present in leukocytes. The B-lymphocytes have lactoferrin-binding sites on their surface, which have high affinity for gallium. Additionally, macrophages engulf protein iron complexes and cellular debris, thereby accumulating gallium. Bacteria and fungi contain siderophores which are released for the purpose of scavenging iron and consequently bind gallium as a gallium-siderophore complex [32]. The agent is excreted partly via the kidneys (especially during the first 24 hours after injection) and via the gastrointestinal tract; therefore colon is the target organ. Oral laxatives to reduce bowel activity and to reduce dose to large bowel are not required [33, 34]. Physiological uptake of the radiolabel also occurs in liver, bone, bone marrow, salivary glands, nasopharynx, and lacrimal glands. For infection or inflammation, imaging can often be accomplished at 48 hours, or even 24 hours, after injection. Planar imaging is performed in the anterior and posterior projection, to include the head, neck, chest, abdomen, pelvis, and proximal extremities. SPECT imaging is performed at 72 hours, which improves the sensitivity and specificity. Most patients exhibit bowel activity at this time; therefore planar and SPECT imaging of abdomen can be performed at 5–7 days after injection. Inspite of SPECT imaging, there are low spatial resolution and the lack of anatomic landmarks of scintigraphy [35].

Although ^{67}Ga-citrate scintigraphy has high sensitivity for both acute and chronic infection and noninfectious inflammation, there are several shortcomings that limit its clinical application. The specificity of the technique is low, due to physiological bowel excretion and accumulation in malignant tissues and areas of bone remodeling. In addition, the radiopharmaceutical has unfavorable imaging characteristics (long physical half-life and high energy gamma radiations), causing high radiation-absorbed doses. Furthermore, optimal imaging often requires delayed recordings up to 72 hours. These unfavorable characteristics, in combination with the development of newer radiopharmaceuticals, have narrowed the clinical indication for gallium scintigraphy to certain conditions such as lung infections and chronic osteomyelitis. The sensitivity and specificity for chronic osteomyelitis are lower than for acute osteomyelitis [36, 37]. Use of SPECT/CT with ^{67}Ga improves diagnostic efficiency as compared with planar or SPECT scanning [11]. Gallium scan is most often used in patients with fever of known origin (FUO), suspected vertebral osteomyelitis, chronic osteomyelitis, pulmonary/mediastinal infections, tuberculosis, sarcoidosis, and retroperitoneal fibrosis. This agent is also valuable for evaluation and followup of drug-induced pulmonary toxic agents like bleomycin and amiodarone. Immunocompromised and neutropenic patients are also candidates for evaluation with gallium scanning [38].

2.2. Nonspecific Immunoglobulins. Initially it was hypothesized that human polyclonal immunoglobulin (HIG) was retained in infectious foci owing to the interaction with Fc-ϒ receptors as expressed on infiltrating leucocytes [39]. Later studies showed that radiolabelled HIG accumulates in infectious foci by nonspecific extravasation due the locally enhanced vascular permeability [40]. For clinical use, HIG has been labeled with ^{111}In-oxinate as well as with ^{99m}Tc. Both agents have slow blood clearance and physiological uptake in the liver, the spleen, and the kidneys. The ^{99m}Tc-labeled preparation has the known ideal radiation characteristics, while the ^{111}In-labeled preparation allows imaging at time points beyond 24 hours after injection. ^{111}In-oxinate or ^{99m}Tc-labeled HIG has been extensively tested in a large number of clinical studies. It has shown excellent performance in the localization of musculoskeletal infection and inflammation [41]. In addition, good results have been reported in pulmonary infection particularly in immunocompromised patients [42] and abdominal inflammation. A general limitation is the long time span between injection and final diagnosis (24–48 hours) [43, 44].

2.3. Liposomes. Liposomes are spheres consisting of one or more lipid bilayers surrounding an aqueous space. They were proposed as vehicles to image infection some 20 years ago, but the preparations used in those early years were cleared from the circulation very rapidly by the mononuclear phagocyte system (MPS). However, if the surface of the liposomes is coated with a hydrophilic polymer such as polyethylene glycol (PEG), they circumvent recognition by the MPS, leading to a prolonged residence time in the circulation and enhanced uptake at pathological sites by extravasation due to locally enhanced vascular permeability [45]. Such stabilized PEG-liposomes can be labeled with ^{111}In-oxinate and with ^{99m}Tc, either using hexamethylpropylene amine oxime (HMPAO) as an internal label or via HYNIC as an external chelator. Labeling is easy and takes only minutes [46]. The first clinical evaluation showed good imaging of focal infection. In patients suspected of harboring infectious or inflammatory disease, ^{99m}Tc-PEG-liposomes were directly compared with ^{111}In-IgG scintigraphy. ^{99m}Tc-PEG-liposome scintigraphy has shown high sensitivity (94%) and specificity (89%) [47].

2.4. The Avidin-Biotin System. Avidins are a family of proteins present in the eggs of amphibians, reptiles, and birds; streptavidin is a member of the same family. Avidin and streptavidin (mol. wt. 66,000 and 60,000, resp.) bind to biotin with extremely high affinity. Biotin is a compound of low molecular weight that can be radiolabelled. The avidin-biotin approach is based on the fact that avidin (or streptavidin) will nonspecifically localize at sites of infection

owing to increased vascular permeability. Avidin (or streptavidin) is injected as a pretargeting agent, followed hours later by a second injection with radiolabelled biotin. Good diagnostic accuracy was demonstrated in studies of vascular infection and chronic osteomyelitis [48–51].

3. Detection of Infection by Specific Tracers

3.1. Radiolabeled White Blood Cells. Ex vivo labeled autologous leucocytes were developed in the 1970s and 1980s and their use is still considered the "gold standard" nuclear medicine technique for infection and inflammation imaging [5–7]. Although a variety of *in vitro* leukocyte-labeling techniques have been used, the most commonly used procedure makes use of the lipophilic compounds ^{111}In-Oxyquinoline and ^{99m}Tc-HMPAO. The radiolabeling procedure takes about 2-3 hours. Because all the cellular components of the blood can be labeled, it is necessary to separate the leukocytes from the erythrocytes and platelets. After withdrawal, therefore, the syringe containing the blood is kept in the upright position for about 1-2 hour to promote erythrocyte sedimentation. After the erythrocytes have been separated, the leukocytes must be separated from platelets. The leukocyte-rich plasma is centrifuged, and the leukocyte pellet that forms at the bottom of the tube is removed, incubated with the radiolabel, washed, and reinjected into the patient. The usual dose of ^{111}In-labeled leukocytes is 10–18.5 MBq (300–500 μCi); the usual dose of ^{99m}Tc-HMPAO-labeled leukocytes is 185–370 MBq (5–10 mCi). Uptake of labeled leukocytes is dependent on intact chemotoxis, the number and types of cells labeled, and the cellular component of a particular inflammatory response. A total white cell count of at least 2000/mm^3 is needed to obtain satisfactory images. Neutrophils can be radiolabeled and hence the procedure is most useful for identifying neutrophil-mediated inflammatory processes, such as bacterial infections. The procedure is less useful for those illnesses in which the predominant cellular response is other than neutrophilic, such as tuberculosis [52].

3.1.1. ^{111}In-Oxine-Labeled Leukocytes. For over two decades, ^{111}In-oxine-labeled leukocytes have been used to image infection and inflammation. The scintigraphic images reflect the distribution of white blood cells in the body. Since an abscess or other localized infection consists primarily of leukocytes, the radiopharmaceutical localizes at the site of infection [53–61]. After intravenous administration, there is initial sequestration of the labeled leucocytes in the lungs, with subsequent rapid clearance of the activity from the lungs. The radiolabel rapidly clears from the blood and in most cases there is high uptake in granulocytic infiltrates, while a substantial portion of the leucocytes (presumably the damaged cells) accumulate in the spleen. Thus, as a radiopharmaceutical, radiolabelled leucocytes are a specific indicator for leukocytic infiltration, but not for infection [62, 63]. At 24 hour, after injection, the usual imaging time for ^{111}In-labeled leukocytes, the normal distribution of activity is limited to the liver, spleen, and bone marrow. Large field of view gamma camera equipped with medium energy parallel hole collimator is used with 15% window centered on 174-Kev photopeak and 20% window centered on the 247-Kev photopeak. Advantages of the ^{111}In label are a very stable label and constant normal distribution of activity limited to liver, spleen, and bone marrow. The 67-hour half-life of isotope allows delayed imaging, which is particularly valuable in musculoskeletal infection. Another advantage is conduction of bone or bone marrow scan immediately after completion of ^{111}In-labeled study which is a limitation with ^{99m}Tc-labeled tracers [9]. Disadvantages of the ^{111}In label include a low photon flux, less than ideal photon energies, and the fact that a 24-hour interval between injection and imaging is generally required. Causes of false-negative and false-positive ^{111}In-leukocyte study are summarized in Table 1 [64]. Drawbacks of ^{111}In-labeled white blood cells are laborious and time-consuming preparation, requiring specialized equipment and can be hazardous. Almost 3 hours are required for isolating and labeling a patient's white blood cells by a trained technician. In addition, the need to handle potentially contaminated blood can lead to transmission of blood-borne pathogens such as HIV and HBV. As anatomical land marks are not properly outlined with scintigraphy, the same is the limitation with ^{111}In-WBC planar images. However, SPECT/CT with ^{111}In-WBC scintigraphy markedly improves accurate identification of infection sites [11].

Table 1: Causes of false-negative and false-positive ^{111}In leukocyte studies.

False Negative
Encapsulated nonpyogenic abscess
Vertebral osteomyelitis
Chronic low-grade infection
Parasitic, mycobacterial or fungal infections
Intrahepatic, perihepatic, or splenic infection
Hyperglycemia
Steroids
False Positive
Gastrointestinal bleeding
Pseudoaneurysm
Healing fracture
Soft tissue tumor
Surgical wounds, stomas, or catheter sites
Tumors
Accessory spleens

3.1.2. ^{99m}Tc-HMPAO-Labeled Leukocytes. The normal biodistribution of ^{99m}Tc-HMPAO-labeled leukocytes is more variable. In addition to the reticuloendothelial system, activity is also normally present in the genitourinary tract, large bowel, blood pool, and occasionally the gall bladder [65]. The interval between injection and imaging varies with indication; in general, imaging is usually performed within a few hours after injection. ^{99m}Tc-HMPAO has theoretical advantages over ^{111}In-labeled leukocytes. ^{99m}Tc, being generator produced on site, could be immediately available for radiolabeling. The radiation dose to the patient would be

significantly lower, permitting a higher administered activity. The higher photon yield of ^{99m}Tc would result in superior image resolution and improved infection detectability and accuracy.

HMPAO preferentially labels granulocytes, a potential advantage for imaging acute purulent processes. Unlike ^{111}In-oxine-labeled leukocytes, ^{99m}Tc-HMPAO-labeled leukocytes are cleared by the hepatobiliary and renal systems [65–70]. Disadvantages include genitourinary tract activity, which appears shortly after injection and colonic activity which appears 4 hours after injection. The instability of the label and the short half-life of ^{99m}Tc are disadvantages when 24-hour imaging is needed. This occurs in those infections that tend to be indolent and for which several hours may be necessary for accumulation of a sufficient quantity of labeled leukocytes to be successfully imaged. Bone or bone marrow scan if indicated after ^{99m}Tc-HMPAO-WBC scan has to be delayed at least for 48 hours and preferably 72 hours. For better anatomical localization of infection site, SPECT/CT with ^{99m}Tc-HMPAO-WBC scintigraphy is far better than planar/SPECT imaging with other infecting imaging agents [10].

3.2. Antigranulocyte Antibodies and Antibody Fragment. Several monoclonal antibodies reactive with antigens expressed on granulocytes (NCA, CD15, CD66, and CD67) have been developed. At least three antigranulocyte antibodies have been tested for infection imaging: anti-NCA-95 IgG (BW250/183) [71, 72], anti-NCA-90 Fab' (Immu-MN3, LeukoScan: anti-CD66) [73], and anti-SSEA-1 IgM (LeuTech: anti-CD15) [74–76]. Each of these antigranulocyte antibodies labeled with ^{99m}Tc or ^{123}I allowed accurate delineation of infection [59]. The antigranulocyte antibody-based radiopharmaceuticals visualized infectious foci in patients with sensitivity between 80% and 90% [77].

The use of antibody fragments instead of the whole antibody seems to be more advantageous, since such fragments appear to be less immunogenic. In addition, antibody fragments show faster blood clearance and may thus provide earlier diagnosis. ^{99m}Tc-labeled antigranulocyte Fab' fragment (LeukoScan) has been registered in Europe as an infection imaging agent.

3.3. Chemotactic Peptides. A wide variety of peptides that bind to receptors expressed on white blood cells have been tested for the detection of infection. One of the first receptor binding peptide tested for its ability to image infectious foci was chemotactic peptide formyl-Met-Leu-Phe. This tripeptide, which is N-terminally formylated, is a chemotactic factor produced by bacteria which binds to receptors on granulocytes and monocytes with high affinity [78–80]. A drawback of using these biologically potent peptides is a transient but severe reduction in peripheral leukocyte counts. Several antagonists were developed to circumvent this undesirable biological activity of the radiolabelled chemotactic peptide. However, these antagonists had lower uptake in the infectious focus, most likely owing to reduced affinity for the receptor [81].

3.4. Cytokines. The attraction of leukocytes to tissues is essential for inflammation and host response to infection. The process is controlled by chemokines, which are chemotactic cytokines. Over 40 chemokines have been identified to date, most of them in the past few years. Chemokines induce cell migration and activation by binding to specific G-protein-coupled cell surface receptors on target cells. Their receptors are expressed on different types of leukocytes. Some are restricted to certain cells, whereas others are more widely expressed [82]. Labeled cytokines are an interesting class of protein radiopharmaceuticals of low molecular weight (<20,000).

3.5. Interleukin-1. Interleukin-1 (IL-1) binds receptors expressed mainly on granulocytes, monocytes, and lymphocytes, with high affinity. Studies in mice with focal *Staphylococcus aureus* infections showed specific uptake of radioiodinated IL-1 at the site of infection [83]. Fever, haemodynamic and hematological side effects, occurring even at very low concentrations, are the major drawbacks of the use of such a biologically active protein [84].

3.6. Interleukin-2. The IL-2 is considered to bind specifically to IL-2 receptors expressed on activated T lymphocytes. In a study in an animal model of human autoimmune diabetes mellitus, Hashimoto's thyroiditis, Grave's disease, Crohn's disease, Coeliac disease and other autoimmune diseases, demonstrated localization of ^{123}I or ^{99m}Tc-labeled IL-2 at the site of lymphocytic infiltration [85, 86].

3.7. Interleukin-8. IL-8 binds to receptors on neutrophils with high affinity. In rabbits with focal *Escherichia coli* infection, accumulation of ^{123}I-labeled IL-8 in the abscess was rapid and high. The specific activity of this IL-8 preparation was relatively low, resulting in a transient reduction in peripheral leukocyte counts to 45% after a dose of 25 μg/kg ^{123}I-IL-8, followed by leukocytosis for several hours. Recently, a ^{99m}Tc-labelled IL-8 preparation was developed using HYNIC as a chelator. In rabbits with *Escherichia coli* infection, high abscess uptake of ^{99m}Tc-HYNIC-IL-8 and high abscess-to-background ratios were obtained compared with those obtained using the radioiodinated preparation [87–91].

3.8. Platelet Factor-4. Platelet factor 4 (PF-4), like IL-8, is a member of the CXC chemokines. PF-4 binds the CXC type II (= IL-8 type B) receptors expressed on neutrophils and monocytes. In a rabbit model of infection, ^{99m}Tc-P483H clearly delineated the infectious foci as early as 4 hours after injection. No systemic side effects were observed. ^{99m}Tc-P483H has been studied in patients to test its applicability as an imaging agent for scintigraphic detection of infection and inflammation, with fair results (82% sensitivity, 77% specificity) [92, 93].

3.9. Detection of Infection by ^{18}F-Deoxyglucose (FDG). FDG is transported into cells by glucose transporters and is phosphorylated by hexokinase enzyme to ^{18}F-2-FDG-6 phosphate

but is not metabolized. The degree of cellular FDG uptake is related to the cellular metabolic rate and the number of glucose transporters [94–96]. Activated inflammatory cells also demonstrate increased expression of glucose transporters. In addition, in inflammatory conditions, the affinity of glucose transporters for deoxyglucose is apparently increased by various cytokines and growth factors, a phenomenon that has not been observed in tumors [97]. Although FDG uptake can produce false-positive results in patients with known or suspected malignancy, FDG represents another potentially useful radiotracer in the setting of infection and inflammation. The areas of normal distribution of FDG include the brain, myocardium, and genitourinary tract. Activity in the bone marrow, stomach, and bowel is variable [98]. Thymic uptake, especially in children, can also be observed [99]. Hepatic and splenic uptake are generally of low grade and diffuse; however intense uptake in spleen may be visualized in the setting of infection [100].

Positron emission tomography (PET) with ^{18}FDG is now widely used. FDG is taken up by inflammatory cells with increased metabolic requirements. In contrast to glucose, deoxyglucose cannot leave the cell once it is taken up, so it can be used to image scintigraphically cells with high glucose uptake such as tumor cells and inflammatory cells. FDG-PET has been studied in a wide variety of infections, including lesions of bacterial, tuberculous, fungal, soft tissue, and bone infections [101, 102]. Sensitivity and specificity have generally exceeded 90%. This radiotracer has high positive predictive value to localize in infective sites of patients with AIDS and fever of unknown origin (FUO). This technique accurately helps identify sites of infective endocarditis and is promising supplement to conventional echocardiography [103]. FDG-PET has been especially successful in cases of osteomyelitis [104–107]. For vertebral osteomyelitis, high sensitivity, specificity, and accuracy comparable to those of gallium imaging have been reported [108]. High spatial resolution and rapid accumulation in infectious foci are significant advantages over conventional imaging techniques such as the use of labeled leucocytes. However, the fact that uptake occurs in any cell type with high glycolytic activity is a serious limitation of the use of FDG-PET for infection imaging, restricting its specificity [109]. PET is highly sensitive but may be unable to define the anatomic location of a focus of increased ^{18}F-FDG accumulation. The hybrid PET/CT technology improved diagnostic accuracy with precise registration of metabolic and structural imaging data. ^{18}F-FDG PET/CT utilized for workup of osteomyelitis in diabetic foot correctly identified 93% of all infected sites [110]. However, ^{18}F-FDG-WBC is a nonspecific tracer of increased glucose metabolism and does not accumulate only in sites of infection and inflammation but also shows false-positive results in tumor and postoperative changes [111]. ^{18}F-FDG-labeled autologous leukocytes PET/CT for infection detection has demonstrated sensitivity, specificity, and accuracy of 91%, 85%, and 90%, respectively. Negative predictive value of 100% with this technique is a hallmark. ^{18}F-FDG-WBC imaging is superior to ^{18}F-FDG alone for infection detection as well as for assessment of response of infection to antibiotic treatment; however limited availability and cost are the limitations [12].

3.10. Detection of Infection by Radiolabeled Antibiotics

3.10.1. Ciprofloxacin. The first antibiotic developed as a radiopharmaceutical was ^{99m}Tc-ciprofloxacin having many of the properties of an ideal infection-specific agent [3]. Ciprofloxacin is a broad spectrum quinolone which binds specifically to bacterial DNA gyrase, inhibits DNA synthesis, and has been proposed to distinguish infection from inflammation [112, 113]. It is retained at sites of infection and associates freely with metal ions, allowing it to be labeled with technetium. Ciprofloxacin also binds to the equivalent mammalian enzyme, topoisomerase II, but with 100 to 1000 times lesser affinity and the binding is readily reversible. Similarly, it penetrates neutrophils, macrophages, and other cells and tissues, but is not retained for prolonged periods. Thus after the initial distribution phase, as the serum concentration falls, the antibiotic readily leaches out of the cells and tissues into tissue fluid and then the blood and excreted freely, predominantly in the urine. However, it is retained at sites of infection, giving high target to background ratio permitting infection-specific imaging when sequential images are taken at 1, 4 and if required 24 hours after injection [3].

In vitro, ciprofloxacin is taken up by a wide variety of Gram-positive, Gram-negative, and anaerobic bacteria (including ciprofloxacin-resistant bacteria as long as the resistance is not mediated by cell membrane impermeability, which prevents entry of the antibiotic into the bacterial cell) but not by dead bacteria or white cells [114, 115]. Biodistribution and dosimetry of ^{99m}Tc-ciprofloxacin show rapid, predominantly urinary excretion of the tracer, with low-to-absent brain, lung, and bone marrow uptake and low liver uptake and excretion. Highest radiation dose was received by urinary bladder. Imaging conditions were excellent for both thoracic and abdominal regions, even at early time (60 minutes) after injection [116]. In a comparative study in 51 patients, it demonstrated greater specificity (96%) for imaging infection compared with white cell imaging (84%) [113]. High specificity for bacterial infection was confirmed in a subsequent study involving 90 patients [117]. It also showed that some infections due to ciprofloxacin-resistant bacteria could be imaged and that prior antibiotic treatment did not significantly affect the imaging result. The sensitivity and specificity of ciprofloxacin imaging have been validated further in a large multicentre study involving 879 patients, with a wide variety of infective and noninfective conditions (including noninfective inflammatory disorders), in eight countries, under the auspices of the International Atomic Energy Agency (IAEA) [118]. No adverse reactions occurred and antibiotic-resistant organisms did not emerge as a result of the administration of antibiotic into patients. This was expected because only a tracer dose of ciprofloxacin is present in the kit, 2 mg, which is 1/200th of a single therapeutic intravenous dose of ciprofloxacin (400 mg). Sensitivity (85.4%) and specificity (81.7%) for imaging sites of infection were good, but varied according to the type of

infections imaged. The highest sensitivity (in excess of 90%) was seen in osteomyelitis, septic arthritis, infection of orthopedic prostheses (which is often difficult to diagnose by standard techniques and differentiate from aseptic loosening), and culture-proven soft tissue and abdominal infections and tuberculosis. Ciprofloxacin has several advantages over established, for example, radiolabeled leucocytes, and other methods for imaging infection, which include the following: (1) specificity for infection, (2) lack of bone marrow uptake, which is a significant advantage in imaging bone and joint and orthopedic prostheses infections, (3) ease and cost of preparation of the agent, (4) *ex vivo* labeling, which avoids contact with blood and hence the risk of acquiring bloodborne infections such as H1V and hepatitis B and C, (5) independence of the host inflammatory response and neutrophil count and hence it can be used to image infections in immunocompromised patients, including those who are neutropaenic, where culture is often negative and white cell imaging unreliable, and (6) availability in a kit format with long shelf-life, making it user friendly and more widely available [3]. Certain studies have revealed false positive uptake of ^{99m}Tc-ciprofloxacin in sterile inflammation questioning its specificity [14–19].

3.10.2. ^{99m}Tc Sparfloxacin. Sparfloxacin is fluoroquinolon, antibiotic effective against a wide range of Gram-positive bacteria. It was successfully labeled and evaluated in *invitro* animal model in which ^{99m}Tc-labeled antibiotic accumulated in infective sites of live *Staphylococcus aureus* bacteria and revealed no uptake in control models with heat-killed bacteria [119].

3.10.3. ^{99m}Tc-Enroflaxacin. This is also quinolone antibiotic used mainly in veterinary practice. Labeled with ^{99m}Tc, *in vitro* studies did not show encouraging results in differentiating infection from inflammatory foci [120].

3.10.4. ^{99m}Tc-Ceftizoxime. Ceftizoxime is a 3rd-generation cephalosporin effective against a wide range of Gram-positive bacteria especially *Staphylococcus aureus*, *Streptococci,* and *Enterobacteriaceae*. This drug is widely used at surgical and medical floors as prophylactic and treatment antibiotic. As per hypothesis, if such drugs are effectively labeled with radiotracer without altering the efficacy and effective binding with bacteria, localization of infective foci and monitoring the efficacy and duration of antibiotic treatment would be a big hallmark. This drug was effectively labeled with ^{99m}Tc and used to localize bone infections as the penetration of this antibiotic in bone is far better as compared with other antibiotics [121].

3.10.5. ^{99m}Tc-Ethambutol. Ethambutol is a narrow-spectrum antibiotic, which is active against mycobacteria (inhibits cell wall mycolic acid synthesis) and is used as a first-line drug for the treatment of tuberculosis (TB). Hence radiolabeled ethambutol is an attractive candidate for specifically imaging mycobacterial infections, including early TB. Good results were obtained in a thigh model of *Mycobacterium tuberculosis* infection in mice and rabbits. ^{99m}Tc-ethambutol accumulated at the site of infection as early as 2 hours after injection, which increased at 4 hours and persisted till 24 hours. Further studies with this agent are eagerly awaited [122].

3.10.6. ^{99m}Tc-INH. Isoniazid (INH) is a specific antituberculous drug showing selective uptake in live mycobacteria based on its specific interaction with mycolic acid which is an important constituent of bacterial cell wall. This drug was successfully labeled with ^{99m}Tc followed by studies on mice and rabbits for labeling efficiency, *in vitro* and *in vivo* stability, blood kinetics, and organ distribution. Thigh model of localized tubercular lesion was prepared in rabbits after injecting 500 μL of 3×10^8 cells/mL of *Mycobacterium tuberculosis* live bacteria in growing phase (clinical human isolate). The localization of radiolabeled complex was studied with 70–75 MBq of ^{99m}Tc-INH intravenously with successful imaging at 2, 4, and 24 hours after tracer injection with increase in target to nontarget (T/NT) ratio gradually up to 24 hours. Labeling efficiency of the kit was >95% and only 2–3.5% of tracer leaked out from the complex or 24 hours when incubated in serum as 37°C, confirming its stability. Organ distribution studies showed renal source of excretion with no gastric or thyroid uptake suggesting good *in vitro* labeling efficiency and stability. As controls, infection was induced in rabbits with live *Staphylococcus aureus* after injection of 10^7 live bacteria followed by injection of same dose of ^{99m}Tc-INH and imaging under same parameters. Tracer accumulation was visualized in the infective foci from 2 hours after injection; however, delayed imaging revealed gradual clearance at 4 and 24 hours, which was in contradiction to findings with tuberculous lesions. Overall more than 95% sensitivity and high specificity were observed in the animal study. Therefore it was concluded that this radiolabeled agent can be used for detection and followup of tuberculous lesions in patients especially to determine the treatment endpoint of antituberculous drugs [123]. Similar labeling of INH with ^{99m}Tc and study in humans was tried in our set up but we were unable to localize lesions of tuberculous lymphadenitis in humans with this radiotracer.

3.10.7. ^{99m}Tc-Fluconazole. Anticancer therapy, transplantation and AIDS give rise to infections with fungi such as *Candida albicans* and *Aspergillus Fumigatus*. Fluconazole is antifungal drug which was successfully labeled with ^{99m}Tc. This labeled compound successfully detected infections with *Candida albicans* but not bacterial infections or sterile inflammatory sites in animals. There was good correlation between ^{99m}Tc-Fluconazole accumulation and the number of viable *Candida albicans* which could be used as parameter for monitoring antifungal therapy. This agent is mainly excreted via the kidneys with little accumulation in the liver. However, it is not suited to detect *Aspergillus fumigatus* infections. However, this radiotracer is able to distinguish between *Candida albicans* infections from bacterial infections and sterile inflammations [124].

3.11. Detection of Infection by Antimicrobial Peptides. Peptides are composed of relatively small components, the amino acids. A difference between peptides and proteins is their size. Peptides are compounds with up to about 50 amino acids and a molecular mass below about 10,000 Dalton. In contrast, they generally do not possess a well-defined three-dimensional (tertiary) structure. Because of the lack of tertiary structure, small peptides are less susceptible to a loss of integrity through labeling conditions and are less immunogenic than proteins [125, 126]. Antimicrobial peptides, produced by phagocytes, epithelial cells, endothelial cells, and many other cell types, are an important component of innate immunity against infection by a variety of pathogens. They can be expressed constitutively or induced during inflammation or microbial challenge. These peptides, which now number more than 100, with proven microbicidal activity against a variety of microorganisms, share certain properties such as their small size and cationic charge. The later allows them to bind preferentially to a broad spectrum of microorganisms. Interestingly, the antibacterial effect of antimicrobial peptides in experimentally infected animals might also be attributed to synergistic effects with endogenous antimicrobial peptides and proteins such as lysozyme and secretary leukoprotease inhibitor (SLPI), reactive oxygen intermediates, or other local factors (such as pH, Ca^{+2} and Zn^{+2} concentrations) or to interactions with host cells, leading to enhanced antibacterial activities of the cells [127–129].

4. Key Features of Antimicrobial Peptides

(i) Antimicrobial peptides usually contain <50 amino acids with a net positive charge created by an excess of basic residues, such as lysine and arginine, and ~50% hydrophobic amino acids.

(ii) Antimicrobial peptides are essential components of the innate host defense because of their ability to kill a wide range of pathogens.

(iii) They have a wide distribution throughout the animal and plant kingdoms.

(iv) They are effectors of local and systemic immune responses. The latter is essentially found in insects.

(v) Although they share basic features such as small size, hydrophobicity, and cationic character, antimicrobial peptides have a great structural diversity.

(vi) The majority of antimicrobial peptides are derived from larger precursors that harbor a signal sequence, whereas other peptides are generated by proteolysis from larger proteins (such as lactoferrin).

(vii) In addition, some antimicrobial peptides such as mammalian defensins have other activities contributing to host defenses by mediating an acute inflammatory reaction and linking the innate with the acquired immune response [130].

4.1. Preparation of Radiolabeled Peptides. Difficulties arising in purifying natural antimicrobial peptides from various sources have prompted the recombinant production of antimicrobial peptides by genetically engineered bacteria or by peptide synthesis. Such methods result in sufficient amounts of antimicrobial peptides produced under good laboratory practice conditions, which is essential for use in animal and human studies. Synthetic peptides are usually small, rapidly removed from the circulation and other body compartments, and flexible, because they do not hold a particular structure in a hydrophilic environment, and display a favorable adverse effect profile.

Table 2: Natural and synthetic human antimicrobial peptides.

Peptide	Amino acids	Amino acid sequence	Code
Ubiquicidin	1–59	[20]	UBI 1–59
	1–18	KVHGSLARAGKVRGQTPK	UBI 1–18
	29–41	TGRAKRRMQYNRR	UBI 29–41
	18–29	KVAKQEKKKKKT	UBI 18–29
	18–35	KVAKQEKKKKKTGRAKRR	UBI 18–35
	31–38	RAKRRMQY	UBI 31–38
	22–35	QEKKKKKTGRAKRR	UBI 22–35
Lactoferrin	1–692	[27]	hLF
	1–11	GRRRRSVQWCA	hLF 1–11
	2–11	RRRRSVQWCA	hLF 2–11
	3–11	RRRSVQWCA	hLF 3–11
	4–11	RRSVQWCA	hLF 4–11
	5–11	RSVQWCA	hLF 5–11
	6–11	SVQWCA	hLF 6–11
	21–31	FQWQRNMRKVR	hLF 21–30
Defensin 1–3	1–30	[28]	—

4.2. Radiolabeling of Peptides. The aim of radiolabeling techniques is to firmly attach or incorporate the radionuclide into the peptide without altering its biological functions, thus allowing a reliable evaluation of its pharmacokinetics after intravenous administration. The various methods of labeling peptides with ^{99m}Tc including indirect labeling using the preformed chelate approach or bifunctional chelating agents and the direct labeling method have been discussed extensively [131]. The direct labeling method is a simple procedure in which the peptide is labeled in absence of an exogenous chelator. The labeling of antimicrobial peptides is rapid (within 10 min), effective (impurities, 5% of the total radioactivity), stable (minimal release of radioactivity from the ^{99m}Tc-peptide in diluted human serum), and safe (no adverse effects in mice and rabbits). Unfortunately, the reaction mechanism underlying this ^{99m}Tc-labeling of peptides has not been elucidated. It may, however, involve the reduction of ^{99m}Tc, the production of a ^{99m}Tc intermediate, and the substitution reaction transferring the reduced ^{99m}Tc from this intermediate to the peptide [132].

4.3. Selection of ^{99m}Tc-Labeled Antimicrobial Peptides for Scintigraphic Studies. In vitro binding studies were used to select peptides displaying a preferential binding to microorganisms over human cells from a range of ^{99m}Tc-labeled

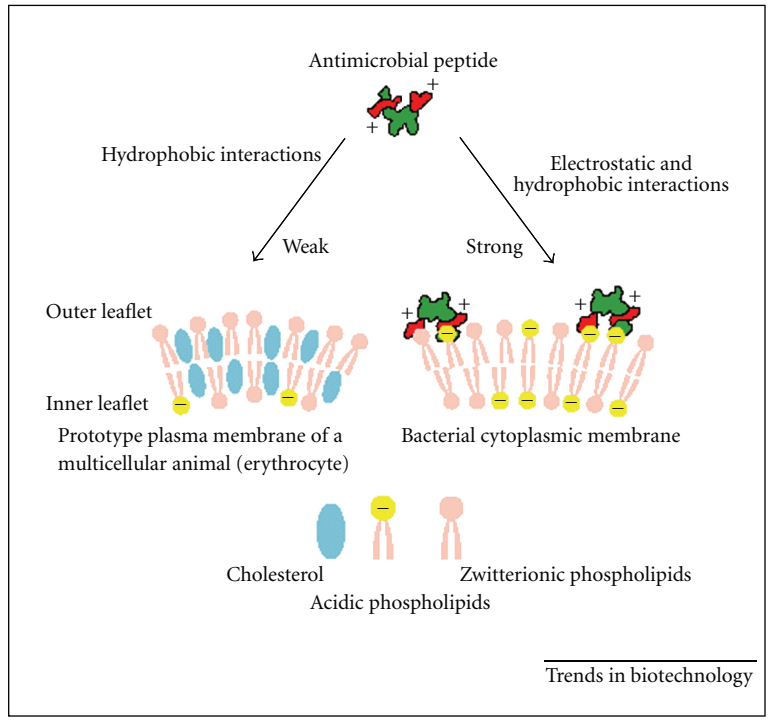

Figure 1: The membrane target of antimicrobial peptides and the basis of their specific binding.

human antimicrobial peptides/proteins and synthetic peptides derived from these natural peptides/proteins (Table 2). Thereafter, a peritoneal infection model was used to assess the *in vivo* binding of ^{99m}Tc-peptides to bacteria and host cells. Next, radiolabeled peptides that had been selected by this assay were injected into animals to find out whether they can be used to discriminate infections from sterile inflammatory lesions using scintigraphic techniques. Peptides were also selected on the basis of favorable pharmacokinetics. After these phases of selection, α-defensins and several peptides derived from ubiquicidin were seen to be the most likely candidates for infection detection [133].

4.4. Mechanism of Labeled Peptides for Infection Detection. Although antimicrobial peptides have different chemical structures, the basis of their antimicrobial activities is the interaction of the cationic (positively charged) domains of the peptides with the (negatively charged) surface of microorganisms (Figure 1). Given that microbial membranes expose negatively charged phospholipids, such as LPS or teichoic acids, on their surface, whereas mammalian cells segregate lipids with negatively charged head groups into the inner leaflet, it is conceivable that antimicrobial peptides bind preferentially to pathogens over mammalian cells [130].

4.5. Antimicrobial Peptides in Experimental Use. One of the best-studied antimicrobial peptides is human neutrophil peptide-1 (HNP-1), which is a member of the family defensins. Initially, the potential use of HNP-1 for antibacterial therapy of experimental infections in mice was studied. The antibacterial effect was found to be associated with an increased influx of neutrophils into the infected area [134]. Use of this agent in experimental thigh muscle infection in mice allowed rapid visualization of bacterial infections, but abscess to background ratios were low and decreased with time [135, 136].

4.6. Imaging of Infections in Immunocompromised Mice. Immunocompromised mice produced by an injection of cyclophosphamide were utilized for detection of infection site induced by microorganisms which confirmed that accumulation of tracer was due to microorganisms, not due to inflammatory cells [24]. In immunocompromised animals the accumulation of the peptide at the infection site was similar to that in immunocompetent rabbits, thus confirming insignificant contribution of the labeling with activated leukocytes and other inflammatory cells [27, 28].

4.7. Discrimination between Infection and Inflammation. Antimicrobial peptides labeled with ^{99m}Tc selectively localized the infection sites of bacteria and fungi through binding with their cell membranes and revealed minimum or no uptake in inflammatory model induced by LPS or heat-killed microorganisms [24]. Similarly, no binding of labeled ^{99m}Tc-antimicrobial peptide UBI (29–41) was appreciated in inflammatory models in rabbits induced with formalin-killed *Staphylococcus aureus* bacteria or turpentine oil [27].

4.8. Ubiquicidin (UBI 29–41): New Antimicrobial Peptide. UBI (29–41) (TGRAKRRMQYNRR, 1,693 Da) was originally

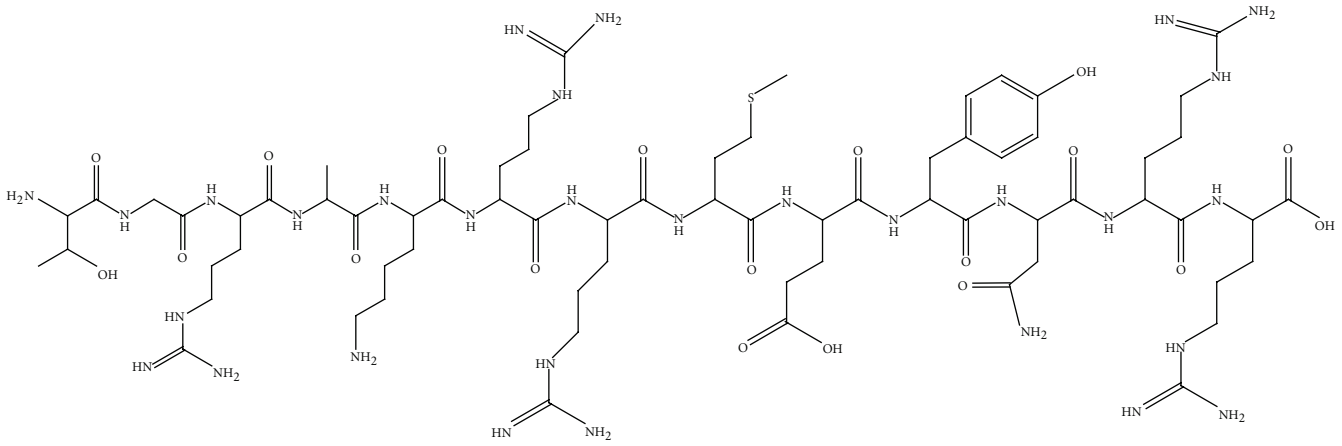

Figure 2: Structure of UBI 29–41.

isolated from the cytosolic fraction of IFN-γ-activated cells of mouse macrophage cell line RAW264.7 (Figure 2). Later, an identical UBI was isolated from human H292 airway epithelial cells. Ubiquicidin is identical or highly homologous to S30, a protein that was purified from the small ribosomal subunit fraction of rat liver and shown to be present in various human and murine tissues. The homology of the precursor element of this protein to ubiquitin and the fact that it is probably widely expressed named this protein ubiquicidin (Latin "ubique," everywhere) [137].

4.8.1. Radiochemical Analysis. HPLC chromatograms for UBI peptides indicated that the preparations were more than 95% pure. ITLC analysis of the preparation containing radiolabeled peptide showed peptide-labeling yield of 98% after 10 minutes of incubation and these values remained unchanged up to 24 hours [20].

4.8.2. Stability of ^{99m}Tc-Labeled UBI in Human Serum. Stability of the ^{99m}Tc-labeled UBI peptides was assessed by incubating one volume of the labeling solution with one volume of 20% (v/v) human serum in saline for 1 and 24 hours at 37°C. Next, the amounts of free pertechnetate and ^{99m}Tc-peptide in the samples were determined by ITLC using methyl ethyl ketone as eluent. Results showed minimal release of radioactivity from the ^{99m}Tc-UBI peptides. ITLC analysis of the samples after 1 and 24 hours of incubation in human serum revealed small amounts of released/free ^{99m}Tc (<3% of the total activity at both intervals) [138].

4.8.3. Binding of UBI to Bacteria and Murine Blood Cells. Analysis of murine blood revealed that only a small proportion of the intravenously injected ^{99m}TC-UBI is associated with blood cells. Moreover, injection of excess unlabeled UBI 29–41 into *Staphylococcus-aureus*-infected mice prior to injection of ^{99m}Tc UBI 29–41 significantly ($P < 0.05$) reduced the accumulation of this radiopharmaceutical at the site of infection. In addition, significantly ($P < 0.01$) higher amounts of ^{99m}Tc-UBI 29–41 accumulated at the site of infection in mice using a carrier-free radiolabeled UBI 29–41 as compared with unpurified preparation containing radiolabeled UBI 29–41 [20].

4.8.4. In Vitro Binding of UBI and Two Other Cationic Peptides to Bacteria and Tumor Cell Lines. A comparative study of the *in vitro* binding of ^{99m}Tc-UBI and two different ^{99m}Tc-labeled cationic peptides (^{99m}Tc-Tat-1-Scr and ^{99m}Tc-Tat-2-Scr) to bacteria and to two tumor cell lines (LS174T and ACHN) was performed. The binding of ^{99m}Tc-UBI, ^{99m}Tc-Tat-1-Scr, and ^{99m}Tc-Tat-2-Scr to *Staphylococcus aureus* was 35%, 78%, and 87%, respectively. While the binding of ^{99m}Tc-Tat-1-Scr and ^{99m}Tc-Tat-2-Scr was 37% and 33% to colon tumor cells (LS174T) and 39% and 41% to renal tumor cells (ACHN), respectively. Binding of ^{99m}Tc-UBI to both cell types was much lower (<4%) [138].

4.8.5. In Vivo Binding Studies. Experimental peritoneal infection in mice showed highest binding of ^{99m}Tc-labeled UBI peptides to bacteria. The mean ratio between binding of UBI peptides to bacteria and that to leukocytes, determined at 2 and 24 hours, amounted to 73–220 [20]. The *in vivo* specificity of ^{99m}Tc-UBI for infection in mice was also evaluated using dual labels in the same animal and comparing the target/nontarget ratio for ^{67}Ga-citrate and ^{99m}Tc-UBI at sites of induced infection and sterile inflammation. This study revealed that there is a significant difference ($P < 0.05$) in the radioactive accumulation of ^{99m}Tc-UBI between the sites of infection and inflammation compared to ^{67}Ga-citrate. Thus, ^{99m}Tc-UBI showed an average infection/inflammation ratio of 2.08 ± 0.49 compared to 1.14 ± 0.45 for ^{67}Ga-citrate. In conclusion, the *in vitro* and *in vivo* results provide evidence that a specific mechanism is responsible for the ^{99m}Tc-UBI bacterial intracellular accumulation [138].

4.8.6. Infection Imaging in Animal Models. In experimental animals, various ^{99m}Tc-labeled UBI peptides visualized the bacterial or fungal infected tissues within 30 minutes after injection. A good correlation between the accumulations of ^{99m}Tc-labeled UBI peptides in *Staphylococcus-aureus*-infected thigh muscles in mice and the number of viable bacteria present at the site of infection was recorded. In immunocompromised animals the accumulation of the peptide at the site of infection seemed to be similar to that in immunocompetent mice, confirming the insignificant contribution

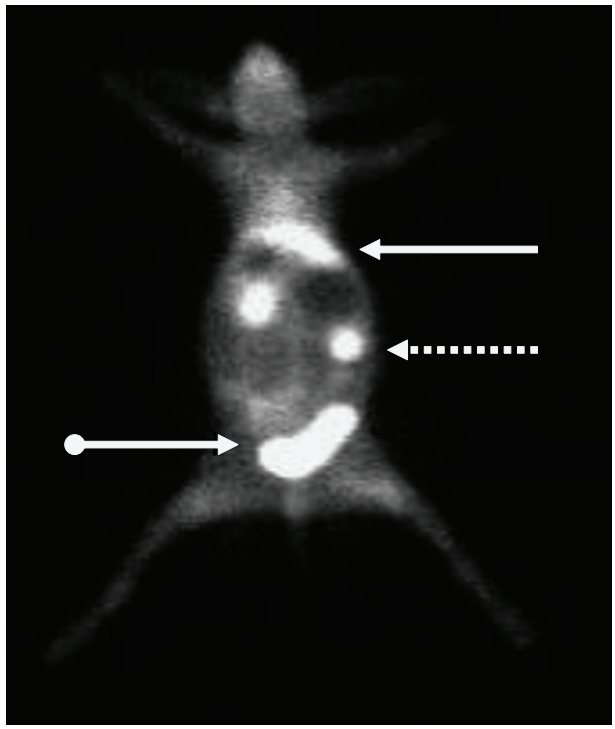

Figure 3: Biodistribution of ^{99m}Tc UBI 29–41 in a normal rabbit at 30 minutes after injection.

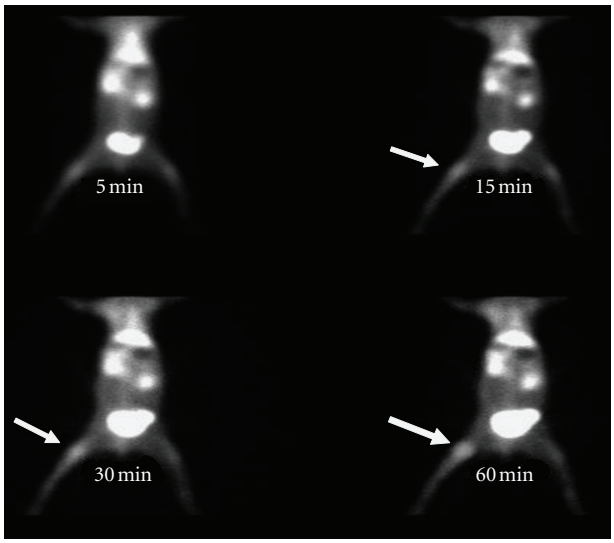

Figure 4: ^{99m}Tc-UBI (29–41) scintigram of rabbit with *Staphylococcus aureus* thigh muscle infection (arrow). Maximum tracer uptake visualized at 60 minutes after tracer injection.

of the direct binding of the tracer to infiltrating leucocytes [133].

4.8.7. Discrimination between Bacterial Infection and Sterile Inflammation. Various experimental thigh muscle infections in mice and rabbits with both Gram-positive and Gram-negative bacteria revealed accumulation of ^{99m}Tc-labeled UBI at the site of infection within 15–30 minutes after injection. No significant accumulation of labeled peptide was observed in thighs of rabbits and mice previously injected with LPS or heat-killed bacteria (i.e., sterile inflammation) [133]. Only one animal model study provided results against its binding to bacteria and concluded its affinity for ^{3}H-deoxyglucose and macrophage accumulation at the site of infection [139].

4.8.8. Biodistribution of UBI in Mice and Rabbits. After injection, ^{99m}Tc-labeled UBI peptides are rapidly removed from the circulation via the kidneys. Scintigraphic analysis revealed that, within the first hour after injection of tracer, major part of activity was found in kidneys and urinary bladder with little accumulation in liver, lungs, and spleen (Figure 3) [20, 27, 133].

4.8.9. Infection Detection with ^{99m}Tc UBI 29–41 in Animal Model. ^{99m}Tc UBI was evaluated as bacterial infection seeking agent in *Staphylococcus aureus* and *Escherichia coli* infections in rabbit model. It was concluded that the agent can detect both bacterial infections from sterile inflammatory sites and showed more tracer accumulation in *Staphylococcus aureus* infections compared with *Escherichia coli* infections. Optimum time for imaging was 60 minutes after tracer injection (Figure 4) [20]. This peptide also permitted early specific detection of experimental *Staphylococcus aureus* prosthetic joint infections in animal model and resulted in early detection of acute prosthetic joint infection and differentiated well from chronic sterile prosthetic joint inflammation [140]. Endocarditis is another difficult diagnostic question from cardiologist. In an animal study radiolabeled UBI

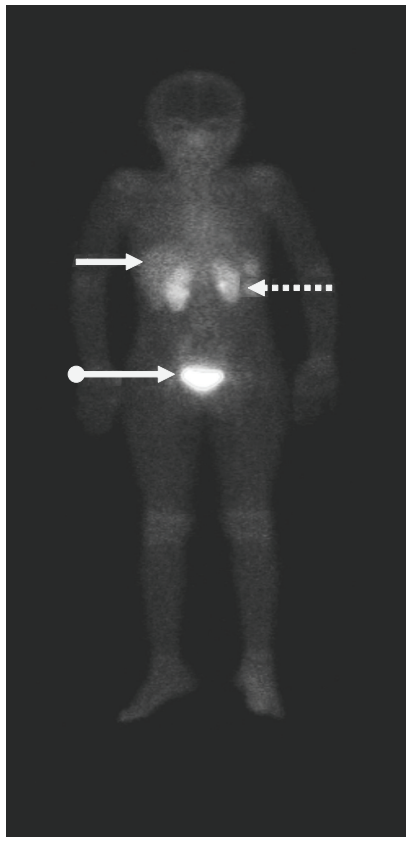

Figure 5: Anterior whole body image at 30 minutes after ^{99m}Tc-UBI 29–41 injection in normal human subject showing kidneys (dotted arrows), liver (solid arrows), and urinary bladder (ball arrow).

29–41 scintigraphy revealed early and specific detection of multidrug-resistant *Staphylococcus-aureus*-induced endocarditis. Furthermore it was concluded that accumulation of tracer depends on the number of viable bacteria in the vegetation and declared it as dedicated noninvasive imaging tool for early detection of infective endocarditis [141].

4.8.10. ^{99m}Tc UBI Scan for Detection of Fungal Infections in Animals. ^{99m}Tc UBI imaging was also studied in animal models for localization of infection induced with *Candida albicans*. It was observed that this antimicrobial peptide showed significant accumulation at the site of infection compared with sterile inflammation [142]. This peptide showed binding with *Candida albicans* and *Aspergillus fumigatus* in addition to viable bacteria. Therefore this agent is useful for detection of fungal infections; however differentiation would be difficult from bacterial infections. However ^{99m}Tc-fluconazole can be used later on, which binds only with *Candida albicans,* shows no binding to bacteria and no accumulation at site of sterile inflammation [143].

4.8.11. ^{99m}Tc UBI for Monitoring Efficacy of Antibacterial Agents. ^{99m}Tc-UBI when injected into *Staphylococcus-aureus*-infected mice after treatment with various doses of cloxacillin and erythromycin showed inverse correlation between accumulation of the peptide at the site of infection and the dose of antibacterial agents. Good correlation was observed between the accumulation of ^{99m}Tc-UBI and the number of viable bacteria. These results indicated the potential of the peptide for evaluating the efficacy of antibiotic therapy. However, minimum number of bacteria that can be detected was 10^3–10^4, which is the limitation for monitoring the effects of the antibacterial agents [144]. Same conclusion was drawn in another study in which commonly used broad-spectrum antibiotic ciprofloxacin was used in a rabbit model. It also revealed that the radiotracer can be used for monitoring efficacy and duration of antibiotic treatment [28].

4.8.12. Biodistribution in Humans. ^{99m}Tc-UBI was investigated in a biokinetic model to evaluate its feasibility as an infection imaging agent in humans. Whole body images from 6 children with suspected bone infection were acquired at 1, 30, 120, 240 minutes and 24 hours after tracer administration. Regions of interest (ROIs) were drawn around source organs (heart, liver, kidneys, and bladder) on each time frame. The same set of ROIs was used for all 6 scans and the counts per minutes (cpm) of each ROI were converted to activity using the conjugate view counting method. Counts were corrected by physical decay and by the background correction factor derived from preclinical phantom studies. The image sequence was used to extrapolate ^{99m}Tc-UBI time-activity curves in each organ and calculate the cumulated activity. Urine samples were used to obtain the cumulative percent of injected activity versus time renal elimination. The absorbed dose in organs was evaluated according to the general equation described in the MIRD formula. In addition, ^{67}Ga-citrate images were obtained from all the patients and used as a control. Biokinetic data showed a fast blood clearance with a mean residence time of 0.52 hour. Approximately 85% of the injected activity was eliminated by renal clearance 24 hours after ^{99m}Tc-UBI administration. Images showed minimal accumulation in nontarget tissues with an average target/nontarget ratio of 2.18 ± 0.74 in positive lesions at 2 hours. All infection positive images were in agreement with those obtained with ^{67}Ga-citrate. The mean radiation-absorbed dose calculated was 0.13 mGy/MBq for kidneys and the effective dose was 4.34×10^{-3} mSv/MBq [145]. Biodistribution of the peptide was also studied in 3 normal subjects in another study by taking anterior and posterior whole body images and using geometric mean method. It was observed that the tracer mainly excreted through the kidneys into urinary bladder followed by liver with no other site of accumulation in the body (Figure 5) [27].

4.8.13. Bacterial Infection Detection in Humans with ^{99m}Tc UBI 29–41. ^{99m}Tc UBI 29–41 showed good correlation for infection detection in humans when compared with ^{67}Ga imaging of the same subjects [145]. In another study the agent was tested in patients suffering from bone, soft tissue, or prosthesis infections and encouraging results were observed with overall sensitivity, specificity, and accuracy of 100%, 80%, and 94.4%, respectively. Maximum tracer accumulation was noted at 30 minutes after tracer injection (Figure 6) [29].

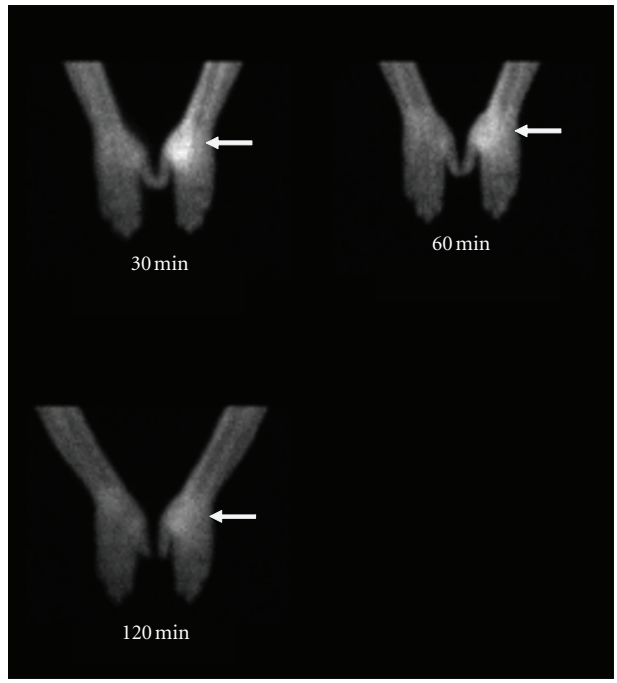

Figure 6: Positive ^{99m}Tc-UBI 29–41 scan in a patient with infection in medial aspect of right hand (arrow). Maximum focal increased tracer uptake was seen at 30 minutes after tracer injection.

This peptide yielded fast and promising results in patients with suspected mediastinitis after cardiac surgery. Qualitative analysis correctly identified infection in 5/6 patients with proven mediastinitis on bacterial culture [146]. Fever of unknown origin (FUO) is also a diagnostic dilemma for physicians and surgeons. Antibiotics are blindly used without localizing the infective focus. This antimicrobial peptide revealed specificity of 95.35% for localizing infection and discarding sterile inflammation. Sensitivity was 97.52% with high accuracy [147]. Vertebral osteomyelitis is difficult to diagnose by noninvasive diagnostic modalities including CT, MRI, radionuclide bone scan, and X-Ray. Even ^{67}Ga scan is nonspecific test which is considered better than other diagnostic techniques. As UBI 29–41 has special affinity for binding to viable bacteria, this has been used for confirmation of vertebral infection which showed 100% sensitivity and 88% specificity [148]. Noninvasive diagnostic techniques including three-phase bone scan, MRI, and ^{99m}Tc-UBI 29–41 scan for detection of osteomyelitis were compared. Antimicrobial peptide showed 100% accuracy with maximum mean target to nontarget ratio at 15 minutes after tracer injection, while three-phase bone scan and MRI revealed 90% and 75% accuracy, respectively. This study revealed superiority of antimicrobial peptide imaging over bone scan and MRI [149].

4.8.14. ^{99m}Tc-UBI Scan for Monitoring Efficacy of Antibiotic Treatment in Human Infections. As mentioned in animal studies, binding of ^{99m}Tc UBI 29–41 to viable bacteria is proportional to their number in the infective focus. Intensity of tracer uptake decreased when number of viable bacteria was reduced. Therefore it was concluded that this tracer can be used for monitoring efficacy and duration of treatment [28, 144]. Similar study for monitoring antibiotic therapy in patients with orthopaedic infections showed better results on quantitative analysis of scan at 30, 60, and 120 minutes after tracer injection after 10–14, day interval with antibiotic treatment when compared with erythrocyte sedimentation rate, C-reactive protein, and radioisotope bone scan [150].

5. Limitations of Antimicrobial Peptides

5.1. Lack of Discrimination between Different Infectious Agents. ^{99m}Tc-labeled antimicrobial peptides bind to fungi in addition to bacterial cell membranes; however, infection either from bacteria or fungi can be differentiated from sterile inflammatory sites [24]. Similarly, there is nonuniform accumulation of radiolabeled peptides in different types of bacteria. *Staphylococcus aureus* showed more uptake than *Escherichia coli* which may be due to different mode of toxicity [27].

5.2. Lack of Detection of Intracellular Pathogens. Radiolabeled peptides bind to the cell membranes of the bacteria. However, if the bacteria are engulfed by the anti-inflammatory cells or become intracellular after invasion of the host immune cells, their detection would become difficult with scintigraphy [123].

5.3. Resistance against Antimicrobial Peptides. Major concern with use of the labeled antibiotics as specific infection localization tracers is the development of resistance. Similar situation may also be encountered with antimicrobial peptides. Some Gram-negative bacteria can modify the lipid-A moiety of the endotoxin [151]. Similarly Gram-positive bacteria can reduce negative charge of the bacterial surface

by esterification of phospholipids of *Staphylococcus aureus* [152]. Inactivation of antimicrobial peptides by bacterial serine proteases can prevent intracellular accumulation of the peptides [153]. However, in multiple studies conducted with different radiolabeled antimicrobial peptides including UBI (29–41) have not revealed such evidence up till now.

6. Conclusion

The medical community often faces the dilemma of discrimination between infection and inflammation on medical as well as on surgical floors. Nonspecific radiotracers for localization of infection/inflammation do not solve the problem. Among the specific radiotracers for localization of infection, antibiotics gained more popularity due to easy availability, labeling, low cost, and high sensitivity. Among the labeled antibiotics ciprofloxacin was the most successful specific bacterial localization agent which showed sensitivity of 85.4% and specificity of 81.7% [117]. However, emerging antibiotic resistance against antibiotics is also associated with ciprofloxacin [154]. False uptake of ^{99m}Tc-ciprofloxacin in sterile inflammation is also a big disadvantage [14]. Due to nonspecific accumulation in inflammatory sites, this agent has been proposed for identifying the presence and distribution of inflammation in joints [18].

On the other hand, antimicrobial peptides labeled with isotopes are better specific infection localizing agents as they bind specifically to bacterial cell membranes. These tracers detect Gram-positive, Gram-negative bacteria, *Candida albicans* and *Aspergillus Fumigatus* infections. The amount of radiolabeled peptides at the site of infection depends on the number of viable organisms present at the focus. Recently investigated antimicrobial peptide, ubiquicidin UBI (29–41) has shown encouraging results in human clinical trials. This peptide can also be used for monitoring efficacy and duration of antibiotic treatment in patients which is very important issue from prophylactic, therapeutic, and socioeconomic point of view. No doubt, there are limitations attributed to synthesis/isolation of such peptides, labeling with isotopes, minimum detection limit of 10^3 Colony-Forming Unit (CFU) of bacteria, and inability to distinguish between bacterial and fungal infections. In addition, different bacterial types reveal different tracer accumulation (*Staphylococcus aureus* versus *Escherichia coli*). Currently no evidence regarding resistance against antimicrobial peptides has been reported. Considering the merits and demerits of radiolabeled peptides and radiolabeled antibiotics, it can currently be concluded that radiolabeled peptides are better specific infection localizing agents.

References

[1] O. Levy, "Antimicrobial proteins and peptides of blood: templates for novel antimicrobial agents," *Blood*, vol. 96, no. 8, pp. 2664–2672, 2000.

[2] M. R. Yeaman, A. S. Ibrahim, J. E. J. Edwards, A. S. Bayer, and M. A. Ghannoum, "Thrombin-induced rabbit platelet microcidal protein is fungicidal in vitro," *Antimicrob Agents Chemother*, vol. 37, pp. 546–553, 1993.

[3] S. S. Das, A. V. Hall, D. W. Wareham, and K. E. Britten, "Infection imaging with radiopharmaceuticals in the 21st century," *Brazilian Archives of Biology and Technology*, vol. 45, pp. 25–37, 2002.

[4] F. H. M. Corstens and J. W. M. Van Der Meer, "Nuclear medicine's role in infection and inflammation," *Lancet*, vol. 354, no. 9180, pp. 765–770, 1999.

[5] A. M. Peters, H. J. Danpure, S. Osman et al., "Preliminary clinical experience with ^{99m}Tc-hexamethylpropylene-amineoxime for labelling leucocytes and imaging infection," *The Lancet*, vol. 2, pp. 945–949, 1986.

[6] A. M. Peters, "The utility of [^{99m}Tc]HMPAO-leukocytes for imaging infection," *Seminars in Nuclear Medicine*, vol. 24, no. 2, pp. 110–127, 1994.

[7] S. Gratz, H. J. J. M. Rennen, O. C. Boerman et al., "^{99m}Tc-HMPAO-labeled autologous versus heterologous leukocytes for imaging infection," *Journal of Nuclear Medicine*, vol. 43, no. 7, pp. 918–924, 2002.

[8] W. Becker and J. Meller, "The role of nuclear medicine in infection and inflammation," *Lancet Infectious Diseases*, vol. 1, no. 5, pp. 326–333, 2001.

[9] C. Love and C. J. Palestro, "Radionuclide imaging of infection," *Journal of Nuclear Medicine Technology*, vol. 32, no. 2, pp. 47–57, 2004.

[10] L. Filippi and O. Schillaci, "Usefulness of hybrid SPECT/CT in ^{99m}TC-HMPAO-labeled leukocyte scintigraphy for bone and joint infections," *Journal of Nuclear Medicine*, vol. 47, no. 12, pp. 1908–1913, 2006.

[11] R. Bar-Shalom, N. Yefremov, L. Guralnik et al., "SPECT/CT using 67Ga and 111In-labeled leukocyte scintigraphy for diagnosis of infection," *Journal of Nuclear Medicine*, vol. 47, no. 4, pp. 587–594, 2006.

[12] N. Dumarey, D. Egrise, D. Blocklet et al., "Imaging infection with 18F-FDG-labeled leukocyte PET/CT: initial experience in 21 patients," *Journal of Nuclear Medicine*, vol. 47, no. 4, pp. 625–632, 2006.

[13] B. Fournier, X. Zhao, T. Lu, K. Drlica, and D. C. Hooper, "Selective targeting of topoisomerase IV and DNA gyrase in Stphylococcus aureus: different patterns of quinolone-induced inhibition of DNA Synthesis," *Antimicrob Agents Chemother*, vol. 44, pp. 2160–2165, 2000.

[14] Z. Yapar, M. Kibar, A. F. Yapar, E. Toğrul, U. Kayaselçuk, and Y. Sarpel, "The efficacy of technetium-99m ciprofloxacin (Infecton) imaging in suspected orthopaedic infection: a comparison with sequential bone/gallium imaging," *European Journal of Nuclear Medicine*, vol. 28, no. 7, pp. 822–830, 2001.

[15] K. Sonmezoglu, M. Sonmezoglu, M. Halac et al., "Usefulness of ^{99m}Tc-ciprofloxacin (infecton) scan in diagnosis of chronic orthopedic infections: comparative study with ^{99m}Tc-HMPAO leukocyte scintigraphy," *Journal of Nuclear Medicine*, vol. 42, no. 4, pp. 567–574, 2001.

[16] M. J. Larikka, A. K. Ahonen, O. Niemela et al., "^{99m}Tc-ciprofloxacin (infection) imaging in the diagnosis of knee prosthesis infections," *Nuclear Medicine Communications*, vol. 23, pp. 167–170, 2002.

[17] L. Sarda, A. C. Crémieux, Y. Lebellec et al., "Inability of ^{99m}Tc-ciprofloxacin scintigraphy to discriminate between septic and sterile osteoarticular diseases," *Journal of Nuclear Medicine*, vol. 44, no. 6, pp. 920–926, 2003.

[18] T. Appelboom, P. Emery, L. Tant, N. Dumarey, and A. Schoutens, "Evaluation of technetium-99m-ciprofloxacin (infection) for detecting sites of inflammation in arthritis," *Rheumatology*, vol. 42, no. 10, pp. 1179–1182, 2003.

[19] M. E. Jones, N. M. Boenink, J. Verhoef, K. Kohrer, and F. J. Schmitz, "Multiple mutations conferring ciprofloxacin resistance in staphylococcus aureus demonstrate long-term stability in an antibiotic free environment," *Journal of Antimicrobial Chemotherapy*, vol. 45, pp. 353–356, 2000.

[20] M. Zasloff, "Antimicrobial peptides of multicellular organisms," *Nature*, vol. 415, no. 6870, pp. 389–395, 2002.

[21] M. M. Welling, P. H. Nibbering, A. Paulusma-Annema, P. S. Hiemstra, E. K. J. Pauwels, and W. Calame, "Imaging of bacterial infections with ^{99m}Tc-labeled human neutrophil peptide-1," *Journal of Nuclear Medicine*, vol. 40, no. 12, pp. 2073–2080, 1999.

[22] P. S. Hiemstra, M. T. Van Den Barselaar, M. Roest, P. H. Nibbering, and R. Van Furth, "Ubiquicidin, a novel murine microbicidal protein present in the cytosolic fraction of macrophages," *Journal of Leukocyte Biology*, vol. 66, no. 3, pp. 423–428, 1999.

[23] M. M. Welling, S. Mongera, A. Lupetti et al., "Radiochemical and biological characteristics of ^{99m}Tc-UBI 29-41 for imaging of bacterial infections," *Nuclear Medicine and Biology*, vol. 29, no. 4, pp. 413–422, 2002.

[24] M. M. Welling, A. Lupetti, H. S. Balter et al., "^{99m}Tc-labeled antimicrobial peptides for detection of bacterial and Candida albicans infections," *Journal of Nuclear Medicine*, vol. 42, no. 5, pp. 788–794, 2001.

[25] R. M. Epand and H. J. Vogel, "Diversity of antimicrobial peptides and their mechanisms of action," *Biochimica et Biophysica Acta*, vol. 1462, no. 1-2, pp. 11–28, 1999.

[26] M. Edgerton, S. E. Koshlukova, T. E. Lo, B. G. Chrzan, R. M. Straubinger, and P. A. Raj, "Candidacidal activity of salivary histatins: identification of a histatin 5-binding protein on Candida albicans," *Journal of Biological Chemistry*, vol. 273, no. 32, pp. 20438–20447, 1998.

[27] M. S. Akhtar, J. Iqbal, M. A. Khan et al., "^{99m}Tc-labeled antimicrobial peptide ubiquicidin (29-41) accumulates less in Escherichia coli infection than in Staphlococcus aureus infection," *Journal of Nuclear Medicine*, vol. 45, no. 5, pp. 849–856, 2004.

[28] M. S. Akhtar, M. E. Khan, B. Khan et al., "An imaging analysis of ^{99m}Tc-UBI (29-41) uptake in S. aureus infected thighs of rabbits on ciprofloxacin treatment," *European Journal of Nuclear Medicine and Molecular Imaging*, vol. 35, no. 6, pp. 1056–1064, 2008.

[29] M. S. Akhtar, A. Qaisar, J. Irfanullah et al., "Antimicrobial peptide ^{99m}Tc-Ubiquicidin 29-41 as human infection-imaging agent: clinical trial," *Journal of Nuclear Medicine*, vol. 46, no. 4, pp. 567–573, 2005.

[30] Y. Ito, S. Okuyama, T. Awano, K. Takahashi, and T. Sato, "Diagnostic evaluation of 67 Ga scanning of lung cancer and other diseases.," *Radiology*, vol. 101, no. 2, pp. 355–362, 1971.

[31] R. D. Neuman and J. G. McAfee, "Gallium-67 imaging in infection," in *Diagnostic Nuclear Medicine*, M. P. Sandler, J. A. Patton, R. E. Coleman, A. Gottschalk, F. J. Wackers, and P. B. Hoffer, Eds., pp. 1493–1507, Williams and Wilkins, Baltimore, Md, USA, 3rd edition, 1996.

[32] M. F. Tsan, "Mechanism of gallium-67 accumulation in inflammatory lesions," *Journal of Nuclear Medicine*, vol. 26, no. 1, pp. 88–92, 1985.

[33] R. K. Zeman and T. W. Ryerson, "The value of bowel preparation in Ga-67 citrate scanning: concise communication," *Journal of Nuclear Medicine*, vol. 18, no. 9, pp. 886–889, 1977.

[34] O. James, E. J. Wood, and S. Sherlock, "67Gallium scanning in the diagnosis of liver disease," *Gut*, vol. 15, no. 5, pp. 404–410, 1974.

[35] D. Front, O. Israel, R. Epelbaum et al., "Ga-67 SPECT before and after treatment of lymphoma," *Radiology*, vol. 175, no. 2, pp. 515–519, 1990.

[36] C. J. Palestro, "The current role of gallium imaging in infection," *Seminars in Nuclear Medicine*, vol. 24, no. 2, pp. 128–141, 1994.

[37] E. V. Staab and W. H. McCartney, "Role of Gallium 67 in inflammatory disease," *Seminars in Nuclear Medicine*, vol. 8, no. 3, pp. 219–234, 1978.

[38] M. A. Auler, S. Bagg, and L. Gordon, "The role of nuclear medicine in imaging infection," *Seminars in Roentgenology*, vol. 42, no. 2, pp. 117–121, 2007.

[39] A. J. Fischman, R. H. Rubin, J. A. White et al., "Localization of Fc and Fab fragments of nonspecific polyclonal IgG at focal sites of inflammation," *Journal of Nuclear Medicine*, vol. 31, no. 7, pp. 1199–1205, 1990.

[40] A. J. Fischman, A. J. Fucello, J. L. Pellegrino-Gensey et al., "Effect of carbohydrate modification on the localization of human polyclonal IgG at focal sites of bacterial infection," *Journal of Nuclear Medicine*, vol. 33, no. 7, pp. 1378–1382, 1992.

[41] M. W. Nijhof, W. J. G. Oyen, A. Van Kämpen, R. A. M. J. Ciaessens, J. W. M. Van Der Meer, and F. H. M. Corstens, "Evaluation of infections of the locomotor system with indium-111 -labeled human IgG scintigraphy," *Journal of Nuclear Medicine*, vol. 38, no. 8, pp. 1300–1305, 1997.

[42] J. R. Buscombe, W. J. G. Oyen, A. Grant et al., "Indium-111-labeled polyclonal human immunoglobulin: identifying focal infection in patients positive for human immunodeficiency virus," *Journal of Nuclear Medicine*, vol. 34, no. 10, pp. 1621–1625, 1993.

[43] L. Mairal, P. A. De Uma, J. Martin-Comin et al., "Simultaneous administration of 111In-human immunoglobulin and ^{99m}Tc-HMPAO labelled leucocytes in inflammatory bowel disease," *European Journal of Nuclear Medicine*, vol. 22, no. 7, pp. 664–670, 1995.

[44] W. Becker, J. Bair, T. Behr et al., "Detection of soft-tissue infections and osteomyelitis using a technetium- 99m-labeled anti-granulocyte monoclonal antibody fragment," *Journal of Nuclear Medicine*, vol. 35, no. 9, pp. 1436–1443, 1994.

[45] O. C. Boerman, G. Storm, W. J. G. Oyen et al., "Sterically stabilized liposomes labeled with Indium-111 to image focal infection," *Journal of Nuclear Medicine*, vol. 36, no. 9, pp. 1639–1644, 1995.

[46] P. Laverman, E. T. M. Dams, W. J. G. Oyen et al., "A novel method to label liposomes with ^{99m}Tc by the hydrazino nicotinyl derivative," *Journal of Nuclear Medicine*, vol. 40, no. 1, pp. 192–197, 1999.

[47] E. T. M. Dams, W. J. G. Oyen, O. C. Boerman et al., "^{99m}Tc-PEG liposomes for the scintigraphic detection of infection and inflammation: clinical evaluation," *Journal of Nuclear Medicine*, vol. 41, no. 4, pp. 622–630, 2000.

[48] D. J. Hnatowich, F. Virzi, and M. Rusckowski, "Investigations of avidin and biotin for imaging applications," *Journal of Nuclear Medicine*, vol. 28, no. 8, pp. 1294–1302, 1987.

[49] M. Rusckowski, B. Fritz, and D. J. Hnatowich, "Localization of infection using streptavidin and biotin: an alternative to nonspecific polyclonal immunoglobulin," *Journal of Nuclear Medicine*, vol. 33, no. 10, pp. 1810–1815, 1992.

[50] A. Samuel, G. Paganelli, R. Chiesa et al., "Detection of prosthetic vascular graft infection using avidin/indium-111-biotin scintigraphy," *Journal of Nuclear Medicine*, vol. 37, no. 1, pp. 55–61, 1996.

[51] M. Rusckowski, G. Paganelli, D. J. Hnatowich et al., "Imaging osteomyelitis with streptavidin and Indium-111-labeled biotin," *Journal of Nuclear Medicine*, vol. 37, no. 10, pp. 1655–1662, 1996.

[52] C. J. Palestro and M. A. Torres, "Radionuclide imaging of nonosseous infection," *Quarterly Journal of Nuclear Medicine*, vol. 43, no. 1, pp. 46–60, 1999.

[53] E. Outwater, E. Oates, and R. C. Sarno, "Indium-111-labeled leukocyte scintigraphy: diagnosis of subperiosteal abscesses complicating osteomyelitis in a child," *Journal of Nuclear Medicine*, vol. 29, no. 11, pp. 1871–1874, 1988.

[54] F. L. Datz and D. A. Thorne, "Cause and significance of cold bone defects on Indium-111-labeled leukocyte imaging," *Journal of Nuclear Medicine*, vol. 28, no. 5, pp. 820–823, 1987.

[55] K. Uno, N. Matsui, and K. Nohira, "Indium-111 leukocyte imaging in patients with rheumatoid arthritis," *Journal of Nuclear Medicine*, vol. 27, no. 3, pp. 339–344, 1986.

[56] D. S. Schauwecker, H. M. Park, R. W. Burt, B. H. Mock, and H. N. Wellman, "Combined bone scintigraphy and indium-111 leukocyte scans in neuropathic foot disease," *Journal of Nuclear Medicine*, vol. 29, no. 10, pp. 1651–1655, 1988.

[57] L. M. Lamki, L. P. Kasi, and T. P. Haynie, "Localization of Indium-111 leukocytes in noninfected neoplasms," *Journal of Nuclear Medicine*, vol. 29, no. 12, pp. 1921–1926, 1988.

[58] C. J. Palestro, H. H. Mehta, M. Patel et al., "Marrow versus infection in the Charcot joint: indium-111 leukocyte and technetium-99m sulfur colloid scintigraphy," *Journal of Nuclear Medicine*, vol. 39, no. 2, pp. 346–350, 1998.

[59] W. J. G. Oyen, R. A. M. J. Claessens, J. W. M. Van der Meer, and F. H. M. Corstens, "Detection of subacute infectious foci with indium-111-labeled autologous leukocytes and indium-111-labeled human nonspecific immunoglobulin G: a prospective comparative study," *Journal of Nuclear Medicine*, vol. 32, no. 10, pp. 1854–1860, 1991.

[60] J. G. McAfee, G. Gagne, G. Subramanian, and R. F. Schneider, "The localization of indium-111-leukocytes, gallium-67-polyclonal IgG and other radioactive agents in acute focal inflammatory lesions," *Journal of Nuclear Medicine*, vol. 32, no. 11, pp. 2126–2131, 1991.

[61] C. J. Palestro, C. K. Kim, A. J. Swyer, S. Vallabhajosula, and S. J. Goldsmith, "Radionuclide diagnosis of vertebral osteomyelitis: indium-111-leukocyte and technetium-99m-methylene diphosphonate bone scintigraphy," *Journal of Nuclear Medicine*, vol. 32, no. 10, pp. 1861–1865, 1991.

[62] F. L. Datz, "Indium-111-labeled leukocytes for the detection of infection: current status," *Seminars in Nuclear Medicine*, vol. 24, no. 2, pp. 92–109, 1994.

[63] S. L. Kipper, "Radiolabelled leukocyte imaging of the abdomen," in *Nuclear Medicine Annual*, L. M. Freeman, Ed., pp. 81–126, Raven Press, New York, NY, USA, 1995.

[64] J. H. Thrall and H. A. Ziessman, "Infection and inflammation," in *Nuclear Medicine: The Requisites*, J. H. Thrall, Ed., pp. 167–192, Mosby, 2nd edition, 2001.

[65] M. E. Roddie, A. M. Peters, H. J. Danpure et al., "Inflammation: imaging with Tc-99m HMPAO-labeled leukocytes," *Radiology*, vol. 166, no. 3, pp. 767–772, 1988.

[66] M. Vorne, I. Soini, T. Lantto, and S. Paakkinen, "Technetium-99m HM-PAO-labeled leukocytes in detection of inflammatory lesions: comparison with Gallium-67 citrate," *Journal of Nuclear Medicine*, vol. 30, no. 8, pp. 1332–1336, 1989.

[67] I. Hovi, M. Taavitsainen, T. Lantto, M. Vorne, R. Paul, and K. Remes, "Technetium-99m-HMPAO-labeled leukocytes and technetium-99m-labeled human polyclonal immunoglobulin G in diagnosis of focal purulent disease," *Journal of Nuclear Medicine*, vol. 34, no. 9, pp. 1428–1434, 1993.

[68] E. H. Lantto, T. J. Lantto, and M. Vorne, "Fast diagnosis of abdominal infections and inflammations with technetium-99m-HMPAO labeled leukocytes," *Journal of Nuclear Medicine*, vol. 32, no. 11, pp. 2029–2034, 1991.

[69] E. H. Lantto, T. J. Lantto, and M. Vorne, "Fast diagnosis of abdominal infections and inflammations with technetium-99m-HMPAO labeled leukocytes," *Journal of Nuclear Medicine*, vol. 32, no. 11, pp. 2029–2034, 1991.

[70] F. Palermo, F. Boccaletto, A. Paolin et al., "Comparison of technetium-99m-MDP, technetium-99-m-WBC and technetium- 99m-HIG in musculoskeletal inflammation," *Journal of Nuclear Medicine*, vol. 39, no. 3, pp. 516–521, 1998.

[71] W. Becker, U. Borst, W. Fischbach, B. Pasurka, R. Schafer, and W. Borner, "Kinetic data of in-vivo labeled granulocytes in humans with a murine Tc-99m-labelled monoclonal antibody," *European Journal of Nuclear Medicine*, vol. 15, no. 7, pp. 361–366, 1989.

[72] W. S. Becker, A. Saptogino, and F. G. Wolf, "The single late 99Tcm granulocyte antibody scan in inflammatory diseases," *Nuclear Medicine Communications*, vol. 13, no. 3, pp. 186–192, 1992.

[73] W. Becker, J. Bair, T. Behr et al., "Detection of soft-tissue infections and osteomyelitis using a technetium- 99m-labeled anti-granulocyte monoclonal antibody fragment," *Journal of Nuclear Medicine*, vol. 35, no. 9, pp. 1436–1443, 1994.

[74] M. L. Thakur, C. S. Marcus, P. Henneman et al., "Imaging inflammatory diseases with neutrophil-specific technetium-99m-labeled monoclonal antibody anti-SSEA-1," *Journal of Nuclear Medicine*, vol. 37, no. 11, pp. 1789–1795, 1996.

[75] S. L. Kipper, E. B. Rypins, D. G. Evans, M. L. Thakur, T. D. Smith, and B. Rhodes, "Neutrophil-specific ^{99m}Tc-labeled anti-CD 15 monoclonal antibody imaging for diagnosis of equivocal appendicitis," *Journal of Nuclear Medicine*, vol. 41, no. 3, pp. 449–455, 2000.

[76] S. Gratz, T. Behr, A. Herrmann et al., "Intraindividual comparison of ^{99m}Tc-labelled anti-SSEA-1 antigranulocyte antibody and ^{99m}Tc-HMPAO labelled white blood cells for the imaging of infection," *European Journal of Nuclear Medicine*, vol. 25, no. 4, pp. 386–393, 1998.

[77] W. Becker, D. M. Goldenberg, and F. Wolf, "The use of monoclonal antibodies and antibody fragments in the imaging of infectious lesions," *Seminars in Nuclear Medicine*, vol. 24, no. 2, pp. 142–153, 1994.

[78] A. J. Fischman, M. C. Pike, D. Kroon et al., "Imaging focal sites of bacterial infection in rats with indium-111- labeled chemotactic peptide analogs," *Journal of Nuclear Medicine*, vol. 32, no. 3, pp. 483–491, 1991.

[79] J. W. Babich, W. Graham, S. A. Barrow et al., "Technetium-99m-labeled chemotactic peptides: comparison with Indium-111- labeled white blood cells for localizing acute bacterial infection in the rabbit," *Journal of Nuclear Medicine*, vol. 34, no. 12, pp. 2176–2181, 1993.

[80] A. J. Fischman, D. Rauh, H. Solomon et al., "In vivo bioactivity and biodistribution of chemotactic peptide analogs in nonhuman primates," *Journal of Nuclear Medicine*, vol. 34, no. 12, pp. 2130–2134, 1993.

[81] J. W. Babich, Q. Dong, W. Graham et al., "A novel high affinity chemotactic peptide antagonist for infection imaging," *Journal of Nuclear Medicine*, vol. 38: 268, 1997.

[82] A. D. Luster, "Mechanisms of disease: chemokines-chemotactic cytokines that mediate inflammation," *New England Journal of Medicine*, vol. 338, no. 7, pp. 436–445, 1998.

[83] C. J. Van der Laken, O. C. Boerman, W. J. G. Oyen et al., "Specific targeting of infectious foci with radioiodinated human recombinant interleukin-1 in an experimental model," *European Journal of Nuclear Medicine*, vol. 22, no. 11, pp. 1249–1255, 1995.

[84] C. J. vanderLaken, O. C. Boerman, W. J. G. Oyen et al., "Comparison of radiolabeled human recombinant interleukin-1 with its receptor antagonist in a model of infection," *European Journal of Nuclear Medicine*, vol. 22: 916, 1995.

[85] A. Signore, M. Chianelli, A. Annovazzi et al., "123I-Interleukin-2 scintigraphy for in vivo assessment of intestinal mononuclear cell infiltration in Crohn's disease," *Journal of Nuclear Medicine*, vol. 41, no. 2, pp. 242–249, 2000.

[86] A. Signore, M. Chianelli, A. Annovazzi et al., "Imaging active lymphocytic infiltration in coeliac disease with iodine- 123-interleukin-2 and the response to diet," *European Journal of Nuclear Medicine*, vol. 27, no. 1, pp. 18–24, 2000.

[87] M. D. Gross, B. Shapiro, R. S. Skinner, P. Shreve, L. M. Fig, and R. V. Hay, "Scintigraphy of osteomyelitis in man with human recombinant interleukin-8," *Journal of Nuclear Medicine*, vol. 37: 25, 1996.

[88] R. V. Hay, R. S. Skinner, O. C. Newman et al., "Scintigraphy of acute inflammatory lesions in rats with radliolabelled recombinant human interleukin-8," *Nuclear Medicine Communications*, vol. 18, no. 4, pp. 367–378, 1997.

[89] C. J. Van Der Laken, O. C. Boerman, W. J. G. Oyen, M. T. P. Van De Ven, J. W. M. Van Der Meer, and F. H. M. Corstens, "Radiolabeled interleukin-8: specific scintigraphic detection of infection within a few hours," *Journal of Nuclear Medicine*, vol. 41, no. 3, pp. 463–469, 2000.

[90] H. J. J. M. Rennen, O. C. Boernan, W. J. G. Oyen, J. W. M. Van der Meer, and F. H. M. Corstens, "Specific and rapid scintigraphic detection of infection with ^{99m}Tc-labeled interleukin-8," *Journal of Nuclear Medicine*, vol. 42, no. 1, pp. 117–123, 2001.

[91] S. Gratz, H. J. J. M. Rennen, O. C. Boerman, W. J. G. Oyen, and F. H. M. Corstens, "Rapid imaging of experimental colitis with ^{99m}Tc-interleukin-8 in rabbits," *Journal of Nuclear Medicine*, vol. 42, no. 6, pp. 917–923, 2001.

[92] B. R. Moyer, S. Vallabhajosula, J. Lister-James et al., "Technetium-99m-White Blood Cell-Specific Imaging Agent Developed from Platelet Factor 4 to Detect Infection," *Journal of Nuclear Medicine*, vol. 37, no. 4–6, pp. 673–679, 1996.

[93] C. J. Palestro, M. B. Tomas, K. K. Bhargava et al., "Tc-99m P483H for imaging infection: phase 2 multicenter trial results," *Journal of Nuclear Medicine*, vol. 40:15, 1999.

[94] G. I. Bell, C. F. Burant, J. Takeda, and G. W. Gould, "Structure and function of mammalian facilitative sugar transporters," *Journal of Biological Chemistry*, vol. 268, no. 26, pp. 19161–19164, 1993.

[95] E. K. J. Pauwels, M. J. Ribeiro, J. H. M. B. Stoot, V. R. McCready, M. Bourguignon, and B. Mazière, "FDG accumulation and tumor biology," *Nuclear Medicine and Biology*, vol. 25, no. 4, pp. 317–322, 1998.

[96] H. Zhuang and A. Alavi, "18-Fluorodeoxyglucose positron emission tomographic imaging in the detection and monitoring of infection and inflammation," *Seminars in Nuclear Medicine*, vol. 32, no. 1, pp. 47–59, 2002.

[97] J. Y. Paik, K. H. Lee, S. C. Yearn, Y. Choi, and B. T. Kim, "Augmented 18F-FDG uptake in activated monocytes occurs during the priming process and involves tyrosine kinases and protein kinase C," *Journal of Nuclear Medicine*, vol. 45, no. 1, pp. 124–128, 2004.

[98] P. D. Shreve, Y. Anzai, and R. L. Wahl, "Pitfalls in oncologic diagnosis with FDG PET imaging: physiologic and benign variants," *Radiographics*, vol. 19, no. 1, pp. 61–77, 1999.

[99] T. Nakahara, H. Fujii, M. Ide et al., "FDG uptake in the morphologically normal thymus: comparison of FDG position emission tomography and CT," *British Journal of Radiology*, vol. 74, pp. 821–824, 2001.

[100] C. Love, M. B. Tomas, G. G. Tronco, and C. J. Palestro, "FDG PET of infection and inflammation," *Radiographics*, vol. 25, no. 5, pp. 1357–1368, 2005.

[101] A. Guhlmann, D. Brecht-Krauss, G. Suger et al., "Fluorine-18-FDG PET and technetium-99m antigranulocyte antibody scintigraphy in chronic osteomyelitis," *Journal of Nuclear Medicine*, vol. 39, no. 12, pp. 2145–2152, 1998.

[102] Y. Sugawara, D. K. Braun, P. V. Kison, J. E. Russo, K. R. Zasadny, and R. L. Wahl, "Rapid detection of human infections with fluorine-18 fluorodeoxyglucose and positron emission tomography: preliminary results," *European Journal of Nuclear Medicine*, vol. 25, no. 9, pp. 1238–1243, 1998.

[103] R. F. Yen, Y. C. Chen, Y. W. Wu, M. H. Pan, and S. C. Chang, "Using 18-fluoro-2-deoxyglucose position emission tomography in detecting infectious endocarditis/endoarteritis: a preliminary report," *Academic Radiology*, vol. 11, pp. 316–321, 2004.

[104] A. Guhlmann, D. Brecht-Krauss, G. Suger et al., "Chronic osteomyelitis: detection with FDG PET and correlation with histopathologic findings," *Radiology*, vol. 206, no. 3, pp. 749–754, 1998.

[105] T. Kälicke, A. Schmitz, J. H. Risse et al., "Fluorine-18 fluorodeoxyglucose PET in infectious bone diseases: results of histologically confirmed cases," *European Journal of Nuclear Medicine*, vol. 27, no. 5, pp. 524–528, 2000.

[106] K. D. M. Stumpe, H. Dazzi, A. Schaffner, and G. K. Von Schulthess, "Infection imaging using whole-body FDG-PET," *European Journal of Nuclear Medicine*, vol. 27, no. 7, pp. 822–832, 2000.

[107] M. Schiesser, K. D. M. Stumpe, O. Trentz, T. Kossmann, and G. K. Von Schulthess, "Detection of metallic implant-associated infections with FDG PET in patients with trauma: correlation with microbiologic results," *Radiology*, vol. 226, no. 2, pp. 391–398, 2003.

[108] C. Love and C. J. Palestro, "18F-FDG and 67Ga-SPECT imaging in suspected vertebral osteomyelitis: an intraindividual comparison," *Journal of Nuclear Medicine*, vol. 45, supplement: 148, 2003.

[109] S. Yamada, K. Kubota, R. Kubota, T. Ido, and N. Tamahashi, "High accumulation of fluorine-18-fluorodeoxyglucose in turpentine-induced inflammatory tissue," *Journal of Nuclear Medicine*, vol. 36, no. 7, pp. 1301–1306, 1995.

[110] Z. Keidar, D. Militianu, E. Melamed, R. Bar-Shalom, and O. Israel, "The diabetic foot: initial experience with 18F-FDG PET/CT," *Journal of Nuclear Medicine*, vol. 46, no. 3, pp. 444–449, 2005.

[111] A. Kjaer, A. M. Lebech, A. Eigtved, and L. Højgaard, "Fever of unknown origin: prospective comparison of diagnostic value of 18F-FDG PET and 111In-granulocyte scintigraphy," *European Journal of Nuclear Medicine and Molecular Imaging*, vol. 31, no. 5, pp. 622–626, 2004.

[112] D. C. Hooper, J. S. Wolfson, E. Y. Ng, and M. N. Swartz, "Mechanisms of action of and resistance to ciprofloxacin," *American Journal of Medicine*, vol. 82, no. 4, pp. 12–20, 1987.

[113] S. Vinjamuri, A. V. Hall, K. K. Solanki et al., "Comparison of ^{99m}Tc infecton imaging with radiolabelled white-cell imaging in the evaluation of bacterial infection," *Lancet*, vol. 347, no. 8996, pp. 233–235, 1996.

[114] A. V. Hall, K. K. Solanki, S. Vinjamuri et al., "Evaluation of the efficacy of ^{99m}Tc-Infecton: a novel agent for detecting sites of infection," *Journal of Clinical Pathology*, vol. 51, pp. 215–219, 1996.

[115] J. L. Martinez, A. Alonso, J. M. Gonez-Gomez, and F. Baquero, "Quinolone resistance by mutations in chromosomal gyrase genes," *Journal of Antimicrobial Chemotherapy*, vol. 42, pp. 683–671, 1998.

[116] F. De Winter, C. Van de Wiele, F. Dumont et al., "Biodistribution and dosimetry of ^{99m}Tc-ciprofloxacin, a promising agent for the diagnosis of bacterial infection," *European Journal of Nuclear Medicine*, vol. 28, no. 5, pp. 570–574, 2001.

[117] K. E. Britton, S. Vinjamuri, A. V. Hall et al., "Clinical evaluation of technetium-99m infecton for the localisation of bacterial infection," *European Journal of Nuclear Medicine*, vol. 24, no. 5, pp. 553–556, 1997.

[118] K. E. Britton, D. W. Wareham, S. S. Das et al., "Imaging bacterial infection with ^{99m}Tc-Ciprofloxacin (infecton)," *Journal of Clinical Pathology*, vol. 55, pp. 817–823, 2002.

[119] A. K. Singh, J. Verma, A. Bhatnagar, and A. Ali, "^{99m}Tc-labelled sparfloxacin: a specific infection imaging agent," *World Journal of Nuclear Medicine*, vol. 1, pp. 103–109, 2003.

[120] R. H. Siaens, H. J. Rennen, O. C. Boerman, R. Dierckx, and G. Slegers, "Synthesis and comparison of ^{99m}Tc-enrofloxacin and ^{99m}Tc-ciprofloxacin," *Journal of Nuclear Medicine*, vol. 45, no. 12, pp. 2088–2094, 2004.

[121] V. Gomes Barreto, F. Iglesias, M. Roca, F. Tabau, and J. Martin-Comin, "Labelling of cefizoxime with ^{99m}Tc," *Revista Española de Medicina Nuclear*, vol. 19, pp. 479–483, 2000.

[122] J. Verma, A. k. Singh, A. Bhatnagar et al., "Radio-labeling of Ethambutol with technetium-99m and its evaluation for detection of tuberculosis," *World Journal of Nuclear Medicine*, vol. 4, pp. 35–46, 2005.

[123] A. K. Singh, J. Verma, A. Bhatnagar, S. Sen, and M. Bose, "Tc-99m isoniazid: a specific agent for diagnosis of tuberculosis," *World Journal of Nuclear Medicine*, vol. 2, pp. 292–305, 2003.

[124] A. Lupetti, M. M. Welling, U. Mazzi, P. H. Nibbering, and E. K. Pauwels, "Technetium-99m labelled fluconazole and antimicrobial peptides for imaging of Candida albicans and Aspergillus fumigatus infections," *European Journal of Nuclear Medicine*, vol. 29, no. 5, pp. 674–679, 2002.

[125] A. Lupetti, M. M. Welling, E. K. J. Pauwels, and P. H. Nibbering, "Radiolabelled antimicrobial peptides for infection detection," *Lancet Infectious Diseases*, vol. 3, no. 4, pp. 223–229, 2003.

[126] A. J. Fischman, J. W. Babich, and H. W. Strauss, "A ticket to ride: peptide radiopharmaceuticals," *Journal of Nuclear Medicine*, vol. 34, no. 12, pp. 2253–2263, 1993.

[127] D. Blok, R. I. J. Feitsma, P. Vermeij, and E. J. K. Pauwels, "Peptide radiopharmaceuticals in nuclear medicine," *European Journal of Nuclear Medicine*, vol. 26, no. 11, pp. 1511–1519, 1999.

[128] P. H. Nibbering, M. M. Welling, P. J. Van Den Broek, K. E. Van Wyngaarden, E. K. J. Pauwels, and W. Calame, "Radiolabelled antimicrobial peptides for imaging of infections: a review," *Nuclear Medicine Communications*, vol. 19, no. 12, pp. 1117–1121, 1998.

[129] R. M. Epand and H. J. Vogel, "Diversity of antimicrobial peptides and their mechanisms of action," *Biochimica et Biophysica Acta*, vol. 1462, no. 1-2, pp. 11–28, 1999.

[130] A. Lupetti, P. H. Nibbering, M. M. Welling, and E. K. J. Pauwels, "Radiopharmaceuticals: new antimicrobial agents," *Trends in Biotechnology*, vol. 21, no. 2, pp. 70–73, 2003.

[131] S. M. Okarvi, "Recent developments in 99Tcm-labelled peptide-based radiopharmaceuticals: an overview," *Nuclear Medicine Communications*, vol. 20, no. 12, pp. 1093–1112, 1999.

[132] E. K. J. Pauwels, M. M. Welling, R. I. J. Feitsma, D. E. Atsma, and W. Nieuwenhuizen, "The labeling of proteins and LDL with ^{99m}Tc: a new direct method employing KBH4 and stannous chloride," *Nuclear Medicine and Biology*, vol. 20, no. 7, pp. 825–833, 1993.

[133] M. M. Welling, A. Paulusma-Annema, H. S. Balter, E. K. J. Pauwels, and P. H. Nibbering, "Technetium-99m labelled antimicrobial peptides discriminate between bacterial infections and sterile inflammations," *European Journal of Nuclear Medicine*, vol. 27, no. 3, pp. 292–301, 2000.

[134] M. M. Welling, P. S. Hiemstra, M. T. Van Den Barselaar et al., "Antibacterial activity of human neutrophil defensins in experimental infections in mice is accompanied by increased leukocyte accumulation," *Journal of Clinical Investigation*, vol. 102, no. 8, pp. 1583–1590, 1998.

[135] M. M. Welling, P. H. Nibbering, A. Paulusma-Annema, P. S. Hiemstra, E. K. J. Pauwels, and W. Calame, "Imaging of bacterial infections with ^{99m}Tc-labeled human neutrophil peptide-1," *Journal of Nuclear Medicine*, vol. 40, no. 12, pp. 2073–2080, 1999.

[136] P. H. Nibbering, M. M. Welling, A. Paulusma-Annema, M. T. vandenBarselaar, and E. K. J. Pauwels, "Monitoring the efficacy of antibacterial treatments of infections with Tc-99m labeled antimicrobial peptides," *Nuclear Medicine Communications*, vol. 21, pp. 575–576, 2000.

[137] P. S. Hiemstra, M. T. Van Den Barselaar, M. Roest, P. H. Nibbering, and R. Van Furth, "Ubiquicidin, a novel murine microbicidal protein present in the cytosolic fraction of macrophages," *Journal of Leukocyte Biology*, vol. 66, no. 3, pp. 423–428, 1999.

[138] G. Ferro-Flores, C. Arteaga De Murphy, M. Pedraza-López et al., "In vitro and in vivo assessment of ^{99m}Tc-UBI specificity for bacteria," *Nuclear Medicine and Biology*, vol. 30, no. 6, pp. 597–603, 2003.

[139] D. Salber, J. Gunawan, K.-J. Langen et al., "Comparison of ^{99m}Tc-and 18F-ubiquicidin autoradiography to anti-staphylococcus aureus immunoflorescence in rat muscle abscesses," *Journal of Nuclear Medicine*, vol. 49, pp. 995–999, 2008.

[140] L. Sarda-Mantel, A. Saleh-Mghir, M. M. Welling et al., "Evaluation of ^{99m}Tc-UBI 29-41 scintigraphy for specific detection of experimental Staphylococcus aureus prosthetic joint infections," *European Journal of Nuclear Medicine and Molecular Imaging*, vol. 34, no. 8, pp. 1302–1309, 2007.

[141] C. P. J. M. Brouwer, F. F. A. Y. Gemmel, and M. M. Welling, "Evaluation of^{99m}Tc-UBI 29-41 scintigraphy for specific detection of experimental multidrug-resistant Staphylococcus aureus bacterial endocarditis," *Quarterly Journal of Nuclear Medicine and Molecular Imaging*, vol. 54, no. 4, pp. 442–450, 2010.

[142] M. M. Welling, A. Lupetti, H. S. Balter et al., "^{99m}Tc-labeled antimicrobial peptides for detection of bacterial and Candida albicans infections," *Journal of Nuclear Medicine*, vol. 42, no. 5, pp. 788–794, 2001.

[143] A. Lupetti, M. M. Welling, U. Mazzi, P. H. Nibbering, and E. K. Pauwels, "Technetium-99m labelled fluconazole and antimicrobial peptides for imaging of Candida albicans and

Aspergillus fumigatus infections," *European Journal of Nuclear Medicine*, vol. 29, no. 5, pp. 674–679, 2002.

[144] P. H. Nibbering, M. M. Welling, A. Paulusma-Annema, C. P. J. M. Brouwer, A. Lupetti, and E. K. J. Pauwels, "^{99m}Tc-labeled UBI 29–41 peptide for monitoring the efficacy of antimicrobial agents in mice infected with staphylococcus aureus," *Journal of Nuclear Medicine*, vol. 45, pp. 321–326, 2004.

[145] L. Meléndez-Alafort, J. Rodríguez-Cortés, G. Ferro-Flores et al., "Biokinetics of ^{99m}Tc-UBI 29-41 in humans," *Nuclear Medicine and Biology*, vol. 31, no. 3, pp. 373–379, 2004.

[146] E. Vallejo, I. Martinz, A. Tejero, S. Hermandez et al., "Clinical utility of ^{99m}Tc-labeled ubiquicidin 29-41 antimicrobial peptide for sctigraphic detection of mediastinitis after cardiac surgery," *Archives of Medical Research*, vol. 39, no. 8, pp. 768–774, 2008.

[147] J. Supulveda-Mendez, C. A. de Murphy, J. C. Rojas-Bautista, and M. Pedraza-Lopez, "Specificity of 99m-Tc-UBI for detecting foci in patients with fever in study," *Nuclear Medicine Communications*, vol. 31, no. 10, pp. 889–895, 2010.

[148] C. Dillmann-Arroyo, R. Cantu-Leal, H. Camp-Nunez, C. Lopez-Carazosc et al., "Application of the ubiquicidin 29-41 scan in the diagnosis of pyogenic vertebral osteomyelitis," *Acta Ortopédica Mexicana*, vol. 25, no. 1, pp. 27–31, 2011.

[149] M. Assadi, K. Vahdat, I. Nabipour, M. R. Sehhat, F. Hadanvand et al., "Diagnostic value of ^{99m}Tc-ubiquicidin scintigraphy for osteomyelitis and comparison with ^{99m}Tc-methylene diphosphonate scintigraphy and magnetic resonance imaging," *Nuclear Medicine Communications*, vol. 32, no. 8, pp. 716–723, 2011.

[150] B. Nazari, Z. Azizmohammadi, M. Rajaei et al., "Role of ^{99m}Tc-ubiquicidin 29-41 scintigraphy to monitor antibiotic therapy in patients with orthopaedic infection: a preliminary study," *Nuclear Medicine Communications*, vol. 32, no. 8, pp. 745–751, 2011.

[151] R. E. Bishop, H. S. Gibbons, T. Guina, M. S. Trent, S. I. Miller, and C. R. H. Raetz, "Transfer of palmitate from phospholipids to lipid A in outer membranes of Gram-negative bacteria," *EMBO Journal*, vol. 19, no. 19, pp. 5071–5080, 2000.

[152] A. Peschel, R. W. Jack, M. Otto et al., "Staphylococcus aureus resistance to human defensins and evasion of neutrophil killing via the novel virulence factor MprF is based on modification of membrane lipids with L-lysine," *Journal of Experimental Medicine*, vol. 193, no. 9, pp. 1067–1076, 2001.

[153] A. Peschel, "How do bacteria resist human antimicrobial peptides?" *Trends in Microbiology*, vol. 10, no. 4, pp. 179–186, 2002.

[154] M. H. Limoncu, S. Ermertcan, C. B. Cetin, G. Cosar, and G. Dinc, "Emergence of phenotypic resistance to ciprofloxacin and levofloxacin in methicillin resistant and methicillin-sensitive staphylococcus aureus strains," *International Journal of Antimicrobial Agents*, vol. 5, pp. 420–424, 2003.

Hindawi Publishing Corporation
International Journal of Peptides
Volume 2012, Article ID 781785, 3 pages
doi:10.1155/2012/781785

Research Article

Pyrazinamide Effects on Cartilage Type II Collagen Amino Acid Composition

Larysa B. Bondarenko and Valentina M. Kovalenko

SI "Institute of Pharmacology and Toxicology" National Academy of Medical Sciences of Ukraine, Eugene Potier 14, 03680 Kyiv, Ukraine

Correspondence should be addressed to Larysa B. Bondarenko, larabon04@yahoo.com

Received 5 December 2011; Revised 13 February 2012; Accepted 16 February 2012

Academic Editor: Katsuhiro Konno

Introduction. Current therapeutic regimens with first-line antitubercular agents are associated to a high rate of adverse effects which could cause pronounced changes in collagen's contents and structure. Investigation of these changes is very important for optimization of antitubercular therapy and minimization of treatment-caused harm. The aim of present paper was to investigate potential effect of pyrazinamide on male rats' cartilage type II collagen amino acid composition. *Materials and Methods*. Wistar albino male rats (160–200 g b.w.) were divided into three groups: I—received pyrazinamide *per os* at a dose of 1000 mg/kg b.w./day; II—at a dose of 2000 mg/kg b.w./day, in both groups it was given for 60 days; III—control. After 60 days of the experiment, rats of the experimental (groups I and II) and control groups were sacrificed and the amino acids contents of male rat cartilage type II collagens were determined using amino acid analyzer. *Results and Discussion*. The study of pyrazinamide effects (administered in different doses) on rat cartilage type II collagen amino acid contents demonstrated presence of dose-dependent pyrazinamide-mediated quantitative and qualitative changes in these rat extracellular matrix proteins in comparison with control.

1. Introduction

There has been resurgence in tuberculosis worldwide. Approximately 2 billion people have latent infection, 8 million would develop active tuberculosis annually, and 2-3 million would die due to tuberculosis. With this resurgence, cases with extrapulmonary tuberculosis have also shown an increase. Approximately 10-11% of extrapulmonary tuberculosis involves joints and bones, which is approximately 1–3% of all tuberculosis cases. The global prevalence of latent joint and bone tuberculosis is approximately 19–38 million cases [1].

Collagens are major structural proteins of the extracellular matrix, joints, and bones and their correct structure is crucial for the proper functioning of locomotor apparatus. Both tuberculosis per se and its chemotherapy with antitubercular drugs could cause pronounced changes in collagen's contents and structure [1, 2]. Investigation of these changes is very important for improving first-line antitubercular therapy and minimization of its adverse effects.

Previously we have demonstrated putative changes in rat bone and skin type I collagens amino acid contents with using different doses of pyrazinamide [2, 3]. Type II collagen has been classically recognized as the major collagenous component of cartilage.

The aim of present study was to investigate potential effect of pyrazinamide on male rats cartilage type II collagen amino acid composition.

2. Materials and Methods

Cartilage type II collagens were extracted and purified according to Trelstad et al. [4]. All procedures were carried out at 4°C. Cartilages (20 g) were grinded. Extraction of proteoglycans was carried out by 100 mL 2 M $MgCl_2$, 0.05 M Tris (pH 7.6) during 3 days. Extract was decanted. Cartilages were washed by distilled water (3 times). Collagen was extracted by 100 mL 0.1 M acetic acid (pH 2.5) with pepsin. Pepsin (20 mg/g of tissue) was added into this solution and mixtures were left for 3 days in refrigerator at 4°C.

Table 1: Male rats cartilage type II collagen amino acid contents in control and with pyrazinamide administration at doses 1000 mg/kg and 2000 mg/kg of body weight (M ± m, $n = 5$, residues/1000 residues).

Amino acid	Control (norm)	Pyrazinamide 1000 mg/kg	Pyrazinamide 2000 mg/kg
Hydroxylysine	5.60 ± 1.20	4.20 ± 0.80	3.50 ± 0.40
Lysine	29.9 ± 1.80	31.80 ± 2.70	33.30 ± 2.50
Histidine	8.30 ± 1.20	7.10 ± 1.30	5.60 ± 0.30
Arginine	53.83 ± 3.35	53.00 ± 5.80	39.90 ± 3.00*#
Hydroxyproline	95.80 ± 2.70	91.70 ± 4.70	85.90 ± 2.90
Aspartic acid	53.50 ± 5.10	62.30 ± 6.40	72.10 ± 10.60
Threonine	29.80 ± 6.60	29.20 ± 1.30	33.70 ± 2.10
Serine	34.00 ± 1.98	49.80 ± 1.60*	56.30 ± 2.30*#
Glutamic acid	88.10 ± 3.47	115.40 ± 6.30*	110.80 ± 12.20*
Proline	91.70 ± 1.60	91.20 ± 4.10	86.10 ± 3.70
Glycine	310.20 ± 7.70	282.10 ± 9.90	294.00 ± 6.40
Alanine	105.62 ± 2.78	92.60 ± 1.80*	72.10 ± 5.50*#
Valine	24.80 ± 1.89	16.70 ± 3.60*	32.90 ± 1.57*#
Methionine	7.60 ± 1.50	3.80 ± 1.00	2.70 ± 0.70
Isoleucine	13.35 ± 0.79	8.30 ± 0.80*	10.60 ± 1.80
Leucine	23.43 ± 1.85	34.30 ± 2.00*	32.90 ± 1.00*
Tyrosine	7.30 ± 0.80	6.80 ± 0.30	7.50 ± 0.50
Phenylalanine	18.80 ± 0.80	20.80 ± 2.30	20.60 ± 2.10

M ± m: mean ± mean standard error.
*$P < 0.05$ statistically significant in comparison with control.
#$P < 0.05$ statistically significant pyrazinamide, 1000 mg/kg group versus pyrazinamide, 2000 mg/kg group.

After that for pepsin inactivation pH in each mixture was neutralized by addition of powdered crystalline Tris (to pH 7.6). Solutions were centrifuged: 35000 g, 40 min, 4°C. Pellets were discarded and supernatants were used for further collagen types fractionation. Fractionation of pure type II collagens was carried out by growing concentrations of NaCl according to method [4]. Protein fraction from pellet which was formed at 4.4 M NaCl concentration contained type II collagen. Fractions were separated by centrifugation (65000 g, 60 min, at 4°C). Obtained pellets were recrystallized (3 times) by dialysis (against 15% KCl in 0.02 M $NaHPO_4$ at 4°C) and centrifugation (65000 g, 60 min, at 4°C) [5]. Collagen preparations purity was controlled electrophoretically [6].

Collagen fractions were hydrolyzed: 24 h, 6 N HCl, 105°C [7]. Their amino acid compositions were analyzed by ion exchange chromatography on the amino acid analyzer AAA-881 (Czech Republic).

In statistical processing of experimental data mean of corresponding parameter (for each animal) was used as independent variable. The obtained data were calculated by one-way analysis of variance (ANOVA). Data were compared using Tukey test. Differences were considered to be statistically significant at $P < 0.05$.

3. Results and Discussion

Changes in male rat cartilage type II collagen amino acid contents induced by pyrazinamide were profound as compared to control (Table 1). Statistically significant changes were registered in cartilage collagen with pyrazinamide administration at dose 1000 mg/kg for 6 amino acids and at dose 2000 mg/kg for 6 amino acids.

Cartilage type II collagen of male rats with pyrazinamide at dose 1000 mg/kg contains lower contents of alanine (−12.3%) and isoleucine (−37.8%) simultaneously with higher contents of serine (+46.5%), glutamic acid (+31.0%), and leucine (+46.6%). Collagen of rats with pyrazinamide at dose 2000 mg/kg contains lower contents of arginine (−25.9%) and alanine (−31.7%) simultaneously with higher contents of serine (+65.6%), valine (+32.7%), and leucine (+40.6%). For the majority of amino acids pyrazinamide effects were dose dependent.

Our experiments demonstrated presence of qualitative changes in male rats' cartilage type II collagens with pyrazinamide (in comparison with norm) (Table 1). With pyrazinamide administration possibly could be formed cartilage type II collagen molecules with changed surface charge (changes in number of arginine, serine, and glutamic acid residues), rigidity (changes in quantity of alanine, valine, isoleucine residues), number of specific loci responsible for cell adhesion, interaction with chaperons, and procollagen processing to collagen (changes in arginine residues) [8–14]. Such collagen molecules changes could hence affect the properties of connective tissues, mineralisation processes, and calcium metabolism.

Comparative analysis of present results with our previous data on skin and bone type I collagens demonstrated analogous character of changes in regard to contents of serine, glutamic acid, alanine, valine, and leucine residues [2, 3]. This could be the evidence of existence some general mechanisms of pyrazinamide effects on collagen's contents

and structure. Moreover, having compared these data with our previous experiments, we found out analogous character of these changes in regard to changes of free serine, glutamic acid, alanine, valine, and leucine contents in liver, kidney, lung and spleen pools with different doses of pyrazinamide [8]. Thus adverse effects of pyrazinamide (this widely used antitubercular drug) are much more serious and more profound than it was considered earlier. Among this pyrazinamide treatment could cause qualitative changes in nucleic acid molecules, change their length, and structure [9].

We can suppose that such changes could be caused by pyrazinamide via its influence on nucleic acids (coding information for this proteins synthesis) as it was mentioned previously [2, 9, 10]. In our previous experiments we demonstrated epigenetic changes induced by pyrazinamide treatment, pyrazinamide-mediated alterations in male rats DNA fragmentation processes, bone type I collagen amino acid composition, spermatogenesis indices, reproductive capability, and posterity antenatal and postnatal development. Besides these, on changes in collagen metabolism and structure pathologic changes in amino acid metabolism could also be affected [8]. And at last, due to collagen genes polymorphism [11–14], collagen structures contain in norm 4 different α-chains of the same type in different concentrations. Pathology [14] changed concentrations in which these 4 different α-chains of the same type of collagen are present in connective tissue structures. Possibly pyrazinamide-caused disturbances in amino acid compositions in our experiments could be a result of such changes in transcription rates of genes coding different α-chains from the same type collagen superfamily as it was previously demonstrated for other pathology [14].

References

[1] A. N. Malaviya and P. P. Kotwal, "Arthritis associated with tuberculosis," *Best Practice and Research*, vol. 17, no. 2, pp. 319–343, 2003.

[2] L. B. Bondarenko, G. M. Shayakhmetova, T. F. Byshovets, and V. M. Kovalenko, "Pyrazinamide-mediated changes in rat type I collagen and spermatogenesis indices," *Acta Poloniae Pharmaceutica—Drug Research*, vol. 68, no. 2, pp. 285–290, 2011.

[3] L. B. Bondarenko, G. M. Shayakhmetova, T. F. Byshovets, and V. M. Kovalenko, *Acta Poloniae Pharmaceutica*. In press.

[4] R. L. Trelstad, V. M. Catanese, and D. F. Rubin, "Collagen fractionation: separation of native types I,II and III by differential precipitation," *Analytical Biochemistry*, vol. 71, no. 1, pp. 114–118, 1976.

[5] A. L. Rubin, M. P. Drake, P. F. Davison, D. Pfahl, P. T. Speakman, and F. O. Schmitt, "Effects of pepsin treatment on the interaction properties of tropocollagen macromolecules," *Biochemistry*, vol. 4, no. 2, pp. 181–190, 1965.

[6] G. Maurer, in *The Disk-Electrophoresis*, p. 247, Mir, Moscow, Russia, 1971.

[7] T. Deveni and J. Gherghey, in *The Aminoacids, Peptides and Proteins*, p. 364, Mir, Moscow, Russia, 1976.

[8] L. B. Bondarenko, N. A. Saprykina, and V. M. Kovalenko, "Lung and spleen contents of free amino acids after pyrazinamide treatment," *Acta Toxicologica*, vol. 14, no. 1-2, pp. 79–86, 2006.

[9] V. M. Kovalenko, T. V. Bagnyukova, O. V. Sergienko et al., "Epigenetic changes in the rat livers induced by pyrazinamide treatment," *Toxicology and Applied Pharmacology*, vol. 225, no. 3, pp. 293–299, 2007.

[10] L. Bondarenko, G. Shayakhmetova, T. Byshovets, and V. Kovalenko, *International Journal of Infectious Diseases*, vol. 15, supplement S99, 2011.

[11] S. R. Kimball, M. Yancisin, R. L. Horetsky, and L. S. Jefferson, "Translational and pretranslational regulation of protein synthesis by amino acid availability in primary cultures of rat hepatocytes," *International Journal of Biochemistry and Cell Biology*, vol. 28, no. 3, pp. 285–294, 1996.

[12] J. Inamasu, B. H. Guiot, and D. C. Sachs, "Ossification of the posterior longitudinal ligament: an update on its biology, epidemiology, and natural history," *Neurosurgery*, vol. 58, no. 6, pp. 1027–1038, 2006.

[13] J. D. Kurt, S. Makoto, K. Tomoatsu, and Y. Yoshihiko, "Complete coding sequence and deduced primary structure of the human cartilage large aggregating proteoglycan, aggrecan," *The Journal of Biological Chemistry*, vol. 266, no. 2, pp. 894–902, 1991.

[14] B. Lee, M. D'Alessio, H. Vissing, F. Ramirez, B. Steinmann, and A. Superti-Furga, "Characterization of a large deletion associated with a polymorphic block of repeated dinucleotides in the type III procollagen gene (COL3AI) of a patient with Ehlers-Danlos syndrome type IV," *American Journal of Human Genetics*, vol. 48, no. 3, pp. 511–517, 1991.

Hindawi Publishing Corporation
International Journal of Peptides
Volume 2012, Article ID 731293, 10 pages
doi:10.1155/2012/731293

Research Article

Molecular Cloning and Sequence Analysis of the cDNAs Encoding Toxin-Like Peptides from the Venom Glands of Tarantula *Grammostola rosea*

Tadashi Kimura,[1,2] Seigo Ono,[1] and Tai Kubo[1,2]

[1] *Molecular Neurophysiology Group, Neuroscience Research Institute, National Institute of Advanced Industrial Science and Technology (AIST), Central 6, 1-1-1 Higashi, Tsukuba, Ibaraki 305-8566, Japan*
[2] *United Graduate School of Drug Discovery and Medical Information Science, Gifu University, 1-1 Yanagido, Gifu 501-1193, Japan*

Correspondence should be addressed to Tadashi Kimura, tadashi.kimura@aist.go.jp and Tai Kubo, tai.kubo@aist.go.jp

Received 16 September 2011; Accepted 26 November 2011

Academic Editor: Mirian A. F. Hayashi

Tarantula venom glands produce a large variety of bioactive peptides. Here we present the identification of venom components obtained by sequencing clones isolated from a cDNA library prepared from the venom glands of the Chilean common tarantula, *Grammostola rosea*. The cDNA sequences of about 1500 clones out of 4000 clones were analyzed after selection using several criteria. Forty-eight novel toxin-like peptides (GTx1 to GTx7, and GTx-TCTP and GTx-CRISP) were predicted from the nucleotide sequences. Among these peptides, twenty-four toxins are ICK motif peptides, eleven peptides are MIT1-like peptides, and seven are ESTX-like peptides. Peptides similar to JZTX-64, aptotoxin, CRISP, or TCTP are also obtained. GTx3 series possess a cysteine framework that is conserved among vertebrate MIT1, Bv8, prokineticins, and invertebrate astakines. GTx-CRISP is the first CRISP-like protein identified from the arthropod venom. Real-time PCR revealed that the transcripts for TCTP-like peptide are expressed in both the pereopodal muscle and the venom gland. Furthermore, a unique peptide GTx7-1, whose signal and prepro sequences are essentially identical to those of HaTx1, was obtained.

1. Introduction

Venoms are complex mixtures of many different components proven to be useful tools for biochemical, physiological, and pharmacological studies of ion channels and receptors. Toxins that recognize ion channel subgroups are versatile tools for channel studies and thus contribute to drug discovery [1, 2]. For example, a 25-amino-acid peptide isolated from the marine fish-hunting cone snail *Conus magus*, ω-conotoxin-MVIIA, blocks N-type voltage-dependent calcium channels. In 2004, ziconotide, the synthetic version of ω-conotoxin-MVIIA, was approved in the United States for the treatment of chronic severe pain refractory to other current pain medications.

About 40000 different kinds of spiders are known at present. Spider venoms contain peptide neurotoxins and are expected to be a rich source of ion channel blockers [3–5]. Tarantulas, comprising more than 860 species, like all other spiders are predators that feed on a variety of vertebrate and invertebrate prey [6]. Tarantulas do not use webs for capture but are well-equipped predators, possessing a variety of venoms that target receptors in the nervous system, probably with adaptation to a certain type of prey [7, 8]. Tarantula venom has been suggested to contain 1000 or more peptide toxins [8]. Despite their diverse activities, these toxins display only a few widely conserved structural motifs that share remarkable similarities in their primary sequences and tertiary structures [9–11]. In a similar fashion to the evolution of snake toxins, several molecular scaffolds have been used during the evolution of toxin "cocktails" in spider venoms. The selected genes are duplicated several times, and, while the core of each protein scaffold is conserved, the loops and surfaces are altered through mutations [12]. We recently found T-type voltage-dependent calcium channel blocker from venom of Chilean common tarantula, *Grammostola rosea* [13].

Expressed sequence tags (ESTs) are short single-pass sequence reads generated from either 5′ or 3′ end of cDNAs. They provide a quick and inexpensive route for discovering new genes and obtaining data on gene expression. The ESTs approach has been used in several reports, because it is a rapid and reliable method for gene discovery in general, mainly in this case, related to secretory glands from venomous animals [14–16].

In this paper, we focused on the tarantula toxins, and by applying improved molecular biological techniques, we revealed novel peptide sequences after ESTs techniques applied to a cDNA library prepared from the Chilean common tarantula *Grammostola rosea* venom glands.

2. Materials and Methods

2.1. Animals and Venom Glands. *Grammostola rosea* tarantulas were obtained from a local pet supplier. The venom glands were dissected from the chelicera and the pereopodal muscles were from the prosoma using sharp forceps, frozen immediately with liquid nitrogen, and then stored at −80°C until use.

2.2. cDNA Library Construction. Preparation of the venom gland cDNA library was reported previously [13]. Briefly, the venom glands were dissected from 30 spiders, and total RNA was extracted using TRIZOL reagent (Invitrogen, Carlsbad, CA). Poly(A)$^+$ RNA was prepared using Oligotex-dT30 Super (Takara Bio, Otsu, Japan). The first-strand cDNAs were synthesized from 2.5 μg of poly(A)$^+$ RNA using the primer, VNXho$(dT)_{30}$, which installs oligo dT and *Xho*I sequences, by ReverTra Ace (Toyobo, Osaka, Japan) and Superscript II (Invitrogen). The second strands were synthesized with DNA polymerase I (Takara Bio), RNase H (Takara Bio), and *Escherichia coli* DNA ligase (Takara Bio). *Eco* RI adaptors (Clontech, Palo Alto, CA) were ligated to the cDNAs after both ends of the double-stranded cDNAs were filled in with a DNA blunting kit (Takara Bio). The cDNAs were then digested with *Xho*I and fractionated by 1.2% agarose gel electrophoresis. DNA fragments with lengths of 0.8–2.0 kbp were eluted from dissected gel. The resulting DNA fragments were ligated into *Eco*RI and *Xho*I restriction sites of pSD64TR$_{ER}$ [17]. *E. coli* XL1-Blue MRA (Agilent Technologies, Santa Clara, CA) was transformed with the plasmid. An aliquot of the cDNA library in *E. coli* was spread onto LB agar plates containing 50 μg/mL ampicillin, and the plasmid DNA was prepared for the PCR template.

2.3. Fingerprinting of Clones. An aliquot of cDNA library was spread onto LB agar plates with ampicillin (50 μ g/mL) and incubated at 37°C overnight. Formed colonies were picked up by automated colony picker (Microtec Nichion, Japan) and inoculated into1 mL of 2 × LB medium supplemented with ampicillin (50 μg/mL) in 96 deep-well plates and incubated at 37°C overnight with vigorous shaking. Plasmids were purified with an automated machine, BIOMEK2000, (Beckman Coulter, USA) using MultiScreen-FB and -NA (Millipore, USA) and eluted by 50 μL TE solution, then stored −20°C until use. PCR was performed with an SP6 primer and a pSD64-specific reverse primer, SDA (5′-TTATGTAGCTTAGAGACT-3′), to amplify the inserts of the cDNA library. Each PCR reaction mixture consists of 10 pmol of the forward and reverse primers, 0.25 U EX Taq polymerase (Takara Bio), 200 mM each of dATP, dCTP, dGTP and dTTP, 2 mM $MgCl_2$, PCR buffer, and 1 μL DNA template. The reaction was performed in a thermal cycler PTC-200 (MJ research, USA) for 30 cycles, each consisting of denaturation at 94°C for 30 s, annealing at 42°C for 45 s, and polymerization at 72°C for 1 min, after the initial cycle of 94°C for 5 min. At the end of all the cycles, samples were maintained at 72°C for 9 min and then kept at 4°C.

PCR reaction products were digested by *Dde*I restriction enzyme at 37°C and analyzed by electrophoresis in 3% agarose/TBE gel, then visualized with ethidium bromide, and digitized using gel documentation system, Gel Doc 1000 (Bio-Rad, USA). The band patterns of the digested PCR products were clustered by the similarity using Molecular Analyst Fingerprinting plus software (Bio-Rad).

2.4. Sequencing and Data Analysis. We manually selected clones to be sequenced based on the fingerprinting categorization described previously. Single run DNA sequencings were performed using an SP6 primer by a sequencer Model ABI Prism 377 (Applied Biosystems, CA, USA) or performed by Shimadzu. The obtained DNA sequences were translated into amino acid sequences with all three frames using the Vector NTI program (Invitrogen, USA). After translation into three amino acid sequences, both protein and cDNA sequences were stored into in-house database software, KIROKU (World Fusion, Tokyo, Japan). Homology search of translated protein sequences was performed at in-house sequence database using the BLAST program. The prediction of signal sequence was performed by SignalP 3.0 program (http://www.cbs.dtu.dk/services/SignalP/). Amino acid alignment and phylogenetic tree construction were performed using the MegAlign program by Clustal W and neighbor-joining method (DNASTAR, Madison, USA).

2.5. PCR Cloning Based on the Signal Sequence of Toxins. We synthesized oligonucleotide primers based on the conserved initiation codon (ATG) and its juxtaposed sequences including 5′-noncoding region and the signal sequences of the GTxs (Table 1). Using these primers and an SDA primer, PCR amplifications were carried out with the venom glands cDNA library as a template. The reaction conditions were essentially the same as described in Section 2.3. Amplified fragments were cloned into pCR 2.1-TOPO (Invitrogen). The full-length nucleotide sequences of the clones were determined by Hitachi Soft Co Ltd.

2.6. Quantification of Tissue Expression of GTx-TCTP and GTx-CRISP cDNAs

2.6.1. Cloning and Sequence Analysis of GTx-TCTP and GTx-CRISP cDNAs. Single run sequencings of the venom gland cDNA library revealed the first half of GTx-TCTP and GTx-CRISP cDNA including 5′-UTR region with start

Table 1: Primers for PCR cloning.

Primers	Nucleotide sequence	Referred sequences
PC1	5′-TAARCGACAATGAAGAC-3′	GTx1-11, 12, 14, 15, 16
PC2	5′-TTCGATAACATGAAGAC-3′	GTx1-1, 2; GTx7-1
PC3	5′-AAAGCATGAAAACCTC-3′	GTx1-3
PC4	5′-ACTCTAAAAATGAAGGC-3′	GTx1-4, 5, 7, 8, 9
PC5	5′-TCAGCAGAAATGAAGGC-3′	GTx2-2, 3
PC6	5′-TCCATCATGAAGITNGC-3′	GTx3-4, 5, 6, 7, 8
PC7	5′-ATAACGATGAAGITINT-3′	GTx5-1
PC8	5′-GCAGCCATGAAAICINT-3′	GTx6-1
PC9	5′-GTTAAGATGAAITWYNC-3′	GTx3-1, 2, 3
PC10	5′-GCAACGATGAGRTCINT-3′	GTx4-1, 2
PC11	5′-GGAAACATGAGRAAINC-3′	GTx1-13

Oligonucleotide primers are synthesized based on the conserved signal sequences and the sequcences of 5–9 nucleotides upstream of initiation codon of the GTxs indicated in the right column. Underline indicates initiation codon, ATG. R: A/G; W: T/A; Y: T/C; N: A/T/C/G; I: inosine.

codon. To obtain the latter halves of GTx-TCTP and GTx-CRISP cDNA including 3′-UTR region with the stop codon from the cDNA library, PCRs were performed using the gene-specific primers, 5′-TCAAGGATATGATTACTGGT-3′ for GTx-TCTP and 5′-AGGTGGGCTGAATCCTGT-3′ for GTx-CRISP, and an SDA primers (see Section 2.3) as forward and reverse primers, respectively. The PCR was carried out in a PTC-200 DNA thermal cycler (MJ Research, South San Francisco, CA) using 30 cycles as follows: denaturation at 94°C for 30 s, annealing at 54°C for 30 s, and extension at 72°C for 1 min using LA Taq polymerase (Takara Bio). The amplified fragments were gel purified using QIAquick Gel Extraction Kit (QIAGEN, Valencia, CA), subcloned into pCR 2.1-TOPO vector (Invitrogen), and sequenced using BigDye Terminator Cycle Sequencing Ready Reaction Kit (version 3.1) and an ABI PRIZM 310 DNA sequencer (Applied Biosystems, Foster City, CA).

2.6.2. Real Time PCR. The gene expressions of GTx-TCTP and GTx-CRISP in the venom gland and pereopodal muscle were quantified by real-time PCR. Tarantula G3PDH (GTx-G3PDH) cDNA was cloned and used as an expression control. Primers for the real-time PCR were designed using Roche ProbeFinder version 2.45 (http://qpcr.probefinder.com/roche3.html). Primers for GTx-G3PDH were 5′-CATGCTTGGCTAAGGGAGTAA-3′ and 5′-TGTATTTGACATCAATAAATGGATCA-3′; primers for GTx-TCTP, 5′-CTCGGAGAATGGGAGACATT-3′ and 5′-CATCTGCCTCCTCCTGAGAC-3′; and primers for GTx-CRISP, 5′-GCACAATTTCTTCAGGTCACG-3′ and 5′-CAGCTCATTGCCAGCATATC-3′. The venom glands and the pereopodal muscles were stored at −80°C and thawed in TRIZOL reagent (Invitrogen), homogenized, and directly subjected to total RNA extraction according to manufacturer's instructions. Total RNA was reverse transcribed with PrimeScript RT reagent Kit (Takara Bio). Real-time PCR mixtures were prepared with SYBR Premix Ex Taq II (Takara Bio) according to manufacturer's instructions. The reaction and monitoring were performed with Thermal Cycler Dice Real-Time System, PT800 (Takara Bio) for 40 cycles of 2 step shuttle PCR (95°C for 5 s, 60°C for 30 s).

3. Results and Discussion

We constructed a tarantula venom gland cDNA library from 2.5 μg of poly $(A)^+$ RNA. The independency of the library is about 4.4×10^5. We chose about 1500 clones out of 4000 clones based on the restriction-enzyme digestion patterns determined by fingerprinting software and sequenced by single run sequencing from the upstream region of the protein-coding sequence. After eliminating vector and low-quality sequences, 869 high-quality ESTs were obtained. We found that 284 clones (=32.7%) encode toxin-like sequences among them. This ratio is comparable to the results from the EST analysis of the venom glands of Theraphosidae family tarantulas *Chilobrachys jingzhao* and *Citharischius crawshayi*, in which 30.6% and 32.5% of analyzed clones encode toxin-like sequences, respectively [16, 18, 19]. In the present study, eight types of toxin-like scaffold were found mainly based on a cysteine framework. It is noteworthy that 15 and 5 peptide scaffolds were reported from the EST studies of the tarantulas *Chilobrachys jingzhao* and *Citharischius crawshayi*, respectively, [16, 18, 19]. Thirty-four cDNAs were additionally revealed by PCR cloning using primers designed from the conserved initiation codon (ATG) and its juxtaposed sequences including 5′-noncoding region and the signal sequences.

We focused on unique 48 peptides belonging to eight types of toxin-like scaffold. The resulted sequence analysis and the database search are described here in after.

3.1. GTx1 Family, Long Loop ICK Motif Toxins; and GTx2 Family, Short Loop ICK Motif Toxins. Twenty long loop ICK motif toxins and four short loop ICK motif toxins were obtained (Figure 1(a)). In the mature sequences, the N-terminal and the C-terminal sequence stretches separated by cysteine residues are termed "loops" and numbered 1–6 from N- to C-terminus. The toxins with more than 6 amino acids and the toxins with only three amino acids in the loop 5 are designated as "long-loop" and "short-loop" ICK toxins group, respectively. Among these toxins, we previously showed that GTx1-15 preferentially block the currents of the T-type voltage-dependent calcium channel $Ca_v3.1$ [13]. Among the GTx1 and GTx2 families, we identified additional peptide cDNAs; those translated sequences are the same as the previously reported ones, HaTx1 and 2, VSTx1 and 2, GsMTx4, GsAFI and II, GrTx1, and ω-GrTx SIA. HaTx1 and 2 are well-known toxins that inhibit $K_v2.1$ and $K_v4.2$ voltage-gated potassium channels [20]. VSTx1 is a voltage sensor toxin from the spider *Grammostola rosea* that inhibits K_vAP, an archeabacterial voltage-activated potassium channel whose X-ray structure has been reported [21]. GsMTx4 is known as a toxin for stretch-activated mechanosensitive channels [22]. GsAFI and II have been first reported to be an analgesic and an antiarrhythmic peptides from the venom of spider *Grammostola rosea*, respectively [23, 24]. GsAFI, GsAFII, and GrTx1 have been shown to have

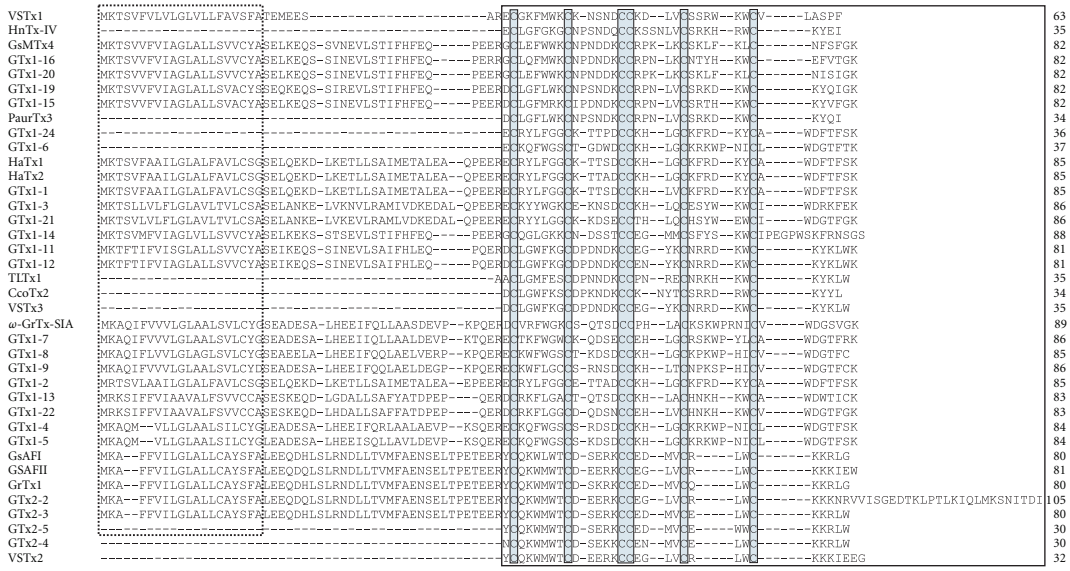

(a)

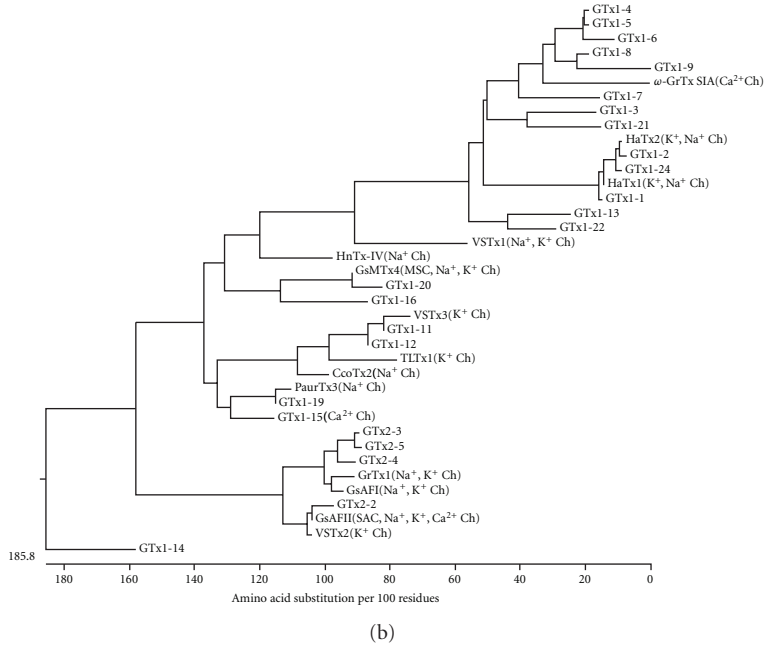

(b)

Figure 1: Homology analysis of ICK motif toxins. (a) Homology alignment of ICKs. The putative signal sequences deduced by SignalP 3.0 server (**http://www.cbs.dtu.dk/services/SignalP/**) are indicated by dotted box. Signal sequences and prepro-sequences of GTx1-6, GTx1-24, GTx2-4, GTx2-5, HnTx-IV, PaurTx3, TLTx1, CcoTx2, and VSTx1, 2, 3 are not determined. Mature toxin regions are indicated by closed box. Conserved cysteine residues are indicated by closed boxes filled with gray color. (b) Phylogenetic tree of ICK toxins. Amino acid alignment and phylogenetic tree construction were performed using the MegAlign program by Clustal W and neighbor-joining method (DNASTAR, Madison, USA) based on the alignment (a) of mature peptides. A scale below the tree indicates the number of amino acid substitutions per 100 residues for protein sequences. Known molecular targets are indicated following to the peptide names. Accession numbers: GTx1 and GTx2 families, AB200996-AB201024 and AB671302-AB671308; HaTx1, AB200991; HaTx2, AB200992; VSTx1, AB200994; GsAFI, AB200995; GsAFII, AB612242; GrTx1, AB671300 and AB671301; ω-GrTx SIA, AB612243; GsMTx4, AB201020; PaurTx3, P84510; CcoTx2, P84508; TLTx1, P83745; VSTx2, P0C2P4; VSTx3, P0C2P5.

similar blockade spectra against ion channels such as $Na_v1.1$, $Na_v1.2$, $Na_v1.3$, $Na_v1.4$, $Na_v1.6$, $Na_v1.7$, and $K_v11.1$ [25, 26]. ω-GrTx SIA is reported to inhibit $Ca_v2.1$ and $Ca_v2.2$ voltage-dependent calcium channels by modifying their voltage-dependent gating [27, 28].

As mentioned previously, HaTx1 is known as a potassium channel gating modifier but can inhibit sodium channels at concentrations similar to those that modify the gating of potassium channels [29]. Recently, similar target promiscuity and heterogeneous effects of tarantula venom

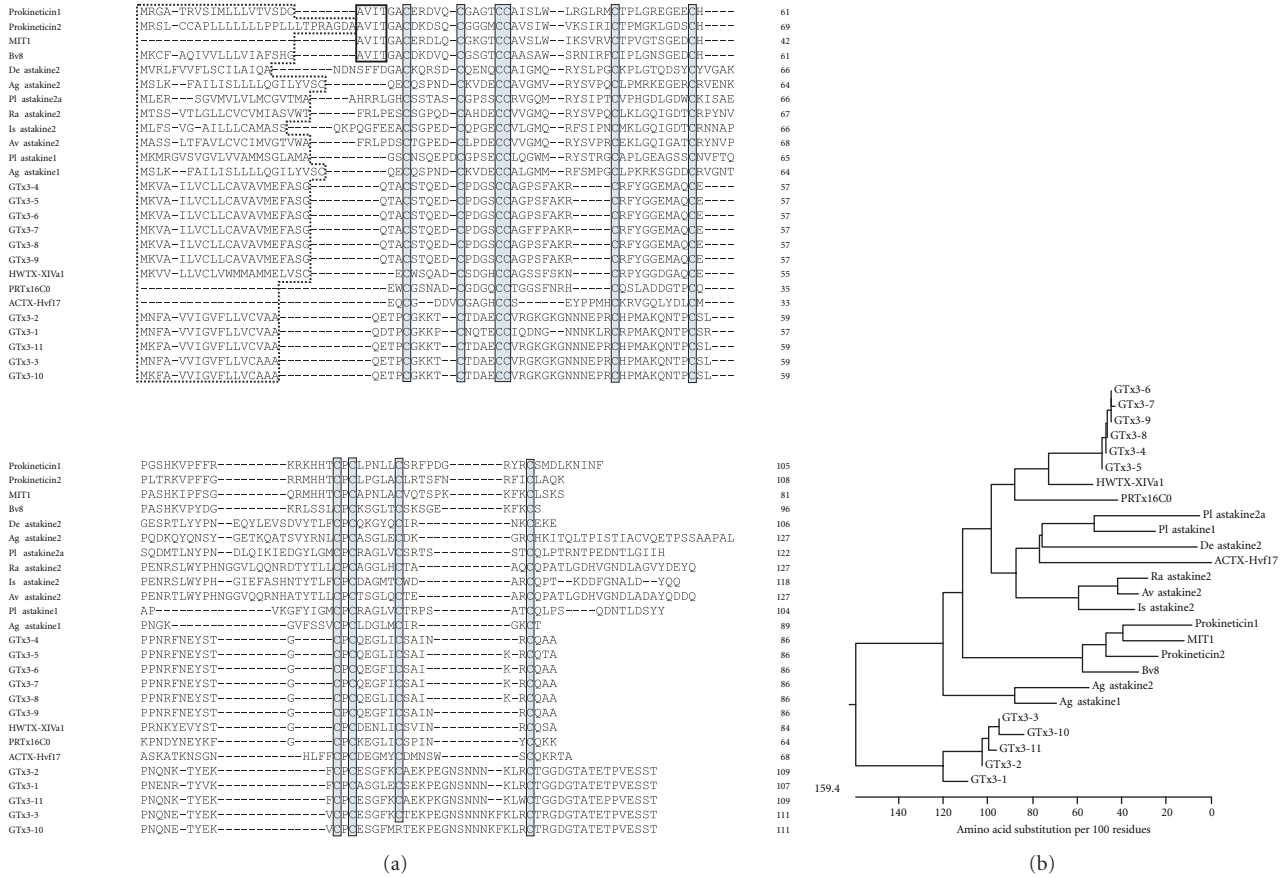

Figure 2: Homology analysis of GTx3 series toxins. (a) Sequence alignment of GTx3 series and their related peptides. The putative signal sequence deduced by SignalP 3.0 server (http://www.cbs.dtu.dk/services/SignalP/) is indicated by dotted box. Signal sequence of MIT1 is not determined. Conserved cysteine residues are indicated by closed boxes filled with gray color. AVIT N-terminals of Prokineticin1, Prokineticin2, MIT1, and Bv8 are indicated closed boxes. (b) Phylogenetic tree of GTx3 series and related peptides. Amino acid alignment and phylogenetic tree construction were performed using the MegAlign program by Clustal W and neighbor-joining method (DNASTAR) based on the alignment (a) of mature peptides. A scale below the tree indicates the number of amino acid substitutions per 100 residues for protein sequences. Accession numbers: GTx3 series, AB201025-AB201034 and AB671309-AB671311; Bv8, AF168790; Prokineticin 1, AF333024; Prokineticin 2, AAH96695; MIT1, P25687; HWTX-XIVa1, ABY77690; ACTX-Hvf17, P81803; *Pacifastacus leniusculus* (Pl) astakine1, AY787656; Pl astakine2a, EF568370; *Acanthoscurria gomesiana* (Ag) astakine1, DR447331; Ag astakine2, DR445103; *Rhipicephalus appendiculatus* (Ra) astakine2, CD794853; *Ixodes scapularis* (Is) astakine2, EW845057; *Amblyomma variegatum* (Av) astakine2, BM292046; *Dysdera erythrina* (De) astakine2, CV178181.

voltage-sensor toxins are discussed including GsAFI and II, GrTx1 described previously [25, 30]. We also suggest similar target promiscuity; that is, a toxin family including GsAFII, GsMTx2, PaTx2, and ProTx-II could affect several types of ion channels such as stretch-activated channels and the voltage-dependent sodium, potassium, and calcium channels [13]. Figure 1(b) shows phylogenetic tree of GTx1, GTx2, and several ICK toxins. The correlations between the peptide groups and their target molecules are not clear. Vega discussed the pharmacological diversification of ICK motif toxin by phylogenetic analysis of 171 homologous ICK toxins using Bayesian inference [31]. Although the relationship between clusters is not satisfactorily solved, several trustable monophyletic groups appear from the analysis. The main conclusion from the tree is a plausible lineage-specific process of paralogous diversification from several independent recruiting events. Further investigation is needed to elucidate the relationships between evolutional processes and the pharmacological diversification and target promiscuity of ICK toxins.

3.2. GTx3 Series: Similar to Mamba Intestinal Toxin 1 (MIT1), Bv8/Prokineticins, and Invertebrate Astakines. Eleven toxins similar to MIT1, Bv8/prokineticins, and invertebrate astakines were identified (Figure 2). Bv8, prokineticins, and MIT1 consist in a group known as AVIT family due to their N-terminal residues A-V-I-T [32]. MIT1 shows contractile effects on longitudinal ileal muscle and distal colon [33]. The solution structure of MIT1 was determined at a resolution of 0.5 Å and revealed a new type of folding for venom toxins similar to that of colipase, a protein involved in fatty acid digestion [34]. Bv8 is bioactive peptide found from frog skin to induce hyperalgesic effects [35] and belongs to a family of secretory proteins (Bv8-prokineticin family)

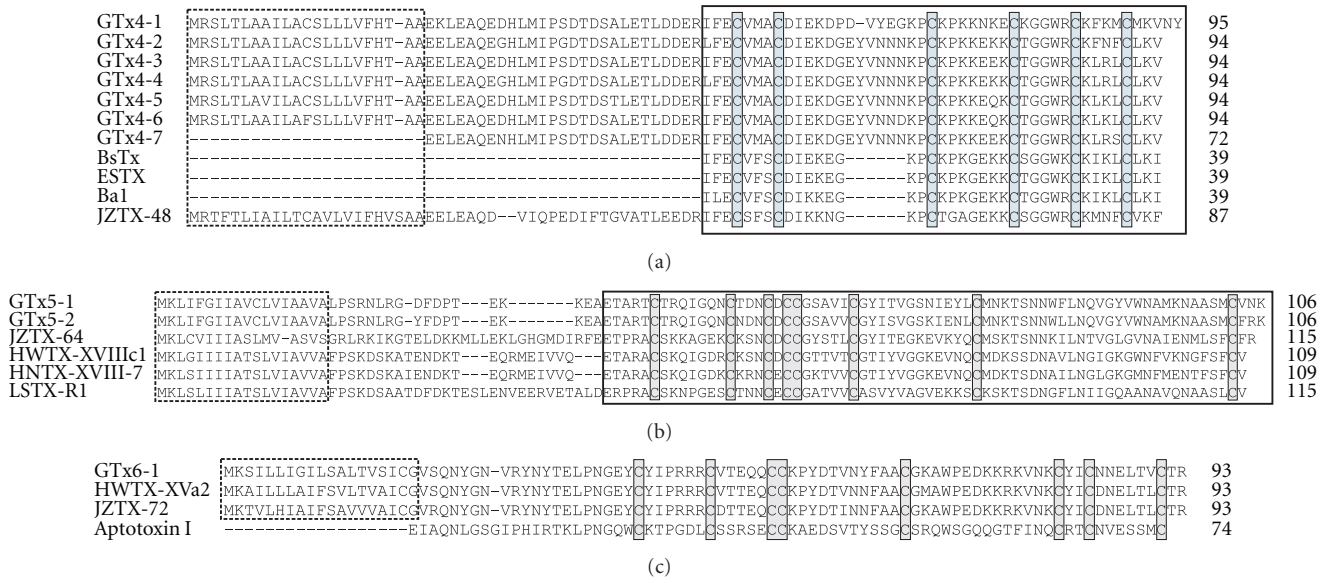

Figure 3: Sequence alignments of GTx4 (a), GTx5 (b), and GTx6 (c) series. The putative signal sequence deduced by SignalP 3.0 server (http://www.cbs.dtu.dk/services/SignalP/) is indicated by dotted box. Signal sequences of GTx4-7 and signal sequences and prepro-sequences of BsTx, ESTX, and Ba1 are not determined. Mature toxin regions are indicated by closed box in (a) and (b). Conserved cysteine residues are indicated by closed boxes filled with gray color. Accession numbers: GTx4 series, AB201035-AB201036 and AB671312-AB671317; BsTx, P49265; ESTX, P61509; Ba1, P85497; JZTX-48, EU233840; GTx5-1 and GTx5-2, AB201037 and AB683255; JZTX-64, EU233914; HWTX-XVIIIc1, EU195231; HNTX-XVIII-7, GU293118; LSTX-R1, EU926143; GTx6-1, AB201038; HWTX-XVa2, EU195236; JZTX-72, EU233926; Aptotoxin I, P49267.

whose orthologues have been conserved throughout evolution from invertebrates to human. The prokineticins (PK1 and PK2, also known as endocrine gland vascular endothelial growth factor (EG-VEGF) and Bv8, resp.) are involved in signaling through two highly homologous G-protein-coupled receptors, PKR1 and PKR2 [36]. Bv8/PK2 is upregulated in inflammatory granulocytes and modulates inflammatory pain [37]. Blockade of PKRs might represent a therapeutic strategy in acute and inflammatory pains [38].

Vertebrate PKs are released from damaged tissues and act as regulators of inflammatory responses, including recruitment of new blood cells [39]. Invertebrate astakine, a homologue to vertebrate PKs, was first identified in *Pacifastacus leniusculus* and was found to be necessary for new hemocyte synthesis and release [40]. Although astakines lack the N-terminal AVIT motif, they are designated as prokineticin domain-containing proteins based on their hematopoietic function. No astakine or prokineticin homologue is present in the genome of *Drosophila* or other dipterans, so far. Figure 2(a) shows that the cysteine frameworks of GTx3 series peptides, vertebrate PKs, invertebrate astakines, and several peptide toxins are well conserved. ACTX-Hvf17 from Australian funnel-web spiders lacks the N-terminal AVIT motif and did not affect smooth muscle contractility or block PK1-induced contractions in guinea pig ileum [5]. PRTx16C0 from Brazilian Amazonian armed spider (accession no. P83893) is nontoxic to mice and insects. The effect of HWTX-XIVa1 from Chinese bird spider is unknown [41]. Phyogenetic tree shows that GTx3-4 to GTx3-9, invertebrate astakines, vertebrate prokineticin-related proteins, and spider toxins form large family, while GTx3-1 to GTx3-3, GTx3-10 and GTx3-11 form a distantly related group (Figure 2(b)). For the spider proteins containing prokineticin domain (ACTX-Hvf17, PRTx16C0, HWTX-XIVa1, and GTx3 series), further investigation is needed to reveal their biological functions, especially their effects on the hematopoietic system.

3.3. GTx4, 5, 6 Series: Similar to Other Toxins. GTx4 series are similar to ESTX [42], BsTx [43], JZTX-47, 48 [16], and Ba1, 2 [44] (Figure 3(a)). They are characterized as conserved six cysteine residues. A clear difference between the sequences of GTx4 series and that of the reported ones is the length of the loop 3. ESTX is purified from tarantula *Eurypelma californicum* venom and BsTx is from Mexican red nee tarantula *Brachypelma smithii* venom. The effects of ESTX and BsTx are not clear. Ba1 and Ba2 are insecticidal peptides purified from theraphosid spider *Brachypelma albiceps* venom and an NMR-based 3D model of Ba2 is proposed [44].

GTx5-1 and GTx5-2 are similar to JZTX-64 from *Chilobrachys jingzhao* [16], HWTX-XVIIIc1 from *Ornithoctonus huwena* [41], HNTX-XVIII-7 from *Ornithoctonus hainana* [45], and LSTX-R1 from *Lycosa singoriensis* [46] (Figure 3(b)). These toxins are identified by large-scale venomic strategy and the target molecules are unknown.

GTx6-1 is very similar to HWTX-XVa2 from *Haplopelma schmidti* [41] and JZTX-72 from *Chilobrachys guangxiensis* [16], and similar to aptotoxin I [47], as well (Figure 3(c)).

As mentioned previously, insecticidal effects were reported for Ba1, Ba2, and aptotoxin; however, target

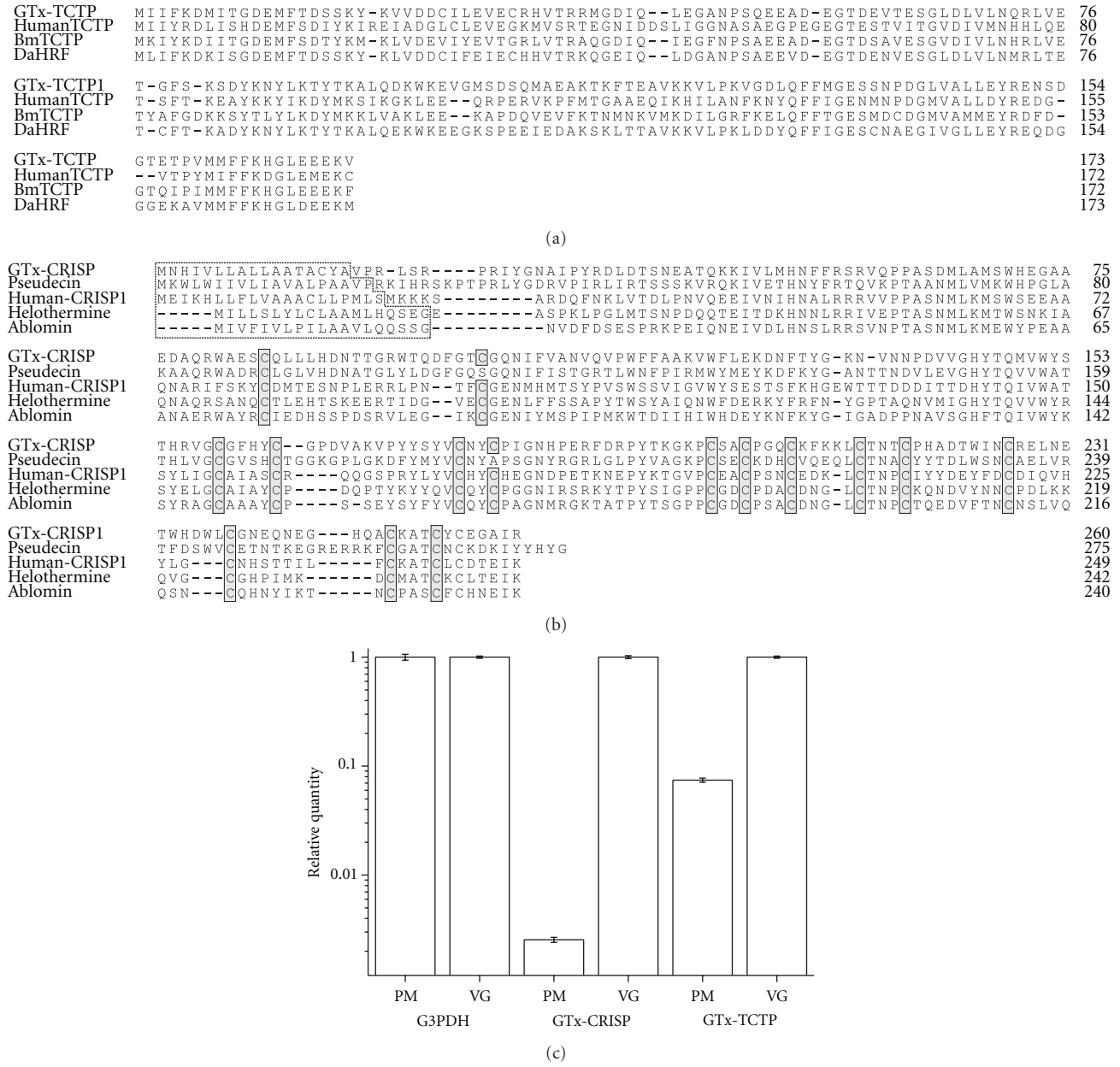

Figure 4: Sequence alignment of GTx-TCTP (a) and GTx-CRISP (b) families. The putative signal sequence deduced by SignalP 3.0 server (http://www.cbs.dtu.dk/services/SignalP/) is indicated by dotted box. Conserved cysteine residues are indicated by closed boxes filled with gray color. (c) The results of real-time PCR. G3PDH is equally expressed in the pereopodal muscle (PM) and the venom gland (VG). GTx-CRISP transcript is predominantly expressed in the venom gland. The GTx-CRISP transcript in the PM is one-400th of that in the VG. GTx-TCTP transcript is expressed in both the pereopodal muscle and the venom gland. The GTx-TCTP transcript in the PM is one-13th of that in the VG. Results were confirmed in triplicate experiments. Accession numbers: GTx-TCTP, AB201040; HumanTCTP, NM_003295; *Bombyx mori* (Bm) TCTP, NM_001044107; *Dermacentor andersoni* (Da) HRF, DQ009480; GTx-CRISP, AB201041; Pseudecin (*Harpegnathos saltator*), EFN80524; Human-CRISP1, NM_001205220; Helothermine, U13619; Ablomin, AF384218.

molecules of GTx4, 5, 6, and their homologues are not yet known.

3.4. GTx-TCTP and GTx-CRISP. We also obtained one translationally controlled tumor protein- (TCTP-) like peptide (Figure 4(a)) and one cysteine-rich secretory protein-(CRISP-) like peptide (Figure 4(b)).

TCTP was first identified as a growth-related tumor protein whose synthesis is controlled mainly at the translational level [48]. This protein has been recognized as a cell

```
GTx7-1   MKTSVFAAILGLALFAVLCSGSELQEKDLKETLLSAIMETALEAQPEERK---ILEKC---GISAEYLSCIGLISTH          71
GTx1-1   MKTSVFAAILGLALFAVLCSGSELQEKDLKETLLSAIMETALEAQPEERECRYLFGGCKTTSDCCKHLVCKFRDKYCAWDFTFSK  85
HaTx1    MKTSVFAAILGLALFAVLCSGSELQEKDLKETLLSAIMETALEAQPEERECRYLFGGCKTTSDCCKHLGCKFRDKYCAWDFTFSK  85
```

Figure 5: Sequence alignment of GTx7-1. The putative signal sequence deduced by SignalP 3.0 server (http://www.cbs.dtu.dk/services/SignalP/) is indicated by dotted box. Mature toxin regions are indicated by closed box. Note that the signal sequences and prepro-sequences are almost same but mature GTx7-1 differs from GTx1-1 and HaTx1. Accession number: GTx7-1, AB201039.

cycle-dependent, tubulin-binding protein having calcium-binding sites [49]. In addition to this growth-related function as a cytosolic protein, TCTP is now known to act as a secretory protein. TCTP has been uniquely characterized as an IgE-dependent histamine-releasing factor [50].

CRISPs are found in a variety of organisms, such as mammals, reptiles, amphibians, and secernentea. The first discovered CRISP (acidic epididymis glycoprotein, also known as protein D/E or CRISP-1) was isolated from mammalian epididymis [51–53]. Two other mammalian CRISPs have been isolated and characterized: CRISP-2 (testis-specific protein 1) [54] and CRISP-3 (specific granule protein of 28 kDa) [55]. Venomic CRISPs were identified mainly from lizard and snake, so far. Helothermine, a CRISP family toxin, is discovered from the lizard of the Central America [56] and blocks voltage-gated calcium and potassium channels and ryanodine receptors [57]. Ablomin is a 25-kDa protein isolated from the venom of the Japanese Mamushi snake (*Agkistrodon blomhoffi*) [58]. Ablomin blocks contraction of rat tail arterial smooth muscle elicited by high K^+-induced depolarization. In insects, it is revealed that an ant (*Harpegnathos saltator*) genome contains a CRISP family protein, Pseudecin [59]. GTx-CRISP is the first CRISP protein identified from the arthropod venom.

To compare the expression levels of the transcripts for GTx-CRISP and GTx-TCTP between the venom gland and the pereopodal muscle, we conducted real-time PCR. The results indicate that transcript of GTx-TCTP was expressed in both the tissues, while that of GTx-CRISP was predominantly expressed in the venom gland (Figure 4(c)). It is tempting to assume that GTx-TCTP acts as both growth-related cytosolic protein and secretory proteins, an IgE-dependent histamine-releasing factor. Further investigation is needed to elucidate the bifunctional feature of GTx-TCTP.

3.5. Other Toxins. The predicted mature portion of the peptide GTx7-1, 21 amino acid residues with two cysteine residues, has a unique sequence (Figure 5). It has no amino acid sequence homology with any other peptide registered in the public database up to now. On the other hand, the preprotoxin sequence of GTx7-1 is very similar to GTx1 family. GTx7-1 slightly and transiently inhibited the contraction of guinea pig right atrial preparation at high concentration (13.2 μM) (Japan patent publication number: 2008-271800).

3.6. Biochemical and Biomedical Applications of Peptide Toxins. Natural peptide toxins contribute to biochemical, physiological, and pharmacological studies especially on cellular/neuronal signal transduction. Furthermore, some of the peptides and its derivatives have been developed as potential therapeutic agents. Their utility is based on an unprecedented selectivity in targeting specific molecular forms, such as subgroups of ion channels and subtypes of receptors, and even specific substates of channel functions.

There are principally two approaches to access to the peptide with some aimed function/property. One is to screen such a peptide from the venom/secreta or tissue extracts, and the other is to screen from cDNA libraries followed by expression and functional assays. Recently, we have developed a new approach by utilizing natural toxin scaffold combined with *in vitro* selection technology. We first constructed a random peptide library based on a three-finger (3F) neurotoxin scaffold. From the 3F peptide library, *in vitro* selections targeting to interleukin-6 receptor were performed, and finally peptide ligands with the antagonist-like and the agonist-like property were generated [60]. Variety of toxin scaffolds are available up to now, and still unknown scaffolds might be revealed by genomic approach for the venom/secretion glands. The new *in vitro* evolution approach will be further applied to different toxin scaffolds including ICK motifs and also will be directed to different targets, such as biomarkers for diagnosis or drug development, or target cells for imaging and drug delivery, and so forth.

4. Conclusions

We have challenged to reveal a peptide repertoire contained in the venom gland of tarantula *Grammostola rosea*. In the previous report, we identified several novel peptides from the spider venom by both proteomic and genomic approaches and reported their modulation activities toward calcium channels [13]. Here in this study, we further presented 48 novel peptides grouped as GTx1 to GTx7, and TCTP- and CRISP-like peptides, and compared the sequences with the homologues. GTx1 and 2 series are mostly homologous to ion channel blockers. GTx3 series are related to the peptides that modulate cell growth and/or cell signaling via GPCRs such as vertebrate prokineticins and invertebrate astakines. GTx-CRISP is the first identified arthropod venom CRISP. GTx-TCTP is expressed in both the venom gland and the pereopodal muscle and assumed to act as both TCTP and HRF. Biochemical and physiological characterizations of these peptides are under investigation. Furthermore, we are now applying the next generation sequencing to totally reveal the transcripts of the tarantula venom gland.

Acknowledgments

A part of this work was supported by Industrial Technology Research Grant Program in 2004 from The New Energy and

Industrial Technology Development Organization (NEDO) (04A02542a), by Grant-in-Aid for Scientific Research (C) from Japan Society for the Promotion of Science (JSPS) KAKENHI (22603016), and by Takeda Science Foundation.

References

[1] P. Escoubas and G. F. King, "Venomics as a drug discovery platform," *Expert Review of Proteomics*, vol. 6, no. 3, pp. 221–224, 2009.

[2] R. J. Lewis and M. L. Garcia, "Therapeutic potential of venom peptides," *Nature Reviews Drug Discovery*, vol. 2, no. 10, pp. 790–802, 2003.

[3] M. E. Adams, "Agatoxins: ion channel specific toxins from the american funnel web spider, *Agelenopsis aperta*," *Toxicon*, vol. 43, no. 5, pp. 509–525, 2004.

[4] G. Corzo, N. Gilles, H. Satake et al., "Distinct primary structures of the major peptide toxins from the venom of the spider *Macrothele gigas* that bind to sites 3 and 4 in the sodium channel," *FEBS Letters*, vol. 547, no. 1–3, pp. 43–50, 2003.

[5] S. Wen, D. T. R. Wilson, S. Kuruppu et al., "Discovery of an MIT-like atracotoxin family: Spider venom peptides that share sequence homology but not pharmacological properties with AVIT family proteins," *Peptides*, vol. 26, no. 12, pp. 2412–2426, 2005.

[6] G. K. Isbister, J. E. Seymour, M. R. Gray, and R. J. Raven, "Bites by spiders of the family Theraphosidae in humans and canines," *Toxicon*, vol. 41, no. 4, pp. 519–524, 2003.

[7] N. Amzallag, B. J. Passer, D. Allanic et al., "TSAP6 facilitates the secretion of translationally controlled tumor protein/histamine-releasing factor via a nonclassical pathway," *The Journal of Biological Chemistry*, vol. 279, no. 44, pp. 46104–46112, 2004.

[8] P. Escoubas and L. Rash, "Tarantulas: eight-legged pharmacists and combinatorial chemists," *Toxicon*, vol. 43, no. 5, pp. 555–574, 2004.

[9] F. Bosmans, L. Rash, S. Zhu et al., "Four novel tarantula toxins as selective modulators of voltage-gated sodium channel subtypes," *Molecular Pharmacology*, vol. 69, no. 2, pp. 419–429, 2006.

[10] R. E. Middleton, V. A. Warren, R. L. Kraus et al., "Two tarantula peptides inhibit activation of multiple sodium channels," *Biochemistry*, vol. 41, no. 50, pp. 14734–14747, 2002.

[11] H. W. Tedford, B. L. Sollod, F. Maggio, and G. F. King, "Australian funnel-web spiders: master insecticide chemists," *Toxicon*, vol. 43, no. 5, pp. 601–618, 2004.

[12] A. M. Torres, H. Y. Wong, M. Desai, S. Moochhala, P. W. Kuchel, and R. M. Kini, "Identification of a novel family of proteins in snake venoms. Purification and structural characterization of nawaprin from *Naja nigricollis* snake venom," *The Journal of Biological Chemistry*, vol. 278, no. 41, pp. 40097–40104, 2003.

[13] S. Ono, T. Kimura, and T. Kubo, "Characterization of voltage-dependent calcium channel blocking peptides from the venom of the tarantula *Grammostola rosea*," *Toxicon*, vol. 58, no. 3, pp. 265–276, 2011.

[14] B. Zhang, Q. Liu, W. Yin et al., "Transcriptome analysis of *Deinagkistrodon acutus* venomous gland focusing on cellular structure and functional aspects using expressed sequence tags," *BMC Genomics*, vol. 7, article 152, 2006.

[15] G. S. Magalhães, I. L. M. Junqueira-de-Azevedo, M. Lopes-Ferreira, D. M. Lorenzini, P. L. Ho, and A. M. Moura-da-Silva, "Transcriptome analysis of expressed sequence tags from the venom glands of the fish *Thalassophryne nattereri*," *Biochimie*, vol. 88, no. 6, pp. 693–699, 2006.

[16] J. Chen, M. Deng, Q. He et al., "Molecular diversity and evolution of cystine knot toxins of the tarantula *Chilobrachys jingzhao*," *Cellular and Molecular Life Sciences*, vol. 65, no. 15, pp. 2431–2444, 2008.

[17] B. Zhao, F. Rassendren, B.-K. Kaang, Y. Furukawa, T. Kubo, and E. R. Kandel, "A new class of noninactivating K^+ channels from aplysia capable of contributing to the resting potential and firing patterns of neurons," *Neuron*, vol. 13, no. 5, pp. 1205–1213, 1994.

[18] J. Chen, L. Zhao, L. Jiang et al., "Transcriptome analysis revealed novel possible venom components and cellular processes of the tarantula *Chilobrachys jingzhao* venom gland," *Toxicon*, vol. 52, no. 7, pp. 794–806, 2008.

[19] E. Diego-García, S. Peigneur, E. Waelkens, S. Debaveye, and J. Tytgat, "Venom components from *Citharischius crawshayi* spider (Family Theraphosidae): exploring transcriptome, venomics, and function," *Cellular and Molecular Life Sciences*, vol. 67, no. 16, pp. 2799–2813, 2010.

[20] K. J. Swartz and R. MacKinnon, "An inhibitor of the Kv2.1 potassium channel isolated from the venom of a *Chilean tarantula*," *Neuron*, vol. 15, no. 4, pp. 941–949, 1995.

[21] Y. Jiang, A. Lee, J. Chen et al., "X-ray structure of a voltage-dependent K^+ channel," *Nature*, vol. 423, no. 6935, pp. 33–41, 2003.

[22] K. L. Ostrow, A. Mammoser, T. Suchyna et al., "cDNA sequence and in vitro folding of GsMTx4, a specific peptide inhibitor of mechanosensitive channels," *Toxicon*, vol. 42, no. 3, pp. 263–274, 2003.

[23] R. A. Lampe, "Analgesic peptides from venom of *Grammostola spatulata* and use thereof," *U. S. Patent*, no. 5877026, 1999.

[24] R. A. Lampe and F. Sachs, "Antiarrhythmic peptide from venom of spider *Grammostola spatulata*," *U. S. Patent*, no. 5968838, 1999.

[25] E. Redaelli, R. R. Cassulini, D. F. Silva et al., "Target promiscuity and heterogeneous effects of tarantula venom peptides affecting Na^+ and K^+ ion channels," *The Journal of Biological Chemistry*, vol. 285, no. 6, pp. 4130–4142, 2010.

[26] H. Clement, G. Odell, F. Z. Zamudio et al., "Isolation and characterization of a novel toxin from the venom of the spider *Grammostola rosea* that blocks sodium channels," *Toxicon*, vol. 50, no. 1, pp. 65–74, 2007.

[27] R. A. Lampe, P. A. Defeo, M. D. Davison et al., "Isolation and pharmacological characterization of ω-grammotoxin SIA, a novel peptide inhibitor of neuronal voltage-sensitive calcium channel responses," *Molecular Pharmacology*, vol. 44, no. 2, pp. 451–460, 1993.

[28] K. Takeuchi, E. J. Park, C. W. Lee et al., "Solution structure of ω-grammotoxin SIA, a gating modifier of P/Q and N-type Ca^{2+} channel," *Journal of Molecular Biology*, vol. 321, no. 3, pp. 517–526, 2002.

[29] F. Bosmans, M. F. Martin-Eauclaire, and K. J. Swartz, "Deconstructing voltage sensor function and pharmacology in sodium channels," *Nature*, vol. 456, no. 7219, pp. 202–208, 2008.

[30] F. Bosmans and K. J. Swartz, "Targeting voltage sensors in sodium channels with spider toxins," *Trends in Pharmacological Sciences*, vol. 31, no. 4, pp. 175–182, 2010.

[31] R. C. Rodríguez de la Vega, "A note on the evolution of spider toxins containing the ICK-motif," *Toxin Reviews*, vol. 24, no. 3-4, pp. 385–397, 2005.

[32] A. Kaser, M. Winklmayr, G. Lepperdinger, and G. Kreil, "The AVIT protein family: secreted cystein-rich vertebrate proteins

with diverse functions," *EMBO Reports*, vol. 4, no. 5, pp. 469–473, 2003.

[33] H. Schweitz, P. Pacaud, S. Diochot, D. Moinier, and M. Lazdunski, "MIT1, a black mamba toxin with a new and highly potent activity on intestinal contraction," *FEBS Letters*, vol. 461, no. 3, pp. 183–188, 1999.

[34] J. Boisbouvier, J. P. Albrand, M. Blackledge et al., "A structural homologue of colipase in black mamba venom revealed by NMR floating disulphide bridge analysis," *Journal of Molecular Biology*, vol. 283, no. 1, pp. 205–219, 1998.

[35] C. Mollay, C. Wechselberger, G. Mignogna et al., "Bv8, a small protein from frog skin and its homologue from snake venom induce hyperalgesia in rats," *European Journal of Pharmacology*, vol. 374, no. 2, pp. 189–196, 1999.

[36] L. Negri, R. Lattanzi, E. Giannini, and P. Melchiorri, "Bv8/Prokineticin proteins and their receptors," *Life Sciences*, vol. 81, no. 14, pp. 1103–1116, 2007.

[37] E. Giannini, R. Lattanzi, A. Nicotra et al., "The chemokine Bv8/prokineticin 2 is up-regulated in inflammatory granulocytes and modulates inflammatory pain," *Proceedings of the National Academy of Sciences of the United States of America*, vol. 106, no. 34, pp. 14646–14651, 2009.

[38] L. Negri, R. Lattanzi, E. Giannini, M. Canestrelli, A. Nicotra, and P. Melchiorri, "Bv8/prokineticins and their receptors: a new pronociceptive system," *International Review of Neurobiology*, vol. 85, pp. 145–157, 2009.

[39] M. Dorsch, Y. Qiu, D. Soler et al., "PK1/EG-VEGF induces monocyte differentiation and activation," *Journal of Leukocyte Biology*, vol. 78, no. 2, pp. 426–434, 2005.

[40] I. Söderhäll, Y. A. Kim, P. Jiravanichpaisal, S. Y. Lee, and K. Söderhäll, "An ancient role for a prokineticin domain in invertebrate hematopoiesis," *The Journal of Immunology*, vol. 174, no. 10, pp. 6153–6160, 2005.

[41] L. Jiang, L. Peng, J. Chen, Y. Zhang, X. Xiong, and S. Liang, "Molecular diversification based on analysis of expressed sequence tags from the venom glands of the Chinese bird spider *Ornithoctonus huwena*," *Toxicon*, vol. 51, no. 8, pp. 1479–1489, 2008.

[42] A. Savel-Niemann, "Tarantula (*Eurypelma californicum*) venom, a multicomponent system," *Biological Chemistry Hoppe-Seyler*, vol. 370, no. 5, pp. 485–498, 1989.

[43] I. I. Kaiser, P. R. Griffin, S. D. Aird et al., "Primary structures of two proteins from the venom of the Mexican red knee tarantula (*Brachypelma smithii*)," *Toxicon*, vol. 32, no. 9, pp. 1083–1093, 1994.

[44] G. Corzo, C. Bernard, H. Clement et al., "Insecticidal peptides from the theraposid spider *Brachypelma albiceps*: an NMR-based model of Ba2," *Biochimica et Biophysica Acta*, vol. 1794, no. 8, pp. 1190–1196, 2009.

[45] X. Tang, Y. Zhang, and S. Liang, "Large-scale identification and analysis of peptide toxins from the tarantula *Ornithoctonus hainana* venom using a venomic strategy," *NCBI, Direct Submission*, 2010, Accession no. GU293118.

[46] Y. Zhang, "Transcriptome analysis of *Lycosa singoriensis* spider venomous gland," *NCBI, Direct Submission*, 2008, Accession no. FM864147.

[47] W. S. Skinner, P. A. Dennis, J. P. Li, and G. B. Quistad, "Identification of insecticidal peptides from venom of the trap-door spider, *Aptostichus schlingeri* (Ctenizidae)," *Toxicon*, vol. 30, no. 9, pp. 1043–1050, 1992.

[48] U. A. Bommer, A. Lazaris-Karatzas, A. De Benedetti et al., "Translational regulation of the mammalian growth-related protein p23: involvement of eIF-4E," *Cellular and Molecular Biology Research*, vol. 40, no. 7-8, pp. 633–641, 1994.

[49] Y. Gachet, S. Tournier, M. Lee, A. Lazaris-Karatzas, T. Poulton, and U. A. Bommer, "The growth-related, translationally controlled protein P23 has properties of a tubulin binding protein and associates transiently with microtubules during the cell cycle," *Journal of Cell Science*, vol. 112, part 8, pp. 1257–1271, 1999.

[50] S. M. MacDonald, T. Rafnar, J. Langdon, and L. M. Lichtenstein, "Molecular identification of an IgE-Dependent histamine-releasing factor," *Science*, vol. 269, no. 5224, pp. 688–690, 1995.

[51] D. A. Ellerman, V. G. Da Ros, D. J. Cohen, D. Busso, M. M. Morgenfeld, and P. S. Cuasnicú, "Expression and structure-function analysis of DE, a sperm cysteine-rich secretory protein that mediates gamete fusion," *Biology of Reproduction*, vol. 67, no. 4, pp. 1225–1231, 2002.

[52] N. J. Charest, D. R. Joseph, E. M. Wilson, and F. S. French, "Molecular cloning of complementary deoxyribonucleic acid for an androgen-regulated epididymal protein: sequence homology with metalloproteins," *Molecular Endocrinology*, vol. 2, no. 10, pp. 999–1004, 1988.

[53] A. L. Kierszenbaum, O. Lea, P. Petrusz, F. S. French, and L. L. Tres, "Isolation, culture, and immunocytochemical characterization of epididymal epithelial cells from pubertal and adult rats," *Proceedings of the National Academy of Sciences of the United States of America*, vol. 78, no. 3, pp. 1675–1679, 1981.

[54] M. Kasahara, H. C. Passmore, and J. Klein, "A testis-specific gene Tpx-1 maps between Pgk-2 and Mep-1 on mouse chromosome 17," *Immunogenetics*, vol. 29, no. 1, pp. 61–63, 1989.

[55] L. Kjeldsen, J. B. Cowland, A. H. Johnsen, and N. Borregaard, "SGP28, a novel matrix glycoprotein in specific granules of human neutrophils with similarity to a human testis-specific gene product and to a rodent sperm-coating glycoprotein," *FEBS Letters*, vol. 380, no. 3, pp. 246–250, 1996.

[56] J. Mochca-Morales, B. M. Martin, and L. D. Possani, "Isolation and characterization of helothermine, a novel toxin from *Heloderma horridum horridum* (Mexican beaded lizard) venom," *Toxicon*, vol. 28, no. 3, pp. 299–309, 1990.

[57] M. Nobile, F. Noceti, G. Prestipino, and L. D. Possani, "Helothermine, a lizard venom toxin, inhibits calcium current in cerebellar granules," *Experimental Brain Research*, vol. 110, no. 1, pp. 15–20, 1996.

[58] Y. Yamazaki, H. Koike, Y. Sugiyama et al., "Cloning and characterization of novel snake venom proteins that block smooth muscle contraction," *European Journal of Biochemistry*, vol. 269, no. 11, pp. 2708–2715, 2002.

[59] R. Bonasio, G. Zhang, C. Ye et al., "Genomic comparison of the ants *Camponotus floridanus* and *Harpegnathos saltator*," *Science*, vol. 329, no. 5995, pp. 1068–1071, 2010.

[60] M. Naimuddin, S. Kobayashi, C. Tsutsui et al., "Directed evolution of a three-finger neurotoxin by using cDNA display yields antagonists as well as agonists of interleukin-6 receptor signaling," *Molecular Brain*, vol. 4, no. 1, article 2, 2011.

Hindawi Publishing Corporation
International Journal of Peptides
Volume 2012, Article ID 532519, 10 pages
doi:10.1155/2012/532519

Review Article

Platelet-Rich Plasma Peptides: Key for Regeneration

Dolores Javier Sánchez-González,[1,2] Enrique Méndez-Bolaina,[3,4] and Nayeli Isabel Trejo-Bahena[2,5]

[1] *Subsección de Biología Celular y Tisular, Escuela Médico Militar, Universidad del Ejército y Fuerza Aérea, 11200 México City, MEX, Mexico*
[2] *Sociedad Internacional para la Terapia Celular con Células Madre, Medicina Regenerativa y Antienvejecimiento S.C. (SITECEM), 53840 Naucalpan, MEX, Mexico*
[3] *Facultad de Ciencias Químicas, Universidad Veracruzana, 94340 Orizaba, VER, Mexico*
[4] *Centro de Investigaciones Biomédicas-Doctorado en Ciencias Biomédicas, Universidad Veracruzana, 91000 Xalapa, VER, Mexico*
[5] *Área de Medicina Física y Rehabilitación, Hospital Central Militar, 11200 México City, MEX, Mexico*

Correspondence should be addressed to Dolores Javier Sánchez-González, javiersglez@yahoo.com

Received 15 September 2011; Revised 13 December 2011; Accepted 14 December 2011

Academic Editor: Frédéric Ducancel

Platelet-derived Growth Factors (GFs) are biologically active peptides that enhance tissue repair mechanisms such as angiogenesis, extracellular matrix remodeling, and cellular effects as stem cells recruitment, chemotaxis, cell proliferation, and differentiation. Platelet-rich plasma (PRP) is used in a variety of clinical applications, based on the premise that higher GF content should promote better healing. Platelet derivatives represent a promising therapeutic modality, offering opportunities for treatment of wounds, ulcers, soft-tissue injuries, and various other applications in cell therapy. PRP can be combined with cell-based therapies such as adipose-derived stem cells, regenerative cell therapy, and transfer factors therapy. This paper describes the biological background of the platelet-derived substances and their potential use in regenerative medicine.

1. Introduction

Platelets are nonnuclear cellular fragments derived from megakaryocytes in the bone marrow; they are specialized secretory elements that release the contents of their intracellular granules in response to activation. They were discovered by Bizzozero in the 19th century [1] and after Wright observed that megakaryocytes are platelet precursors [2]. Actually we know that platelets synthesize proteins and that pattern of peptides synthesis changes in response to cellular activation [3].

Platelets contain a great variety of proteins molecules, among which are the high presence of signaling, membrane proteins, protein processing, cytoskeleton regulatory proteins, cytokines, and other bioactive peptides that initiate and regulate basic aspects of wound healing [3]. It is known, through efforts such as the platelet proteome project, that more than 300 proteins are released by human platelets in response to thrombin activation [4]. Proteome platelet includes 190 membrane-associated and 262 phosphorylated proteins, which were identified via independent proteomic and phospho proteomic profiling [5].

When platelets fall precipitously below critical levels (usually under 10,000 to 20,000 per cubic millimeter), molecular disassembly opens the zippers formed by adjacent intercellular endothelial junctions, causing extravasation of erythrocytes into the surrounding tissues. In addition to their well-known function in hemostasis, platelets also release substances that promote tissue repair, angiogenesis, and inflammation [6]. Furthermore, they induce the migration and adherence of bone-marrow-derived cells to sites of angiogenesis; platelets also induce differentiation of endothelial-cell progenitors into mature endothelial cells [7].

At the site of the injury, platelets release an arsenal of potent regenerative and mitogenic substances that are involved in all aspects of the wound-healing process including a potential point-of-care biologic treatment following myocardial injury [8]. Based on this, platelet called Platelet-rich Plasma (PRP) has been extensively used for orthopaedic

Table 1: Peptidic growth factors present in platelet-rich plasma (PRP).

Name	Cytogenetic location	Biologic activities
Transforming growth factor, beta-I; TGFB1	19q13.2	Controls proliferation, differentiation, and other functions in many cell types
Platelet-derived growth factor, alpha polypeptide; PDGFA	7p22.3	Potent mitogen for connective tissue cells and exerts its function by interacting with related receptor tyrosine kinases
Platelet-derived growth factor, beta polypeptide; PDGFB	22q13.1	Promotes cellular proliferation and inhibits apoptosis
Platelet-derived growth factor C; PDGFC	4q32.1	Increases motility in mesenchymal cells, fibroblasts, smooth muscle cells, capillary endothelial cells, and neurons
Platelet-derived growth factor D; PDGFD	11q22.3	Involved in developmental and physiologic processes, as well as in cancer, fibrotic diseases, and arteriosclerosis
Insulin-like growth factor I; IGF1	12q23.2	Mediates many of the growth-promoting effects of growth hormone
Fibroblast growth factor I; FGF1	5q31.3	Induces liver gene expression, angiogenesis and fibroblast proliferation
Epidermal growth factor; EGF	4q25	Induces differentiation of specific cells, is a potent mitogenic factor for a variety of cultured cells of both ectodermal and mesodermal origin
Vascular endothelial growth factor A; VEGFA	6p21.1	Is a mitogen primarily for vascular endothelial cells, induces angiogenesis
Vascular endothelial growth factor B; VEGFB	11q13.1	Is a regulator of blood vessel physiology, with a role in endothelial targeting of lipids to peripheral tissues
Vascular endothelial growth factor C; VEGFC	4q34.3	Angiogenesis and endothelial cell growth, and can also affect the permeability of blood vessels

Includes, name, cytogenetic location, and biologic activities of platelet growth factors. Furthermore, PRP content other proteins like interleukin-8, macrophage inflammatory protein-1 alpha, and platelet factor-4.

applications; for topical therapy of various clinical conditions, including wounds and soft tissue injuries; and suitable alternative to fetal calf serum for the expansion of mesenchymal stem cells from adipose tissue (see Table 1) [9–12].

In this paper we are going to talk about the platelets, platelet-derived particles, and their biological effects in regenerative medicine.

2. Platelets

Platelets are the first element to arrive at the site of tissue injury and are particularly active in the early inflammatory phases of the healing process [6]. They play a role in aggregation, clot formation, homeostasis through cell membrane adherence, and release of substances that promote tissue repair and that influence the reactivity of blood vessels and blood cell types involved in angiogenesis, regeneration, and inflammation [13]. Platelet secretory granules contain growth factors (GFs), signaling molecules, cytokines, integrins, coagulation proteins, adhesion molecules, and some other molecules, which are synthesized in megakaryocytes and packaged into the granules through vesicle trafficking processes [14]. Three major storage compartments in platelets are alpha granules, dense granules, and lysosomes [14].

Platelets mediate these effects through degranulation, in which platelet-derived GF (PDGF), insulin-like GF (IGF1), transforming GF-beta 1 (TGF-β1), vascular endothelial GF (VEGF), basic fibroblastic GF (bFGF), and epidermal GF (EGF) are released from alpha granules [15]. In fact, the majority of the platelet substances are contained in alpha granules (see Table 2) [15]. When platelets are activated, they exocytose the granules; this process is mediated by molecular mechanisms homologous to other secretory cells, uniquely coupled to cell activation by intracellular signaling events [16].

Among bioactive molecules stored and released from platelets dense granules are catecholamines, histamine, serotonin, ADP, ATP, calcium ions, and dopamine, which are active in vasoconstriction, increased capillary permeability, attract and activate macrophages, tissue modulation and regeneration. These non-GF molecules have fundamental effects on the biologic aspects of wound healing [5].

For their numerous functions, platelets have developed a set of platelet receptors that are the contact between platelets and their surroundings; they determine the reactivity of platelets with a wide range of agonists and adhesive proteins. Some of these receptors are expressed only on activated platelets [6]. Certain biological mechanisms present in the platelets are shared with other cells, and therefore they contain some common cytoplasmic enzymes, signal transduction molecules, and cytoskeletal components [14].

Table 2: Some bioactive peptides present in the alpha granules of platelets.

General activity categories	Specific molecules	Cytogenetic location	Biologic activities
Clotting factors and related proteins	Tissue factor pathway inhibitor; TFPI	2q32.1	Regulates the tissue factor-(TF-) dependent pathway of blood coagulation
	Kininogen; KNG	3q27.3	Plays an important role in assembly of the plasma kallikrein
	Growth arrest-specific 6; GAS6	13q34	Stimulates cell proliferation
	Multimerin; MMRN	4q22	Carrier protein for platelet factor V
	Antithrombin; AT	1q25.1	Is the most important inhibitor of thrombin
	Protein S; PROS1	3q11.1	Inhibits blood clotting
	Coagulation factor V; F5	1q24.2	Acts as a cofactor for the conversion of prothrombin to thrombin by factor Xa
	Coagulation factor XI; F11	4q35.2	It participates in blood coagulation as a catalyst in the conversion of factor IX to factor IXa in the presence of calcium ions
Fibrinolytic factors and related proteins	Plasminogen; PLG	6q26	Induces plasmin production (leads to fibrinolysis)
	Plasminogen activator inhibitor 1; PAI1	7q22.1	Regulation of plasmin production
	Alpha-2-plasmin inhibitor	17p13.3	Inactivation of plasmin
	Osteonectin; ON	5q33.1	Inhibits cell-cycle progression and influences the synthesis of extracellular matrix (ECM)
	Histidine-rich glycoprotein; HRG	3q27.3	Interacts with heparin and thrombospondin
	Thrombin-activatable fibrinolysis inhibitor; TAFI	13q14.13	Attenuates fibrinolysis
	Alpha-2-Macroglobulin; A2M	12p13.31	Carrier of specific growth factors and induces cell signaling
Proteases and antiproteases	Tissue inhibitor of metalloproteinase 4; TIMP4	3p25.2	Inhibits matrix metalloproteinases (MMPs), a group of peptidases involved in degradation of the extracellular matrix
	Complement component 1 inhibitor; C1NH	11q12.1	Inhibits serine proteinases including plasmin, kallikrein, and coagulation factors XIa and XIIa
	Alpha-1-antitrypsin (serpin peptidase inhibitor)	14q32.13	Acute phase protein, inhibits a wide variety of proteases and enzymes
	Nexin 2; SNX2	5q23.2	Modulates intracellular trafficking of proteins to various organelles
Basic proteins	Platelet factor 4; PF4	4q13.3	Inhibition of angiogenesis
	β-thromboglobulin (Pro-platelet basic protein; PPBP)	4q13.3	Platelet activation, inhibition of angiogenesis
	Endostatin (Collagen, type XVIII, Alpha-1; COL18A1)	21q22.3	Inhibitors of endothelial cell migration and angiogenesis
Adhesive proteins	Fibrinogen; FG	4q31.3	Blood clotting cascade (fibrin clot formation)
	Fibronectin; FN	2q35	Binds to cell-surface integrins, affecting cell adhesion, cell growth, migration, and differentiation
	Vitronectin; VTN	17q11.2	Induces cell adhesion, chemotaxis
	Thrombospondin I; THBS1	15q14	Inhibition of angiogenesis
	Laminin-8	18p11.31-p11.23	Modulates cell contact interactions

It is described general activity categories, specific molecules, cytogenetic location and biologic activities. Furthermore, alpha granules include growth factors of Table 1, membrane glycoproteins, and others proteins like albumin and immunoglobulins.

The platelet lifespan is approximately 7 to 9 days, which they spend circulating in the blood in their resting form. When adhered to exposed endothelium or activated by agonists, they change their shape and secrete the contents of the granules (including ADP, fibrinogen, and serotonin), which is followed by platelet aggregation [7]. Initiation of the signaling event within the platelet leads to the reorganization of the platelet cytoskeleton, which is visible as an extremely rapid shape change [17].

3. Platelet-Rich Plasma (PRP)

Platelets are activated either by adhesion to the molecules that are exposed on an injured endothelium, such as von Willebrand Factor (vWF), collagen, fibronectin, and laminin, or by physiologic agonists such as thrombin, ADP, collagen, thromboxane A2, epinephrine, and platelet-activating factors [18].

PRP has been used clinically in humans since the 1970s for its healing properties attributed of autologous GF and secretory proteins that may enhance the healing process on a cellular level [19]. Furthermore, PRP enhances the recruitment, proliferation, and differentiation of cells involved in tissue regeneration [20]. PRP-related products, also known as platelet-rich concentrate, platelet gel, preparation rich in growth factors (PRGF), and platelet releasate, have been studied with in vitro and in vivo experiments in the fields of surgical sciences mainly [21].

Depending on the device and technique used, PRP can contain variable amounts of plasma, erythrocytes, white blood cells, and platelets. The platelet concentration should be increased above baseline or whole blood concentration. It is generally agreed upon that PRP should have a minimum of 5 times the number of platelets compared to baseline values for whole blood to be considered "platelet rich" [22].

This conclusion is supported by in vitro work showing a positive dose-response relationship between platelet concentration and proliferation of human mesenchymal stem cells, proliferation of fibroblasts, and production of type I collagen [23]. This suggests that the application of autologous PRP can enhance wound healing, as has been demonstrated in controlled animal studies for both soft and hard tissues [24, 25].

Autologous PRP represents an efficacious treatment for its use in wound healing like chronic diabetic foot ulceration due to multiple growth factors, is safe for its autologous nature, and is produced as needed from patient blood. Like we said, key for self-regeneration [26].

Upon activation, platelets release their granular contents into the surrounding environment. The platelet alpha granules are abundant and contain many of the GFs responsible for the initiation and maintenance of the healing response [14]. These GFs have been shown to play an important role in all phases of healing. The active secretion of these proteins by platelets begins within 10 minutes after clotting, with more than 95% of the presynthesized GFs secreted within 1 hour. After this initial burst, the platelets synthesize and secrete additional proteins for the balance of their life (5–10 days) [10].

The fibrin matrix formed following platelet activation also has a stimulatory effect on wound healing. The fibrin matrix forms by polymerization of plasma fibrinogen following either external activation with calcium or thrombin or internal activation with endogenous tissue thromboplastin [23]. This matrix traps platelets allowing a slow release of a natural combination of GF while providing a provisional matrix that provides a physical framework for wound stem cells and fibroblast migration and presentation of other biological mediators such as adhesive glycoproteins [27, 28].

PRP with a platelet concentration of at least 1 000 000 platelets/μL in 5 mL of plasma is associated with the enhancement of healing [29]. PRP can potentially enhance healing by the delivery of various GF and cytokines from the alpha granules contained in platelets and has an 8-fold increase in GF concentrations compared with that of whole blood [30].

The use of PRP to enhance bone regeneration and soft tissue maturation has increased dramatically in the fields of orthopedics, periodontics, maxillofacial surgery, urology, and plastic surgery over the last years. However, controversies exist in the literature regarding the added benefit of this procedure. While some authors have reported significant increases in bone formation and maturation rates [21], others did not observe any improvement [31].

The wound-healing process is a complex mechanism characterized by four distinct, but overlapping, phases: hemostasis, inflammation, proliferation, and remodeling [8]. The proliferative phase includes blood vessel formation by endothelial cells and bone synthesis by osteoblasts. All these events are coordinated by cell-cell interactions and by soluble GF released by various cell types. Recent reviews have emphasized the need for additional research aiming to characterize PRP in terms of GF content and their physiological roles in wound healing [32–34].

Thrombin represents a strong inducer of platelet activation leading to GF release [35]. It is also known that particulate grafts, when combined with calcium and thrombin treated PRP, possess better handling characteristics and higher GF content [31]. Typically, thrombin concentrations used in clinical applications vary between 100 and 200 units per mL [21], while platelet aggregation is maximum in the range of 0.5 to 4 units per mL [36].

The basic cytokines identified in platelets play important roles in cell proliferation, chemotaxis, cell differentiation, regeneration, and angiogenesis [28]. A particular value of PRP is that these native cytokines are all present in "normal" biologic ratios. The platelets in PRP are delivered in a clot, which contains several cell adhesion molecules including fibronectin, fibrin, and vitronectin. These cell adhesion molecules play a role in cell migration and thus also add to the potential biologic activity of PRP. The clot itself can also play a role in wound healing by acting as conductive matrix or "scaffold" upon which cells can adhere and begin the wound-healing process [28].

PRP can only be made from anticoagulated blood. Preparation of PRP begins by addition of citrate to whole blood to bind the ionized calcium and inhibit the clotting cascade [15]. This is followed by one or two centrifugation steps. The

first centrifugation step separates the red and white blood cells from plasma and platelets. The second centrifugation step further concentrates the platelets, producing the PRP separate from platelet-poor plasma [19].

An important point is that clotting leads to platelet activation, resulting in release of the GF from the alpha granules, otherwise known as degranulation. Approximately 70% of the stored GFs are released within 10 minutes, and nearly 100% of the GFs are released within 1 hour. Small amounts of GF may continue to be produced by the platelet during the rest of its lifespan (1 week) [21].

A method to delay the release of GF is possible by addition of calcium chloride ($CaCl_2$) to initiate the formation of autogenous thrombin from prothrombin. The $CaCl_2$ is added during the second centrifugation step and results in formation of a dense fibrin matrix. Intact platelets are subsequently trapped in the fibrin matrix and release GF slowly over a 7-day period. The fibrin matrix itself may also contribute to healing by providing a conductive scaffold for cell migration and new matrix formation [27].

4. Growth Factors (GFs)

Platelets are known to contain high concentrations of different GF and are extremely important in regenerative process; activation of the platelet by endothelial injury initiates the wound-healing process [30]. When platelets are activated, their alpha granules are released, resulting in an increased concentration of GF in the wound milieu [14].

There is increasing evidence that the platelet cell membranes themselves also play a crucial role in wound healing through their GF receptor sites [28]. GFs are found in a wide array of cells and in platelet alpha granules [37]. Table 1 gives an overview of some of the more extensively studied GFs and their involvement in wound healing. There are many more, both discovered and undiscovered, GFs. The platelet is an extremely important cell in wound healing because it initiates and plays a major role in the wound regenerative process [38].

The first discovered GF was EGF in 1962 by Cohen [39]. It was not until 1989 before clinical trials with EGF were attempted to demonstrate enhanced wound healing. Studies did demonstrate that EGF can accelerate epidermal regeneration and enhance healing of chronic wounds [40].

PDGF was discovered in 1974 and is ubiquitous in the body. It is known to be released by platelet alpha granules during wound healing and stimulate the proliferation of many cells, including connective tissue cells. In fact, thus far, high-affinity cell-surface receptors specific for PDGF have only been demonstrated on connective tissue cells. When released, PDGF is chemotactic for monocytes, neutrophils, and fibroblasts. These cells release their own PDGF, thus creating a positive autocrine feedback loop [41]. Other functions of PDGF include effects on cell growth, cellular migration, metabolic effects, and modulation of cell membrane receptors [42].

PDGFs were first identified as products of platelets which stimulated the proliferation in vitro of connective tissue cell types such as fibroblasts [43].

The PDGF system, comprising four isoforms (PDGF-A, -B, -C, and -D) and two receptor chains (PDGFR-alpha and -beta), plays important roles in wound healing, atherosclerosis, fibrosis, and malignancy. Components of the system are expressed constitutively or inducibly in most renal cells [42]. They regulate a multitude of pathophysiologic events, ranging from cell proliferation and migration to extracellular matrix accumulation, production of pro- and anti-inflammatory mediators, tissue permeability, and regulation of hemodynamics [43].

Inactivation of PDGF-B and PDGF beta receptor (PDGFRb) genes by homologous recombination in embryonic stem cells shows cardiovascular, hematological, and renal defects. The latter is particularly interesting since it consists of a specific cellular defect: the complete loss of kidney glomerular mesangial cells and the absence of urine collection in the urinary bladder [43].

PDGF-C and PDGFR-alpha contribute to the formation of the renal cortical interstitium. Almost all experimental and human renal diseases are characterized by altered expression of components of the PDGF system. Infusion or systemic overexpression of PDGF-B or -D induces prominent mesangioproliferative changes and renal fibrosis. Intervention studies identified PDGF-C as a mediator of renal interstitial fibrosis and PDGF-B and -D as key factors involved in mesangioproliferative disease and renal interstitial fibrosis [43–45].

Fréchette et al., demonstrated that the release of PDGF-B, TGF-beta1, bFGF, and VEGF is significantly regulated by the amount of calcium and thrombin added to the PRP and that PRP supernatants are more mitogenic for endothelial cells than whole-blood supernatants [11]. Other GFs such as epidermal growth factor (EGF), transforming growth factor-alpha (TGF-alpha), insulin-like growth factor-1 (IGF-1), angiopoietin-2 (Ang-2), and interleukin-1beta (IL-1beta) are also known to play important roles in the wound-healing process [28].

In 2008, Wahlström et al., demonstrated that growth factors released from platelets had potent effects on fracture and wound healing. The acidic tide of wound healing, that is, the pH within wounds and fractures, changes from acidic pH to neutral and alkaline pH as the healing process progresses [44]. They investigated the influence of pH on lysed platelet concentrates regarding the release of growth factors. The platelet concentrates free of leukocyte components were lysed and incubated in buffers with pH between 4.3 and 8.6. Bone morphogenetic protein-2 (BMP-2), platelet-derived growth factor (PDGF), transforming growth factor-beta (TGF-beta), and vascular endothelial growth factor (VEGF) were measured by quantitative enzyme-linked immunosorbent assays. BMP-2 was only detected in the most acidic preparation (pH 4.3), which is interesting since BMP-2 has been reported to be an endogenous mediator of fracture repair and to be responsible for the initiation of fracture healing. These findings indicate that platelets release substantial amounts of BMP-2 only under conditions of low pH, the milieu associated with the critical initial stage of fracture healing [44].

Recently, Bir et al., demonstrated stromal cell-derived factor 1-α (SDF-1α) PRP from diabetic mice. The concentration (pg/mL) of different growth factors was significantly higher in the PRP group than in the platelet-poor plasma (PPP) group. The concentrations (pg/mL) of SDF-1α (10,790 ± 196 versus 810 ± 39), PDGF-BB (45,352 ± 2,698 versus 958 ± 251), VEGF (53 ± 6 versus 30 ± 2), bFGF (29 ± 5 versus 9 ± 5), and IGF-1 (20,628 ± 1,180 versus 1,214 ± 36) were significantly higher in the PRP group than in the PPP group, respectively [46].

5. Platelet GF as Treatment

5.1. In Vitro Studies. Knowledge of GF and their function is far from complete. Many of the known functions were learned through in vitro study. Although many GFs are associated with wound healing, PDGF and TGF-β1 appear to be two of the more integral modulators [46]. PDGF has activity in early wound healing (during the acid tide). In vitro studies have shown that at lower pH (5.0), platelet concentrate lysate has increased concentrations of PDGF, with an increased capacity to stimulate fibroblast proliferation [23]. TGF-β increases the production of collagen from fibroblasts [47]. Its release in vitro is enhanced by neutral or alkaline pH, which correspond to the later phases of healing [10]. Through modulation of interleukin-1 production by macrophages, PRP may inhibit excessive early inflammation that could lead to dense scar tissue formation [48]. Insulin-like GF-I (IGF-1) has also been extensively studied for its ability to induce proliferation, differentiation, and hypertrophy of multiple cell lines. Separate analyses of GF in PRP have shown significant increases in PDGF, VEGF, TGF-β1, and EGF, compared with their concentrations in whole blood [15, 49].

IGF-1 has two important functions: chemotaxis for vascular endothelial cells into the wound which results in angiogenesis and promoting differentiation of several cell lines including chondroblasts, myoblasts, osteoblasts, and hematopoietic cells [50].

TGF-β is a member of the newest family of proteins discovered. Two major sources of this protein are the platelet and macrophage. TGF-β causes chemotactic attraction and activation of monocytes, macrophages, and fibroblasts. The activated fibroblasts enhance the formation of extracellular matrix and collagen and also stimulate the cells ability to contract the provisional wound matrix [51]. Macrophages infiltration promotes TGF-β that induces extracellular matrix such as collagen and fibronectin; however alpha-mangostin prevents the increase in this molecule in rats with Cisplatin-induced nephrotoxicity [52].

5.2. In Vivo Studies. In vivo study is much more complex due to the inability to control the environment. A further complexing matter is the fact that the same GF, depending on the presence or absence of other peptides, may display either stimulatory or inhibitory activity within the same cell. Also, a particular GF can alter the binding affinity of another GF receptor [53].

Release of PDGF can have a chemotactic effect on monocytes, neutrophils, fibroblasts, stem cells, and osteoblasts. This peptide is a potent mitogen for mesenchymal cells including fibroblasts, smooth muscle cells and glial cells [54] and is involved in all three phases of wound healing, including angiogenesis, formation of fibrous tissue, and reepithelialization [41].

TGF beta released from platelet alpha granules is a mitogen for fibroblasts, smooth muscle cells, and osteoblasts. In addition, it promotes angiogenesis and extracellular matrix production [41]. VEGF promotes angiogenesis and can promote healing of chronic wounds and aid in endochondral ossification. EGF, another platelet-contained GF, is a mitogen for fibroblasts, endothelial cells, and keratinocytes and also is useful in healing chronic wounds [55].

IGF, another platelet-contained GF regulates bone maintenance and is also an important modulator of cell apoptosis, and, in combination with PDGF, can promote bone regeneration [56].

However, there are conflicting results with regard to IGF-1, where the majority of studies reported no increase in IGF-1 in PRP, compared with whole blood. There are also conflicting results regarding the correlation between the GF content and platelet counts in PRP [57]. The basis of these contradictions is not fully understood and may be related to variability in patient age, health status, or platelet count. Alternatively, differences in GF content and platelet count may be due to the various methods of processing, handling, and storing of samples, in addition to the type of assay performed. The diversity of PRP products should be taken into account when interpreting and comparing results and methods for generating PRP [10].

VEGF, discovered 25 years ago, was initially referred to as vascular permeability factor [58]. In mammals, there are at least four members of the VEGF family: VEGF-A, VEGF-B, and the VEGF-C/VEGF-D pair, which has a common receptor, VEGF receptor 3 (VEGF-R3) [59]. VEGF-A is a proangiogenic cytokine during embryogenesis and contributes to vascular integrity: selective knockout of VEGF-A in endothelial cells increases apoptosis, which compromises the integrity of the junctions between endothelial cells [60, 61]. VEGF-B, which can form heterodimers with VEGF-A, occurs predominantly in brown fat, myocardium, and skeletal muscle [62]. VEGF-C and VEGF-D seem to regulate lymphangiogenesis. The expression of VEGF-R3 in adults is restricted to the lymphatics and fenestrated endothelium [63]. Neuropilin 1 and neuropilin 2 are receptors that bind specific VEGF family members and are important in neuronal development and embryonic vasculogenesis [64].

Megakaryocytes and platelets contain the three major isoforms of VEGF-A; after exposure to thrombin in vitro, they release VEGF-A [65–67]. VEGF-A alters the endothelial-cell phenotype by markedly increasing vascular permeability, upregulating expression of urokinase, tissue plasminogen activator, connexin, osteopontin, and the vascular-cell adhesion molecule [68].

Table 3: Platelet-plasma-derived peptides are current in clinical use and clinical trials.

Year	Researchers	Health problems	Clinical protocols	Level of evidence	Results
2005	Carreon et al.	Bone healing in instrumented posterolateral spinal fusions	Retrospective cohort study to evaluate rates of nonunionin patients ($n = 76$) with autologous iliac bone graft augmented with platelet gel	Level 4, case control group of 76 randomly selected patients who were matched and grafted with autogenous iliac bone graft with no platelet gel	Nonunion rate in platelet gel group was 25%; 17% in control group ($P = .18$)
2006	Mishra and Pavelko	Chronic elbow tendinitis	Cohort, 15 patients injected with PRP	Level 2, 5 controls	Decreased pain at 2 years (measured by visual analog pain score)
	Savarino et al.	Bone healing in varus HTOs for genu varus	Randomized case control, 5 patients with bone grafted with bone chips and PRP	Level 4, 5 controls bone grafted without PRP	No functional or clinical difference; histology shows increased amounts of osteoid and osteoblasts in PRP group
	Sánchez et al.	Achilles tear healing	Case control, 6 repairs with PRP	Level 3, 6 matched retrospective controls	Improved ROM and early return to activity with PRP by ± 4–7 weeks
2007	Dallari et al.	Bone healing in varus HTOs for genu varus	Prospective randomized control: group A, bone chips with platelet gel ($n = 11$); group B, bone chips, BMC, and platelet gel ($n = 12$)	Level 1, 10 controls treated with bone chips only	Biopsies at 6 weeks after surgery showed increased osteoid and osteoblasts in groups A and B; radiographic differences decreased with time; no clinical difference at 1 year among groups
	Kitoh et al.	Bone healing in distraction osteogenesis for limb lengthening and short stature	Retrospective, comparison case control; at 3 weeks, patients injected with expanded BMC with or without PRP ($n = 32$ bones)	Level 3, 60 bones in retrospective control group (high % of congenital etiologies versus PRP group)	Average healing in BMC + PRP was 34 ± 4 d/cm; control group average was 73.4 ± 27 d/cm ($P = .003$)
2009	Sánchez et al.	Bone healing in nonunions	Retrospective, case series; 16 nonhypertrophic nonunions treated with either surgery and PRGF or percutaneous injections of PRGF to stimulate ($n = 3$) without surgery	Level 4, no control group	84% healed after surgical treatment; unclear if PRGF made a difference

Some published human clinical orthopaedic PRP studies. PRP: platelet-rich plasma; ROM: range of motion; HTO: high tibial osteotomy; BMC: bone marrow cells; PRGF: preparation rich in growth factors [27]. Taken from Foster et al. [27].

6. PRP in Cell Therapy and Regenerative Medicine

PRP can be combined with cell-based therapies such as adipose-derived stem cells, regenerative cell therapy, and transfer factors therapy [69]. While this is a relatively new concept, the strategy is appealing as the regenerative matrix graft delivers a potent trilogy of regenerative cells, fibrin matrix, and GF [15]. The applications are similar to those for PRP alone with the added benefit of regenerative cell enrichment.

Verrier et al., demonstrated that cultures of human mesenchymal stem cell (MSC) supplemented with platelet-released supernatant (PRS) had differentiation towards an osteoblastic phenotype in vitro possibly mediated by bone morphogenetic protein-2 (BMP-2). PRS showed an osteoinductive effect on MSC, as shown by an increased expression of typical osteoblastic marker genes such as collagen I, bone sialoprotein II, BMP-2, and matrix metalloproteinase-13 (MMP-13), as well as by increased Ca^{++} incorporation [70].

Furthermore, the role of platelets in hemostasis may be influenced by alteration of the platelet redox state, the presence of endogenous or exogenous antioxidants, and the formation of reactive oxygen and nitrogen species [71]. As discussed by Sobotková et al., [71], trolox and resveratrol inhibit aggregation of washed platelets and PRP activated by ADP, collagen, and thrombin receptor-activating peptide. Antioxidants, apart from nonspecific redox or radical-quenching mechanisms, inhibit platelet activation also by specific interaction with target proteins. In this context, powerful natural antioxidants, like nordihydroguaiaretic acid (NDGA) extracted from *Larrea tridentata* [72], S-allylcysteine (SAC), the most abundant organosulfur compound in aged garlic extract (AG) [73], sulforaphane (SFN), an isothiocyanate produced by the enzymatic action of myrosinase on glucoraphanin, a glucosinolate contained in

cruciferous vegetables [74], and acetonic and methanolic extracts of *Heterotheca inuloides*, can be administered with ample safety margin in patients treated with PRP [75].

7. Advantages, Limitations, and Precautions

PRP as autologous procedure eliminates secondary effects and unnecessary risks for chemically processed strange molecules, is a natural reserver of various growth factors that can be collected autologously, and is costeffective [76–81] (see Table 3). Thus for clinical use, no special considerations concerning antibody formation and infection risk are needed. The key of our health and our own regeneration resides in our own body. Nevertheless this treatment is not the panacea, it is only the beginning in this new age of the regenerative medicine. Some clinical devices to automatically prepare PRPs are available at present. PRP are consistently being used clinically in the department of orthopedics and plastic surgery (oral, maxillary facial) for a long time. On the basis of research evidence, some publications have reported positive results in either bone or soft tissue healing. It is recommended to avoid the abuse and use generalized of this procedure before any disease. Until now, their clinical applications still are limited. However, some research concludes that there is no or little benefit from PRP. This is likely due to faster degradation of growth factors in PRP since some authors suggest using sustained release form of PRP to deliver optimal effect of PRP. Gelatin hydrogel is also being used clinically as a slow, sustained release of carrier for growth factors in our center recently [47].

8. Conclusions

PRP as therapeutic option is a powerful tool nowadays for the localized delivery of great variety of biologically active GF to the site of injury and is supported by its simplicity, potential cost effectiveness, safety, and permanent availability [11].

Platelet concentrates are potentially useful in wound-healing applications because they function as both a tissue sealant and a drug delivery system that contains a host of powerful mitogenic and chemotactic GFs. However, the method of PRP preparation has a potentially significant impact on the different levels of platelet recovery and activation [10]. Platelet activation during preparation of the platelet concentrate can result in early alpha granule release and loss of the GF during the collection process. It is therefore critical to recognize that each PRP preparation method may differ in regard to platelet number, platelet activation rates, and GF profiles [15].

In this regard, therefore, it is critical to define the extent of platelet activation that occurs during graft preparation. If platelets become activated and release the contents of the alpha granules during the centrifugation process, the GF will be diluted and lost into the plasma. To ensure that platelets are intact until the PRP fraction has been collected, platelet surface marker for platelet activation P selectin can be measured [30]. However, in all methods, the application of PRP is really providing a sufficient dose of these useful bioactive peptides for wound healing and regenerative process [82].

Acknowledgments

This work was supported by award SNI-33834, to D. J. Sánchez-González and SNI-38264 to E. Méndez-Bolaina from CONACYT Investigators National System from México and International Society for Cellular Therapy with Stem Cells, Regenerative Medicine and Anti-aging (SITECEM, México).

References

[1] G. Bizzozero, "Su di un nuovo elemento morfologico del sangue dei mammiferi e della sua importanza nella trombosi e nella coagulazione," *L'Osservatore*, vol. 17, pp. 785–787, 1881.

[2] J. H. Wright, "The origin and nature of blood plates," *Boston Medical Surgical Journal*, vol. 154, pp. 643–645, 1906.

[3] A. S. Weyrich, H. Schwertz, L. W. Kraiss, and G. A. Zimmerman, "Protein synthesis by platelets: historical and new perspectives," *Journal of Thrombosis and Haemostasis*, vol. 7, no. 2, pp. 241–246, 2009.

[4] J. A. Coppinger, G. Cagney, S. Toomey et al., "Characterization of the proteins released from activated platelets leads to localization of novel platelet proteins in human atherosclerotic lesions," *Blood*, vol. 103, no. 6, pp. 2096–2104, 2004.

[5] A. H. Qureshi, V. Chaoji, D. Maiguel et al., "Proteomic and phospho-proteomic profile of human platelets in basal, resting state: insights into integrin signaling," *PLoS One*, vol. 4, no. 10, Article ID e7627, 2009.

[6] R. L. Nachman and S. Rafii, "Platelets, petechiae, and preservation of the vascular wall," *The New England Journal of Medicine*, vol. 359, no. 12, pp. 1261–1270, 2008.

[7] K. Jurk and B. E. Kehrel, "Platelets: physiology and biochemistry," *Semin Thromb Hemost*, vol. 31, pp. 381–392, 2005.

[8] A. Mishra, J. Velotta, T. J. Brinton et al., "RevaTen platelet-rich plasma improves cardiac function after myocardial injury," *Cardiovascular Revascularization Medicine*, vol. 12, no. 3, pp. 158–163, 2011.

[9] P. Borzini and L. Mazzucco, "Platelet-rich plasma (PRP) and platelet derivatives for topical therapy. What is true from the biological view point?" *ISBT Science Series*, vol. 2, pp. 272–281, 2007.

[10] B. Cole and S. Seroyer, "Platelet-rich plasma: where are we now and where are we going?" *Sports Health*, vol. 2, no. 3, pp. 203–210, 2010.

[11] J. P. Fréchette, I. Martineau, and G. Gagnon, "Platelet-rich plasmas: growth factor content and roles in wound healing," *Journal of Dental Research*, vol. 84, no. 5, pp. 434–439, 2005.

[12] A. Kocaoemer, S. Kern, H. Klüter, and K. Bieback, "Human AB serum and thrombin-activated platelet-rich plasma are suitable alternatives to fetal calf serum for the expansion of mesenchymal stem cells from adipose tissue," *Stem Cells*, vol. 25, no. 5, pp. 1270–1278, 2007.

[13] N. Borregaard and J. B. Cowland, "Granules of the human neutrophilic polymorphonuclear leukocyte," *Blood*, vol. 89, no. 10, pp. 3503–3521, 1997.

[14] F. Rendu and B. Brohard-Bohn, "The platelet release reaction: granules' constituents, secretion and functions," *Platelets*, vol. 12, no. 5, pp. 261–273, 2001.

[15] E. Anitua, I. Andia, B. Ardanza, P. Nurden, and A. T. Nurden, "Autologous platelets as a source of proteins for healing and tissue regeneration," *Thrombosis and Haemostasis*, vol. 91, no. 1, pp. 4–15, 2004.

[16] A. Garcia, N. Zitzmann, and S. P. Watson, "Analyzing the platelet proteome," *Seminars in Thrombosis and Hemostasis*, vol. 30, no. 4, pp. 485–489, 2004.

[17] A. I. Mininkova, "Platelet structure and functions (a review of literature). Part 1," *Klinicheschеskaya Laboratornaya Diagnostika*, no. 11, pp. 21–26, 2010.

[18] A. I. Mininkova, "Investigation of platelets by the flow cytofluorometric technique (a review of literature). Part 2," *Klinicheschеskaya Laboratornaya Diagnostika*, no. 4, pp. 25–30, 2011.

[19] O. Mei-Dan, L. Laver, M. Nyska, and G. Mann, "Platelet rich plasma—a new biotechnology for treatment of sports injuries," *Harefuah*, vol. 150, no. 5, pp. 453–457, 2011.

[20] A. T. Nurden, "Platelets, inflammation and tissue regeneration," *Thrombosis and Haemostasis*, vol. 105 suppl 1, pp. S13–S33, 2011.

[21] R. E. Marx, E. R. Carlson, R. M. Eichstaedt, S. R. Schimmele, J. E. Strauss, and K. R. Georgeff, "Platelet-rich plasma: growth factor enhancement for bone grafts," *Oral Surgery, Oral Medicine, Oral Pathology, Oral Radiology, and Endodontics*, vol. 85, no. 6, pp. 638–646, 1998.

[22] L. Brass, "Understanding and evaluating platelet function," *Hematology / the Education Program of the American Society of Hematology Education Program*, vol. 2010, pp. 387–396, 2010.

[23] Y. Liu, A. Kalen, O. Risto, and O. Wahlström, "Fibroblast proliferation due to exposure to a platelet concentrate in vitro is pH dependent," *Wound Repair and Regeneration*, vol. 10, no. 5, pp. 336–340, 2002.

[24] C. A. Carter, D. G. Jolly, C. E. Worden, D. G. Hendren, and C. J. M. Kane, "Platelet-rich plasma gel promotes differentiation and regeneration during equine wound healing," *Experimental and Molecular Pathology*, vol. 74, no. 3, pp. 244–255, 2003.

[25] B. L. Eppley, W. S. Pietrzak, and M. Blanton, "Platelet-rich plasma: a review of biology and applications in plastic surgery," *Plastic and Reconstructive Surgery*, vol. 118, no. 6, pp. 147e–159e, 2006.

[26] K. M. Lacci and A. Dardik, "Platelet-rich plasma: support for its use in wound healing," *Yale Journal of Biology and Medicine*, vol. 83, no. 1, pp. 1–9, 2010.

[27] T. E. Foster, B. L. Puskas, B. R. Mandelbaum, M. B. Gerhardt, and S. A. Rodeo, "Platelet-rich plasma: from basic science to clinical applications," *American Journal of Sports Medicine*, vol. 37, no. 11, pp. 2259–2272, 2009.

[28] S. Werner and R. Grose, "Regulation of wound healing by growth factors and cytokines," *Physiological Reviews*, vol. 83, no. 3, pp. 835–870, 2003.

[29] R. E. Marx, "Platelet-rich plasma (PRP): what is PRP and what is not PRP?" *Implant Dentistry*, vol. 10, no. 4, pp. 225–228, 2001.

[30] B. L. Eppley, J. E. Woodell, and J. Higgins, "Platelet quantification and growth factor analysis from platelet-rich plasma: implications for wound healing," *Plastic and Reconstructive Surgery*, vol. 114, no. 6, pp. 1502–1508, 2004.

[31] S. J. Froum, S. S. Wallace, D. P. Tarnow, and S. C. Cho, "Effect of platelet-rich plasma on bone growth and osseointegration in human maxillary sinus grafts: three bilateral case reports," *International Journal of Periodontics and Restorative Dentistry*, vol. 22, no. 1, pp. 45–53, 2002.

[32] A. R. Sanchez, P. J. Sheridan, and L. I. Kupp, "Is platelet-rich plasma the perfect enhancement factor? A current review," *International Journal of Oral and Maxillofacial Implants*, vol. 18, no. 1, pp. 93–103, 2003.

[33] T. F. Tozum and B. Demiralp, "Platelet-rich plasma: a promising innovation in dentistry," *Journal Canadian Dental Association*, vol. 69, no. 10, p. 664, 2003.

[34] E. G. Freymiller and T. L. Aghaloo, "Platelet-rich plasma: ready or not?" *Journal of Oral and Maxillofacial Surgery*, vol. 62, no. 4, pp. 484–488, 2004.

[35] M. I. Furman, L. Liu, S. E. Benoit, R. C. Becker, M. R. Barnard, and A. D. Michelson, "The cleaved peptide of the thrombin receptor is a strong platelet agonist," *Proceedings of the National Academy of Sciences of the United States of America*, vol. 95, no. 6, pp. 3082–3087, 1998.

[36] J. P. Maloney, C. C. Silliman, D. R. Ambruso, J. Wang, R. M. Tuder, and N. F. Voelkel, "In vitro release of vascular endothelial growth factor during platelet aggregation," *American Journal of Physiology*, vol. 275, no. 3, pp. H1054–H1061, 1998.

[37] N. T. Bennett and G. S. Schultz, "Growth factors and wound healing: biochemical properties of growth factors and their receptors," *American Journal of Surgery*, vol. 165, no. 6, pp. 728–737, 1993.

[38] D. R. Knighton, T. K. Hunt, K. K. Thakral, and W. H. Goodson, "Role of platelets and fibrin in the healing sequence: an in vivo study of angiogenesis and collagen synthesis," *Annals of Surgery*, vol. 196, no. 4, pp. 379–388, 1982.

[39] S. Cohen, "Isolation of a mouse submaxillary gland protein accelerating incisor eruption and eyelid opening in the new born animal," *Journal of Biological Chemistry*, vol. 237, pp. 1555–1562, 1962.

[40] G. L. Brown, L. B. Nancy, J. Griffen et al., "Enhancement of wound healing by topical treatment with epidermal growth factor," *The New England Journal of Medicine*, vol. 321, no. 2, pp. 76–79, 1989.

[41] G. Hosgood, "Wound healing: the role of platelet-derived growth factor and transforming growth factor beta," *Veterinary Surgery*, vol. 22, no. 6, pp. 490–495, 1993.

[42] H. N. Antoniades and L. T. Williams, "Human platelet-derived growth factor: structure and function," *Federation Proceedings*, vol. 42, no. 9, pp. 2630–2634, 1983.

[43] J. Floege, F. Eitner, and C. E. Alpers, "A new look at platelet-derived growth factor in renal disease," *Journal of the American Society of Nephrology*, vol. 19, no. 1, pp. 12–23, 2008.

[44] O. Wahlström, C. Linder, A. Kalén, and P. Magnusson, "Acidic preparations of platelet concentrates release bone morphogenetic protein-2," *Acta Orthopaedica*, vol. 79, no. 3, pp. 433–437, 2008.

[45] C. Betsholtz, "Role of platelet-derived growth factors in mouse development," *International Journal of Development Biology*, vol. 39, no. 5, pp. 817–825, 1995.

[46] S. C. Bir, J. Esaki, A. Marui et al., "Therapeutic treatment with sustained-release platelet-rich plasma restores blood perfusion by augmenting ischemia-induced angiogenesis and arteriogenesis in diabetic mice," *Journal of Vascular Research*, vol. 48, no. 3, pp. 195–205, 2011.

[47] S. C. Bir, J. Esaki, A. Marui et al., "Angiogenic properties of sustained release platelet-rich plasma: characterization in-vitro and in the ischemic hind limb of the mouse," *Journal of Vascular Surgery*, vol. 50, no. 4, pp. 870–879, 2009.

[48] A. Mishra and T. Pavelko, "Treatment of chronic elbow tendinosis with buffered platelet-rich plasma," *American Journal of Sports Medicine*, vol. 34, no. 11, pp. 1774–1778, 2006.

[49] G. Weibrich, W. K. Kleis, G. Hafner, and W. E. Hitzler, "Growth factor levels in platelet-rich plasma and correlations with donor age, sex, and platelet count," *Journal of Craniomaxillofacial Surgery*, vol. 30, no. 2, pp. 97–102, 2002.

[50] M. M. Rechler and S. P. Nissley, "Insulin-like growth factors," in *Handbook of Experimental Pharm: Peptide Growth Factors and Their Receptors*, M. B. Sporn and A. B. Roberts, Eds., vol. 96, pp. 263–367, Springer, Berlin, Germany, 1990.

[51] G. F. Pierce, T. A. Mustoe, J. Lingelbach, V. R. Masakowski, P. Gramates, and T. F. Deuel, "Transforming growth factor β reverses the glucocorticoid-induced wound healing deficit in rats. Possible regulation in macrophages by platelet-derived growth factor," *Proceedings of the National Academy of Sciences of the United States of America*, vol. 86, no. 7, pp. 2229–2233, 1989.

[52] J. M. Pérez-Rojas, C. Cruz, P. García-López et al., "Renoprotection byα-mangostin is related to the attenuation in renal oxidative/nitrosative stress induced by cisplatin nephrotoxicity," *Free Radical Research*, vol. 43, no. 11, pp. 1122–1132, 2009.

[53] M. G. Goldner, "The fate of the second leg in the diabetic amputee," *Diabetes*, vol. 9, pp. 100–103, 1960.

[54] J. Yu, C. Ustach, and H. R. Kim, "Platelet-derived growth factor signaling and human cancer," *Journal of Biochemistry and Molecular Biology*, vol. 36, no. 1, pp. 49–59, 2003.

[55] S. P. Bennett, G. D. Griffiths, A. M. Schor, G. P. Leese, and S. L. Schor, "Growth factors in the treatment of diabetic foot ulcers," *British Journal of Surgery*, vol. 90, no. 2, pp. 133–146, 2003.

[56] E. M. Spencer, A. Tokunaga, and T. K. Hunt, "Insulin-like growth factor binding protein-3 is present in the α-granules of platelets," *Endocrinology*, vol. 132, no. 3, pp. 996–1001, 1993.

[57] T. McCarrel and L. Fortier, "Temporal growth factor release from platelet-rich plasma, trehalose lyophilized platelets, and bone marrow aspirate and their effect on tendon and ligament gene expression," *Journal of Orthopaedic Research*, vol. 27, no. 8, pp. 1033–1042, 2009.

[58] H. F. Dvorak, "Discovery of vascular permeability factor (VPF)," *Experimental Cell Research*, vol. 312, no. 5, pp. 522–526, 2006.

[59] T. Tammela, B. Enholm, K. Alitalo, and K. Paavonen, "The biology of vascular endothelial growth factors," *Cardiovascular Research*, vol. 65, no. 3, pp. 550–563, 2005.

[60] S. Lee, T. T. Chen, C. L. Barber et al., "Autocrine VEGF signaling is required for vascular homeostasis," *Cell*, vol. 130, no. 4, pp. 691–703, 2007.

[61] P. Carmeliet, V. Ferreira, G. Breier et al., "Abnormal blood vessel development and lethality in embryos lacking a single VEGF allele," *Nature*, vol. 380, no. 6573, pp. 435–439, 1996.

[62] B. Olofsson, M. Jeltsch, U. Eriksson, and K. Alitalo, "Current biology of VEGF-B and VEGF-C," *Current Opinion in Biotechnology*, vol. 10, no. 6, pp. 528–535, 1999.

[63] T. A. Partanen, J. Arola, A. Saaristo et al., "VEGF-C and VEGF-D expression in neuroendocrine cells and their receptor, VEGFR-3, in fenestrated blood vessels in human tissues," *FASEB Journal*, vol. 14, no. 13, pp. 2087–2096, 2000.

[64] M. Klagsbrun, S. Takashima, and R. Mamluk, "The role of neuropilin in vascular and tumor biology," *Advances in Experimental Medicine and Biology*, vol. 515, pp. 33–48, 2002.

[65] R. J. Levine, S. E. Maynard, C. Qian et al., "Circulating angiogenic factors and the risk of preeclampsia," *The New England Journal of Medicine*, vol. 350, no. 7, pp. 672–683, 2004.

[66] J. Folkman, "Angiogenesis: an organizing principle for drug discovery?" *Nature Reviews Drug Discovery*, vol. 6, no. 4, pp. 273–286, 2007.

[67] R. Möhle, D. Green, M. A. Moore, R. L. Nachman, and S. Rafii, "Constitutive production and thrombin-induced release of vascular endothelial growth factor by human megakaryocytes and platelets," *Proceedings of the National Academy of Sciences of the United States of America*, vol. 94, no. 2, pp. 663–668, 1997.

[68] M. Lucerna, A. Zernecke, R. de Nooijer et al., "Vascular endothelial growth factor-A induces plaque expansion in ApoE knock-out mice by promoting de novo leukocyte recruitment," *Blood*, vol. 109, no. 1, pp. 122–129, 2007.

[69] D. J. Sánchez-González, C. A. Sosa-Luna, and I. Vásquez-Moctezuma, "Transfer factors in medical therapy," *Medicina Clinica*, vol. 137, no. 6, pp. 273–277, 2011.

[70] S. Verrier, T. R. Meury, L. Kupcsik, P. Heini, T. Stoll, and M. Alini, "Platelet-released supernatant induces osteoblastic differentiation of human mesenchymal stem cells: potential role of BMP-2," *European Cells & Materials*, vol. 20, pp. 403–414, 2010.

[71] A. Sobotková, L. Másová-Chrastinová, J. Suttnar et al., "Antioxidants change platelet responses to various stimulating events," *Free Radical Biology and Medicine*, vol. 47, no. 12, pp. 1707–1714, 2009.

[72] E. Floriano-Sánchez, C. Villanueva, O. N. Medina-Campos et al., "Nordihydroguaiaretic acid is a potent in vitro scavenger of peroxynitrite, singlet oxygen, hydroxyl radical, superoxide anion and hypochlorous acid and prevents in vivo ozone-induced tyrosine nitration in lungs," *Free Radical Research*, vol. 40, no. 5, pp. 523–533, 2006.

[73] C. Cruz, R. Correa-Rotter, D. J. Sánchez-González et al., "Renoprotective and antihypertensive effects of S-allylcysteine in 5/6 nephrectomized rats," *American Journal of Physiology*, vol. 293, no. 5, pp. F1691–F1698, 2007.

[74] C. E. Guerrero-Beltrán, M. Calderón-Oliver, E. Tapia et al., "Sulforaphane protects against cisplatin-induced nephrotoxicity," *Toxicology Letters*, vol. 192, no. 3, pp. 278–285, 2010.

[75] E. Coballase-Urrutia, J. Pedraza-Chaverri, N. Cárdenas-Rodríguez et al., "Hepatoprotective effect of acetonic and methanolic extracts of Heterotheca inuloides against CCl(4)-induced toxicity in rats," *Experimental and Toxicologic Pathology*, vol. 63, no. 4, pp. 363–370, 2011.

[76] M. Sánchez, E. Anitua, J. Azofra, I. Andía, S. Padilla, and I. Mujika, "Comparison of surgically repaired achilles tendon tears using platelet-rich fibrin matrices," *American Journal of Sports Medicine*, vol. 35, no. 2, pp. 245–251, 2007.

[77] L. Savarino, E. Cenni, C. Tarabusi et al., "Evaluation of bone healing enhancement by lyophilized bone grafts supplemented with platelet gel: a standardized methodology in patients with tibial osteotomy for genu varus," *Journal of Biomedical Materials Research*, vol. 76, no. 2, pp. 364–372, 2006.

[78] D. Dallari, L. Savarino, C. Stagni et al., "Enhanced tibial osteotomy healing with use of bone grafts supplemented with platelet gel or platelet gel and bone marrow stromal cells," *Journal of Bone and Joint Surgery*, vol. 89, no. 11, pp. 2413–2420, 2007.

[79] H. Kitoh, T. Kitakoji, H. Tsuchiya, M. Katoh, and N. Ishiguro, "Transplantation of culture expanded bone marrow cells and platelet rich plasma in distraction osteogenesis of the long bones," *Bone*, vol. 40, no. 2, pp. 522–528, 2007.

[80] L. Y. Carreon, S. D. Glassman, Y. Anekstein, and R. M. Puno, "Platelet gel (AGF) fails to increase fusion rates in instrumented posterolateral fusions," *Spine*, vol. 30, no. 9, pp. E243–E247, 2005.

[81] M. Sanchez, E. Anitua, R. Cugat et al., "Nonunions treated with autologous preparation rich in growth factors," *Journal of Orthopaedic Trauma*, vol. 23, no. 1, pp. 52–59, 2009.

[82] P. R. Siljander, "Platelet-derived microparticles - an updated perspective," *Thrombosis Research*, vol. 127, no. 2, suppl 2, pp. S30–S33, 2011.

Hindawi Publishing Corporation
International Journal of Peptides
Volume 2012, Article ID 124163, 5 pages
doi:10.1155/2012/124163

Research Article

Diverse Effects of Glutathione and UPF Peptides on Antioxidant Defense System in Human Erythroleukemia Cells K562

Ceslava Kairane, Riina Mahlapuu, Kersti Ehrlich, Kalle Kilk, Mihkel Zilmer, and Ursel Soomets

The Centre of Excellence of Translational Medicine, Department of Biochemistry, Faculty of Medicine, University of Tartu, Ravila Street 19, 50411 Tartu, Estonia

Correspondence should be addressed to Kersti Ehrlich, kersti.ehrlich@ut.ee

Received 15 September 2011; Accepted 2 December 2011

Academic Editor: Katsuhiro Konno

The main goal of the present paper was to examine the influence of the replacement of γ-Glu moiety to α-Glu in glutathione and in its antioxidative tetrapeptidic analogue UPF1 (Tyr(Me)-γ-Glu-Cys-Gly), resulting in α-GSH and UPF17 (Tyr(Me)-Glu-Cys-Gly), on the antioxidative defense system in K562 cells. UPF1 and GSH increased while UPF17 and α-GSH decreased the activity of CuZnSOD in K562 cells, at peptide concentration of 10 μM by 42% and 38% or 35% and 24%, respectively. After three-hour incubation, UPF1 increased and UPF17 decreased the intracellular level of total GSH. Additionally, it was shown that UPF1 is not degraded by γ-glutamyltranspeptidase, which performs glutathione breakdown. These results indicate that effective antioxidative character of peptides does not depend only on the reactivity of the thiol group, but also of the other functional groups, and on the spatial structure of peptides.

1. Introduction

Glutathione (GSH) system is an attractive target for drug discovery because of its importance and versatility [1]. GSH (γ-L-Glu-L-Cys-Gly) is a prevalent low molecular weight thiol in eukaryotic cells and has antioxidative, detoxificative, and regulatory roles [2, 3]. Decrease of GSH level and shifted GSH redox status are related to several pathological states, including neurodegenerative, cardiovascular, pulmonary, and immune system diseases [4]. Exogenous administration of GSH to compensate the decrease of GSH levels is not reasonable because of its degradation in the plasma and poor cellular uptake [5–7]. GSH and its oxidized disulfide form (GSSG) are degraded by γ-glutamyltranspeptidase (GGT) via cleavage of the amino acid γ-glutamate from the N-terminal end of the peptide. GGT is located in the outer side of the cell membrane, and one of its functions, in cooperation with dipeptidases, is to provide cells with precursor amino acids needed for GSH *de novo* synthesis. To overcome the problems with GSH administration, several GSH analogues have been created to increase the GSH level and support the functionality of the GSH system [8]. We have previously designed and synthesized a library of peptidic GSH analogues [9]. For this study, two of them, UPF1 (Tyr(Me)-γ-Glu-Cys-Gly) and UPF17 (Tyr(Me)-Glu-Cys-Gly), were selected. Both molecules have an *O*-methyl-L-tyrosine residue added to the N-terminus of GSH-like Glu-Cys-Gly sequence to increase the antioxidativity and hydrophobicity. Previously, different groups have shown that various low molecular weight antioxidants, including melatonin, carvedilol, and its metabolite SB 211475, carry a methoxy moiety in their aromatic structures [10, 11]. The only structural difference between the peptides used is that UPF17 contains α-glutamyl moiety while UPF1 has γ-glutamyl moiety similarly to GSH. This switch from γ- to α-glutamyl moiety improved hydroxyl radical scavenging ability of UPF17 by approximately 500-fold compared to UPF1 whereas UPF1 itself is about 60-fold better hydroxyl radical scavenger than GSH [9]. In addition to being an excellent *in vitro* free radical scavenger, UPF1 has shown protective properties against oxidative damage in a global brain ischemia/reperfusion model and in an ischemia/reperfusion

model on an isolated heart of Wistar rats [12, 13]. UPF1 and UPF17 have been shown to be nontoxic for K562 cells up to concentration of 200 μM and UPF1 has no toxic effect on the primary culture of cerebellar granule cells at concentrations up to 100 μM [9, 13].

Superoxide dismutases (SOD, EC 1.15.1.1.) are metalloproteins and the primary enzymes that keep cellular free radical production under control [14]. Cytosolic CuZnSOD is a homodimer (151 amino acids) with a molecular weight of 32500 Da and contains two cysteines (Cys57, Cys148) bound into an intramolecular disulfide bond and two free cysteines (Cys6, Cys111) [15, 16]. SOD catalyses the dismutation of superoxide into oxygen and hydrogen peroxide. Hydrogen peroxide as a diffusible cell damaging agent is further eliminated by glutathione peroxidase or catalase. One of the essential requirements for the biological activity of the glutathione peroxidase is glutathione as a cosubstrate. Consequently, SOD works synergistically with the glutathione against free radical damage.

This study examined the influence of UPF1 and UPF17 on CuZnSOD activity and intracellular GSH level in K562 cells. The aim of studying these tetrapeptides was to get information about whether and how the replacement of γ-peptide bond with α-peptide bond in the structure affects the bioactivities of the peptides. Additionally, we measured the stability of the peptides towards GGT to clarify their status in biologicalsystems and the pK_a values for thiol group dissociation.

2. Materials and Methods

2.1. Peptide Synthesis. UPF peptides were synthesized manually by solid phase peptide synthesis using Fmoc-chemistry and by machine using *tert*-Boc-chemistry as described previously [9, 17]. The purity of the peptides was >99% as demonstrated by HPLC on an analytical Nucleosil 120-3 C18 reversed-phase column (0.4 cm × 10 cm) and the peptides were identified by MALDI-TOF (matrix-assisted laser desorption ionization time-of-flight) mass-spectrometry (Voyager DE Pro, Applied Biosystems).

2.2. CuZnSOD Activity in K562 Cells. The K562 cells (human erythroleukemia cells, obtained from DSMZ, Germany) were grown in T75 cell culture flasks in RPMI 1640 supplemented with 2 mM glutamine (PAA, Austria), 7.5% fetal calf serum, streptomycin (100 μg/mL), and penicillin (100 U/mL) (all from Invitrogen, USA) at 37°C in a humidified 5% carbon dioxide atmosphere. Cells were seeded at concentration of 1.0×10^6 per mL. Experiments were conducted 24 h after passage. Peptides (GSH, α-GSH, UPF1 and UPF17) diluted in DPBS (PAA, Austria) were added to the flasks containing the K562 cells. The cells were incubated with DPBS as control (Co) or with the peptide solution in a concentration range from 0.5 to 10 μM for 24 h at 37°C. The peptide concentrations were chosen based on the GSH concentration in the blood plasma. After treatment, the cells were washed twice with DPBS and then lysed in water by keeping on ice for 20 min. Samples were centrifuged (12000 g) for 10 min and supernatants were transferred for experiments. The protein concentrations in the supernatants were determined by Lowry's method [18]. CuZnSOD activity was measured with the commercially available kit (Randox Laboratories Ltd, UK). This method employs xanthine and xanthine oxidase to generate superoxide radicals, which react with 2-(4-iodophenyl)-3-(4-nitrophenol)-5-phe nyltetrazolium chloride to form a red formazan dye. The superoxide dismutase activity is then measured by the degree of inhibition of this reaction. One unit of SOD inhibited 50% of the rate of reaction.

2.3. Measurement of Total Glutathione. Concentrations of total glutathione (tGSH) were assessed by an enzymatic method of Tietze [19]. The homogenate was deproteinated by 10% solution of metaphosphoric acid (Sigma-Aldrich, Germany) in water and centrifuged at 12000 g for 10 min. The enzymatic reaction was initiated by the addition of NADPH, glutathione reductase, and 5,5′-dithio-*bis*-2-nitrobenzoic acid in buffer containing EDTA (Sigma-Aldrich, Germany). The change in optical density was measured after 15 min at 412 nm spectrophotometrically (Sunrise Tecan). Glutathione content was calculated on the basis of a standard curve.

2.4. Stability towards γ-Glutamyltranspeptidase. 1 mM UPF1 was incubated with 0.3 mg/mL equine kidney γ-glutamyltranspeptidase in 0.1 M Tris-HCl buffer pH 7.4, supplemented with 0.1% EDTA (Sigma-Aldrich, Germany) at 37°C for 1 h. 6 mM Gly-Gly was added as an acceptor for γ-Glu moiety [20]. GSH was incubated with GGT under the same conditions as the control. The samples were heat-inactivated, centrifuged at 10000 g and +4°C for 5 min, and kept on ice until analyzed. Supernatants were analyzed on a Prominence HPLC (Shimadzu, Japan) and Q-Trap 3200 (Applied Biosystems, USA) mass spectrometry tandem. Luna C18 100 × 2 mm, 3 μm column from Phenomenex was used for sample separation. Solvent A was a mixture of 99.9% water and 0.1% HCOOH, and solvent B was a mixture of 99.9% acetonitrile and 0.1% HCOOH (mass spectrometry grade, Riedel-de Haėn, Germany). Samples were eluated at a flow rate of 0.1 mL/min, gradient started with 5 min at isocratic flow of solvent A, concentration of solvent B increased up to 30% in 25 min, followed by wash with 100% solvent B in 20 min. Enhanced MS scans were performed in negative mode with rate 1000 amu/s between mass range 50–1700 Da. Ionspray voltage was set to −4500 V, declustering potential to −30 V and entrance potential to −10 V.

2.5. pK_a of Thiol Groups. The ratio of thiol and thiolate concentrations were measured spectrophotometrically at 240 nm on a PerkinElmer Lambda 25 spectrometer similarly as previously for GSH and α-GSH [21]. 1 mL of 50 μM peptide solution in phosphate buffered saline (Calbiochem, USA) was titrated with 5 μL volumes of 1 M NaOH and pH and absorbance changes were determined after each addition. The results were corrected to consider the dilution of the assay mixture during titration.

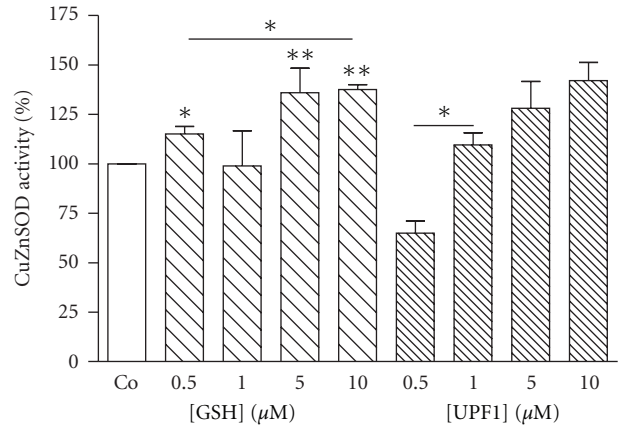

Figure 1: Modulation of CuZnSOD activity by GSH and UPF1 in K562 cells. The CuZnSOD activity of Co is 100%. $^{*}P < 0.05$; $^{**}P < 0.01$, GSH and UPF1 versus Co; $n = 4$–8.

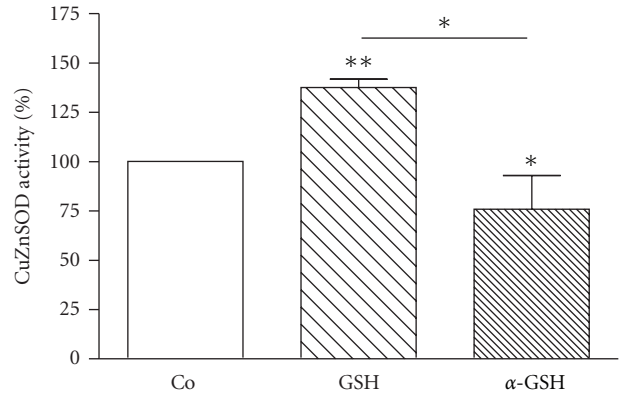

Figure 2: Modulation of CuZnSOD activity by GSH and α-GSH (10 μM) in K562 cells. The CuZnSOD activity of Co is 100%. $^{*}P < 0.05$; $^{**}P < 0.01$, 10 μM GSH or α-GSH versus Co; $n = 4$–8.

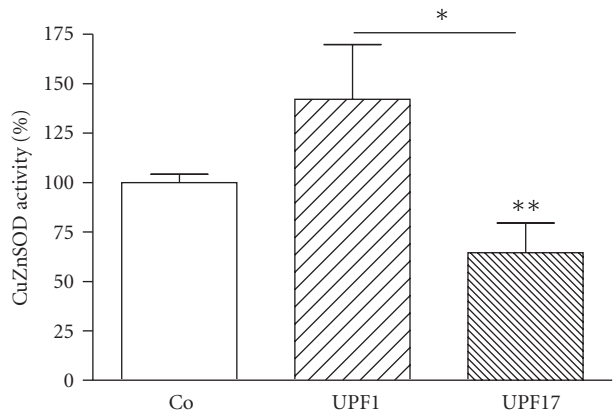

Figure 3: Modulation of CuZnSOD activity by UPF1 and UPF17 (10 μM) in K562 cells. The CuZnSOD activity of Co is 100%. $^{*}P < 0.05$; $^{**}P < 0.01$, 10 μM UPF1 or UPF17 versus Co; $n = 4$–8.

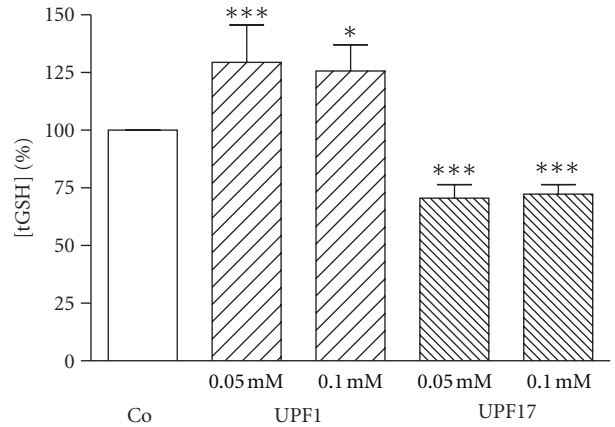

Figure 4: Alteration of tGSH concentration by UPF1 and UPF17 in K562 cells. The tGSH concentration of Co is 100%. $^{*}P < 0.05$, $^{***}P < 0.005$, UPF1 or UPF17 versus Co; $n = 6$–8.

2.6. Statistical Analysis. Data were analyzed using GraphPad Prism version 4.00 for Windows (GraphPad Software, San Diego, CA, USA). The results on the graphs are presented as the mean ± standard error of the mean (SEM).

3. Results

3.1. CuZnSOD Activity. K562 cells were incubated with investigated peptides (GSH, α-GSH, UPF1, and UPF17) for 24 h at four different concentrations: 0.5, 1.0, 5.0, and 10 μM. GSH showed a concentration-dependent activating effect on CuZnSOD activity, whereas 10 μM GSH increased the enzyme activity by 38% (Figure 1). α-GSH had an inhibiting effect (24%) on the enzyme activity but only at the highest concentration used (10 μM) (Figure 2). UPF1 increased the activity of CuZnSOD at concentrations of 1.0, 5.0, and 10 μM, but at concentration of 0.5 μM showed an inhibition of the enzyme activity (Figure 1). The activation rate was concentration dependent. Contrary to UPF1, UPF17 showed an inhibitory effect and the inhibition was not concentration dependent. UPF1 increased and UPF17 decreased the activity of CuZnSOD at peptide concentration of 10 μM by 42% and 35%, respectively (Figure 3). As the peptide concentration of 10 μM was the most effective, it selected for the comparison.

3.2. Intracellular GSH Level. K562 cells were incubated with UPF1 and UPF17 peptides for 3 h at concentrations of 0.05, 0.10, and 0.5 mM. Previous experiments have shown that at these concentrations UPF peptides are effective free radical scavengers and are biologically active. In addition, the 0.5 mM concentration was chosen to match with millimolar GSH concentration in number of cells. UPF1 increased and UPF17 decreased GSH concentration at concentrations of 0.05 and 0.1 mM by 29% and 26% or 26% and 28%, respectively (Figure 4). No statistical difference in tGSH concentration compared to control after incubation with 0.5 mM peptides, the highest concentration used, was detected.

3.3. Degradation by GGT. After incubating GSH with GGT, GSH was degraded and γ-Glu moiety was transferred to an acceptor Gly-Gly dipeptide, resulting in a new compound in

mass spectra with MW 261.2 Da [γ-Glu-Gly-Gly]. The question arose: can the bond between γ-glutamate and cysteine be degraded by GGT in UPF1, where the access to the bond is obstructed by an additional amino acid methylated tyrosine? Results obtained from the mass spectrometry measurements demonstrated that UPF1 is not degraded by GGT as the expected peaks with or without acceptor dipeptide MW 438.4 Da [Tyr(Me)-γ-Glu-Gly-Gly] or 324.3 Da [Tyr(Me)-γ-Glu], respectively, did not appear. During the incubation, UPF1 was dimerised over disulphide bridge. GGT is also able to breakdown dimeric form of GSH, but degradation of dimerised UPF1 was not detected.

3.4. pK_a. The pK_a values of thiol groups of the peptides were measured. For GSH and α-GSH, the values were 9.0 ± 0.3 and 9.1 ± 0.1, respectively, whereas pK_a values for UPF peptides were slightly higher: 9.3 ± 0.1 for UPF1 and 9.4 ± 0.2 for UPF17.

4. Discussion

The present study focused on the effects of UPF1 and UPF17 on CuZnSOD activity and intracellular GSH level in K562 cells. For the first time we described and compared counterpoint biological activities of structural antioxidative peptide analogs differing from each other by spacial arrangement of Glu residue (γ-peptide bond in UPF1 changed to the α-peptide bond in UPF17). Previously we have shown that UPF1 and UPF17 have a tendency for MnSOD activation. However, the γ-glutamyl moiety containing UPF1 needed more time for MnSOD activation compared to UPF17, which had the effect already after 5 min incubation. UPF1 and UPF17 have also different influence on glutathione peroxidase activity (GPx): at higher concentrations than used in *in vivo* experiments, both UPF1 and UPF17 inhibited activity concentration dependently whereas the α-peptide bond containing UPF17 had stronger inhibitory effect [22]. In the present work we investigated how the replacement of γ-peptide bond with α-peptide bond on GSH and its analogue UPF1 affects CuZnSOD activity and level of GSH in K562 cells. The results showed that γ-Glu moiety containing GSH and UPF1 stimulated CuZnSOD activity and increased intracellular tGSH level, whereas α-GSH and UPF17, which have α-Glu moiety in the structure, inhibited enzymatic activity and decreased GSH level. The stability of UPF1 towards GGT activity indicated that UPF1 affects GSH level and CuZnSOD activity as intact molecule instead of being a GSH precursor. Previously, it has been shown that GSH and UPF1 are able to act as signaling molecules through G-protein activation in frontocortical membrane preparations [23]. It has been reported that plasma membranes have specific binding sites of GSH which have an interaction with the glutamate binding sites [24]. By this way GSH and UPF peptides may affect the metabolism of cells as signal molecules. The effects on the level of GSH and CuZnSOD activity may be different depending on the replacement of γ-peptide bond with α-peptide bond. GSH has been shown to bind to ionotropic glutamate receptors via gamma-glutamyl residue in the nervous tissue [25]. Additionally, glutamate receptors have been found also in the plasma membrane of megakaryocytes and rat erythrocytes [26, 27]. By interacting with the latter receptors, GSH and UPF peptides may affect the metabolism of cells as signal molecules through the PKC pathway and affect CuZnSOD activity. The various effects of the studied molecules may be caused by structural differences between the GSH and UPF peptides (replacement of γ-peptide bond with α-peptide bond).

UPF1 and UPF17 have also shown different effects in free radical scavenging experiments. According to the classification of kinetic behavior by Sánches-Moreno et al., UPF17 is classified as fast and UPF1 as intermediate DPPH radical scavenger [9, 28]. *In silica* modeling of noncovalent complex formation by docking calculations revealed a more affine complex between DPPH radical and α-GSH compared to the complex with GSH [21]. This raised a question about pK_a values for the thiol groups of UPF peptides. Previously, the change of γ-peptide bond to α-peptide bond has also been investigated for GSH and its α-analogue: pK_a of thiol groups were similar for GSH and α-GSH (9.0 ± 0.1 and 9.1 ± 0.1) [21]. The comparison of these results with current measurements for UPF1 and UPF17 demonstrated that pK_a value is rather influenced by the addition of a methylated tyrosine moiety to the GSH backbone than by the change of the peptide bond type. Smaller pK_a values for GSH and its α-analogue showed that these molecules donate the sulfhydryl proton more easily than UPF peptides; however, UPF peptides are better radical scavengers. This indicates that reactive species elimination does not depend only of the reactivity of the thiol group.

The results of the current paper show that γ-peptide bond and α-peptide bond containing UPF peptides may influence enzyme activities in different direction, which offers a wider perspective for the usage of glutathione analogues as protective diverse regulators of the oxidative state.

Acknowledgments

This paper was financially supported by the Estonian Science Foundation Grants no. 7856 and 7494, by targeted financing from Ministry of Education and Science of Estonia (SF0180105s08) and by European Union through the European Regional Development Fund.

References

[1] M. Zilmer, U. Soomets, A. Rehema, and U. Langel, "The glutathione system as an attractive therapeutic target," *Drug Design Reviews Online*, vol. 2, no. 2, pp. 121–127, 2005.

[2] N. H. P. Cnubben, I. M. C. M. Rietjens, H. Wortelboer, J. Van Zanden, and P. J. Van Bladeren, "The interplay of glutathione-related processes in antioxidant defense," *Environmental Toxicology and Pharmacology*, vol. 10, no. 4, pp. 141–152, 2001.

[3] D. A. Dickinson, A. L. Levonen, D. R. Moellering et al., "Human glutamate cysteine ligase gene regulation through the electrophile response element," *Free Radical Biology and Medicine*, vol. 37, no. 8, pp. 1152–1159, 2004.

[4] N. Ballatori, S. M. Krance, S. Notenboom, S. Shi, K. Tieu, and C. L. Hammond, "Glutathione dysregulation and the etiology

and progression of human diseases," *Biological Chemistry*, vol. 390, no. 3, pp. 191–214, 2009.

[5] R. Franco, O. J. Schoneveld, A. Pappa, and M. I. Panayiotidis, "The central role of glutathione in the pathophysiology of human diseases," *Archives of Physiology and Biochemistry*, vol. 113, no. 4-5, pp. 234–258, 2007.

[6] O. Ortolani, A. Conti, A. R. De Gaudio, E. Moraldi, Q. Cantini, and G. Novelli, "The effect of glutathione and N-acetylcysteine on lipoperoxidative damage in patients with early septic shock," *American Journal of Respiratory and Critical Care Medicine*, vol. 161, no. 6, pp. 1907–1911, 2000.

[7] A. Wendel and P. Cikryt, "The level and half-life of glutathione in human plasma," *FEBS Letters*, vol. 120, no. 2, pp. 209–211, 1980.

[8] I. Cacciatore, C. Cornacchia, F. Pinnen, A. Mollica, and A. Di Stefano, "Prodrug approach for increasing cellular glutathione levels," *Molecules*, vol. 15, no. 3, pp. 1242–1264, 2010.

[9] K. Ehrlich, S. Viirlaid, R. Mahlapuu et al., "Design, synthesis and properties of novel powerful antioxidants, glutathione analogues," *Free Radical Research*, vol. 41, no. 7, pp. 779–787, 2007.

[10] A. Gozzo, D. Lesieur, P. Duriez, J. C. Fruchart, and E. Teissier, "Structure-activity relationships in a series of melatonin analogues with the low-density lipoprotein oxidation model," *Free Radical Biology and Medicine*, vol. 26, no. 11-12, pp. 1538–1543, 1999.

[11] T. L. Yue, P. J. Mckenna, P. G. Lysko et al., "SB 211475, a metabolite of carvedilol, a novel antihypertensive agent, is a potent antioxidant," *European Journal of Pharmacology*, vol. 251, no. 2-3, pp. 237–243, 1994.

[12] J. Kals, J. Starkopf, M. Zilmer et al., "Antioxidant UPF1 attenuates myocardial stunning in isolated rat hearts," *International Journal of Cardiology*, vol. 125, no. 1, pp. 133–135, 2008.

[13] P. Põder, M. Zilmer, J. Starkopf et al., "An antioxidant tetrapeptide UPF1 in rats has a neuroprotective effect in transient global brain ischemia," *Neuroscience Letters*, vol. 370, no. 1, pp. 45–50, 2004.

[14] I. Fridovich, "Superoxide anion radical ($O_2^{\cdot-}$), superoxide dismutases, and related matters," *Journal of Biological Chemistry*, vol. 272, no. 30, pp. 18515–18517, 1997.

[15] M. D. De Beus, J. Chung, and W. Colón, "Modification of cysteine 111 in Cu/Zn superoxide dismutase results in altered spectroscopic and biophysical properties," *Protein Science*, vol. 13, no. 5, pp. 1347–1355, 2004.

[16] M. A. Hough and S. S. Hasnain, "Structure of fully reduced bovine copper zinc superoxide dismutase at 1.15 Å," *Structure*, vol. 11, no. 8, pp. 937–946, 2003.

[17] U. Soomets, M. Zilmer, and Ü. Langel, "Manual solid-phase synthesis of glutathione analogues: a laboratory-based short course," in *Peptide Synthesis and Applications*, J. Howl, Ed., pp. 241–257, Humana Press, Totowa, NJ, USA, 2006.

[18] O. H. Lowry, N. J. Rosebrough, A. L. Farr, and R. J. Randall, "Protein measurement with the Folin phenol reagent," *The Journal of biological chemistry*, vol. 193, no. 1, pp. 265–275, 1951.

[19] F. Tietze, "Enzymic method for quantitative determination of nanogram amounts of total and oxidized glutathione: applications to mammalian blood and other tissues," *Analytical Biochemistry*, vol. 27, no. 3, pp. 502–522, 1969.

[20] D. Burg, D. V. Filippov, R. Hermanns, G. A. Van der Marel, J. H. Van Boom, and G. J. Mulder, "Peptidomimetic glutathione analogues as novel γGT stable GST inhibitors," *Bioorganic and Medicinal Chemistry*, vol. 10, no. 1, pp. 195–205, 2002.

[21] S. Viirlaid, R. Mahlapuu, K. Kilk, A. Kuznetsov, U. Soomets, and J. Järv, "Mechanism and stoichiometry of 2,2-diphenyl-1-picrylhydrazyl radical scavenging by glutathione and its novel α-glutamyl derivative," *Bioorganic Chemistry*, vol. 37, no. 4, pp. 126–132, 2009.

[22] K. Ehrlich, K. Ida, R. Mahlapuu et al., "Characterization of UPF peptides, members of the glutathione analogues library, on the basis of their effects on oxidative stress-related enzymes," *Free Radical Research*, vol. 43, no. 6, pp. 572–580, 2009.

[23] E. Karelson, R. Mahlapuu, M. Zilmer, U. Soomets, N. Bogdanovic, and U. Langel, "Possible signaling by glutathione and its novel analogue through potent stimulation of frontocortical G proteins in normal aging and in Alzheimer's disease," *Annals of the New York Academy of Sciences*, vol. 973, pp. 537–540, 2002.

[24] R. Janáky, K. Ogita, B. A. Pasqualotto et al., "Glutathione and signal transduction in the mammalian CNS," *Journal of Neurochemistry*, vol. 73, no. 3, pp. 889–902, 1999.

[25] Z. Jenei, R. Janáky, V. Varga, P. Saransaari, and S. S. Oja, "Interference of S-alkyl derivatives of glutathione with brain ionotropic glutamate receptors," *Neurochemical Research*, vol. 23, no. 8, pp. 1085–1091, 1998.

[26] P. G. Genever, D. J. P. Wilkinson, A. J. Patton et al., "Expression of a functional N-methyl-D-aspartate-type glutamate receptor by bone marrow megakaryocytes," *Blood*, vol. 93, no. 9, pp. 2876–2883, 1999.

[27] A. Makhro, J. Wang, J. Vogel et al., "Functional NMDA receptors in rat erythrocytes," *American Journal of Physiology*, vol. 298, no. 6, pp. C1315–C1325, 2010.

[28] C. Sánchez-Moreno, J. A. Larrauri, and F. Saura-Calixto, "A procedure to measure the antiradical efficiency of polyphenols," *Journal of the Science of Food and Agriculture*, vol. 76, no. 2, pp. 270–276, 1998.